Functional Maturation and Glucose Responsiveness in Stem Cell-Derived ß Cells

Functional Maturation and Glucose Responsiveness in Stem Cell-derived β Cells

A dissertation presented

by

Jeffrey Carl Davis

to

the Division of Medical Sciences

in partial fulfillment of the requirements

for the degree of

Doctor of Philosophy

In the subject of

Biological and Biomedical Sciences

Harvard University

Cambridge, Massachusetts

April 2019

Dissertation Advisor: Douglas A. Melton Jeffrey Carl Davis

Functional Maturation and Glucose Responsiveness in Stem Cell-derived β Cells

Abstract

Stem Cell-derived β cells (SC-β cells) are an unlimited source of islet-like material for curative transplantation in patients with Type 1 Diabetes. SC-β cell potential to supplement or replace human islets for transplantation is limited by their ability to sense changes in glucose levels and respond by secreting insulin to restore normoglycemia. SC-β cells respond to glucose *in vitro*, but at a magnitude lower than that of human islets. We have analyzed their capability to sense glucose and undergo glucose stimulated insulin secretion (GSIS) *in vitro* and identified a novel bottleneck in glycolysis, limiting their potential to undergo GSIS. Bypassing this deficiency in metabolism results in an insulin secretion profile indistinguishable from human islets. SC-β cell glucose sensing also improves after transplantation. To study this process, we have analyzed gene expression changes before and after transplantation into immune-compromised mice. In addition to identifying changes in pathways regulating insulin secretion, we have identified Islet Amyloid Polypeptide (IAPP) as a potential marker of more mature SC-β cells. Using a dual knock-in fluorescent reporter line, we have characterized the dynamics of the IAPP-expressing SC-β cell subpopulation before and after transplant, demonstrating IAPP expression marks a more mature, stable population of SC-β cells *in vitro*. In summary, we have identified a glycolytic defect in SC-β cells limiting their function *in vitro*. Bypassing this defect will assist in generating SC-β cells for cell-based therapies for diabetic patients. Analysis of gene expression during *in vivo* functional maturation of SC-β cells revealed IAPP expression is characteristic of more mature SC-β cells *in vitro* and has provided a new marker for SC-β cells during differentiation.

Table of Contents

Acknowledgements

I would first like to thank my mentor, Doug Melton for his unconditional support and offering me tremendous opportunities to grow as a scientist in his lab. I will always look back fondly on this time in my life. You ask big questions and encourage your trainees to think broadly. If I am lucky enough to run a lab of my own in the future, I hope to provide an environment as conducive as yours for great science and important work for my own trainees. Thank you.

I would also like to thank my dissertation defense committee: Dr. Thomas Michel, Dr. Stephan Kissler, Dr. Gustavo Mostoslavsky, and Dr. Richard Lee. Thank you for taking the time to read and critique my work. I appreciate the your effort in this process and am excited for our discussion. I value your advice and comments. Thank you to the other members of my dissertation advisory committee, Dr. Gordon Weir and Dr. Nika Danial. You have both provided tremendous advice for these projects and I have been lucky to have your input.

This work is a culmination of effort from a number of individuals in the lab and external collaborators. I would like to thank Dr. Gordon Weir and Dr. Susan Bonner-Weir for their work in analyzing GAPDH localization and comments. Dr. Maria Ryaboshapkina has contributed tremendously to our work analyzing *in vivo* maturation RNA seq experiments. Within the lab I would like to especially thank Jenny Kenty for her amazing work ethic and help with mouse surgeries and keeping the lab running smoothly. Thank you to Dr. Ronny Helman, Dr. Nadav Sharon, Stephanie Tsai, Christine Griffiths, Dr. Can Kayatekin, and of course Dr. José Rivera-Feliciano. Your conversations, input, and friendship has made this experience even more memorable. Thanks to Dr. Tiago Alves and Dr. Richard Kibbey of Yale University for ideas, analysis, and time.

I would like to thank my entire family for tremendous support and encouragement as I have spent the last seven years pursuing this goal. I would especially like to thank my father, Ray Davis, who has spent countless hours coaching, teaching, and guiding me through my life. I would

also like to thank my brother, Nolan, who I was lucky to have to grow up with. I have too many scientific role models in my family to name individually, but thank you to all of you, especially Jack Serwold, Dr. James Davis, Dr. Thomas Serwold, and Dr. Amy Wagers. You have all played a large role in my choices through life that led me to pursue a PhD at Harvard and I can't think of a more appropriate place to say, "Thank you." I would also like to thank the rest of my family. I have been beyond lucky to have all of you in my life.

I have made amazing friendships in graduate school with truly talented people who will change the world on their own terms. You are too numerous to name but you have made this journey even more rewarding and I look forward with anticipation to following your paths in the future.

To my partner and the light of my life, Dr. Pınar Eser: I am so grateful we found each other in graduate school. The chance to meet you alone made the choice to move to Boston worth it. We have so much ahead of us to experience together and I am enjoying every moment that comes our way. Thank you for your support, humor, compassion, and love of life.

Finally, I would like to dedicate this dissertation to my mother, Theresa Mary Serwold-Davis. You have been a strong role model in my life and are the reason I pursued regenerative medicine. Thank you for the sacrifices you made to raise me. I know you will continue be with me as I move forward in my life and career.

List of Figures

List of Tables

List of Abbreviations

T1D: Type 1 Diabetes

T2D: Type 2 Diabetes

GSIS: Glucose stimulated insulin secretion

OCR: Oxygen consumption rate

SC-β cell: Stem Cell-derived β cell

hES cell: Human embryonic stem cell

iPS: induced Pluripotent Stem Cell

KRB: Kreb's Ringer Buffer

INS: Insulin

IAPP: Islet Amyloid Polypeptide

GCG: Glucagon

GCK: Glucokinase

PEP: Phosphoenolpyruvate

KATP channel: ATP-sensitive Potassium Channel

Chapter 1: Introduction

1.1 Pancreatic Control of Blood Glucose

Energy homeostasis in vertebrates is controlled through intake of nutrients and their subsequent breakdown and distribution to tissues throughout the body, tightly controlled in a tissue-specific manner [1]. Just as a lack of nutrients is fatal in starvation, disturbed transport, metabolism, and storage of fuel sources can have devastating effects on human physiology [2]. The endocrine compartment of the pancreas regulates metabolism and transport of ingested fuel sources [3, 4]. The mammalian pancreas is located inferior the stomach and is structurally comprised of branched ducts, collecting digestive enzymes derived from exocrine acinar cells at edges of these branches which together account for approximately 95% of the pancreas. These ducts converge with the common bile duct, collecting a mix of digestive enzymes from the pancreas and bile from the gallbladder to facilitate nutrient breakdown in the duodenum of the small intestine [3, 4]. Once nutrients are absorbed into the bloodstream via the small intestine, glucose derived from meals or the liver's gluconeogenic functions must be taken up by peripheral tissues to maintain adequate fuel for cellular processes [5]. Regulation of glucose liberation from the liver and its clearance from the blood by peripheral tissues is regulated by several peptide hormones produced in the islets of Langerhans: the neuro-endocrine component of the pancreas organized into small, functional mini-organs located adjacent to the branched duct structures of the pancreas. Islets account for only 1-2% of the pancreatic mass. The human pancreas contains approximately 1 million islets, each composed of 500-5000 cells [3, 6].

Each islet is highly vascularized and innervated to facilitate rapid release of hormones into the blood stream and incorporate autonomic control of energy homeostasis [7, 8]. The adult human islet is comprised mainly of glucagon-producing α cells and insulin-producing β cells as well as smaller populations of somatostatin-producing δ cells, ghrelin-producing ε cells, and pancreatic polypeptide-producing PP cells [3]. Control of the carbohydrate fuel source glucose in the blood stream and peripheral tissues is mostly regulated by the α and β cell populations. Glucagon is

released from α cells which acts to increase glucose in the blood stream through stimulating the liver to undergo gluconeogenesis from glycogen stores in low glucose conditions. The pancreatic β cell makes up 50% of the human islet endocrine population on average [6]. These cells respond to increased blood glucose levels by secreting insulin, driving glucose uptake in peripheral tissues and lowing blood glucose levels.

1.2 Insulin Action

Normal human blood glucose levels range from 80 to 120 mg/dL [9]. This range is maintained through the endocrine actions of glucagon and insulin as described above. Prolonged excursions outside of this range can be fatal if left untreated. Acute episodes of hypoglycemia, defined as a blood glucose level less than 70 mg/dL can be deadly, depriving the brain of its obligate fuel source [10, 11]. Even short periods of hypoglycemia can lead to coma and death if left untreated. In contrast, acute hyperglycemic excursions are not as immediately life threatening as hypoglycemia [12]. Loss of glycemic control due to disrupted insulin action is the defining feature of diabetes. Chronic hyperglycemia is observed in both type 1 and type 2 diabetes when untreated, defined as a fasting plasma glucose level above 126 mg/dL [13].

Insulin is expressed as a 110 amino acid protein. Its signal peptide directs translation at the endoplasmic reticulum where the peptide forms three disulfide bridges between cysteine residues to form a looped structure which is cleaved by prohormone convertases 1 and 2, resulting in a 51 amino acid mature peptide and the liberation of the middle peptide sequence, referred to as the insulin C-peptide [14]. Insulin exerts its glycemic lowering activity by engaging the Insulin Receptor, signaling through the Insulin Receptor Substrate protein to activate PI3K/AKT signaling [5]. This in turn drives translocation of glucose transporter proteins to the cell membrane, allowing them to increase glucose flux into the cell. Loss of insulin signaling is lethal if left untreated and results in a wasting disease-like state in humans, as was the case before discovery of insulin as a treatment for diabetic patients [15]. Paradoxically this results in

pathologically high levels of circulating blood glucose without glucose uptake in peripheral tissues, resulting in hyperglycemic damage to blood vessels due to a lack of glucose clearance and simultaneous starvation of tissues dependent on insulin signaling for sugar transport and cellular uptake. Conversely, overabundance of insulin signaling is more acutely dangerous than chronic hyperglycemia; insulin-driven drops in blood sugar below safe levels results in starvation of peripheral tissues if glucose is cleared to quickly without available dietary or glycogen-derived glucose from gluconeogenesis to replenish absorbed circulating sugars [10]. Hypoglycemic events occur with some frequency among diabetics that require insulin injections. Most type 1 diabetic patients have experienced multiple hypoglycemic events especially when first learning to manage their disease [10, 16, 17]. Some patients experience difficulty in maintaining normoglycemic throughout their lives, a condition termed “brittle diabetes” , and are considered strong candidates for islet replacement therapy as insulin injection alone is insufficient to maintain normoglycemia [18].

1.3 Overview of Diabetes

Diabetes is a disease of disrupted insulin-stimulated glucose uptake in peripheral tissues and is sub-classified into two types of disease. Type 2 Diabetes (T2D), also known as adult onset diabetes, or insulin-independent diabetes, is the most common form of diabetes worldwide [19]. T2D is driven by an insensitivity to insulin signaling in peripheral tissues, causing hyperglycemic excursions in patients due to the lack of glucose uptake from the blood stream, inhibited β oxidation, and induction of glycogen synthesis [5, 20-24]. This lack of insulin sensitivity is driven by a complex set of factors resulting in decreased insulin receptor downstream signaling [5]. However, as only a fraction of individuals with insulin resistance develop T2D [22, 25], other factors also play a role in determining the risk of developing this disease, including genetic predisposition [26], and possibly starting β cell mass in the pancreas as this varies greatly between individuals [25, 27]. Insulin resistance also drives β cell dysfunction and death over

longer periods of time, due to stress of increased insulin demand and toxicity of chronically elevated glucose and triglycerides in the blood stream [28-30].

While T2D is characterized by the lack of insulin sensitivity and the dysfunction of the islet β cell population, type 1 diabetes (T1D) is an autoimmune disease in which the destruction of β cell mass is driven by autoreactive T cells [31, 32]. Disease risk is determined by a combination of genetic predisposition and environmental factors which are incompletely understood [33]. Genome-wide association studies have identified risk gene variants in human leukocyte antigen (HLA) genes as the major risk alleles associated with the disease [34-36]. Ultimately, immune rejection of the host's β cell mass eliminates endogenous insulin signaling and its regulation of glucose uptake in peripheral tissues. For this reason, T1D is referred to as insulin-dependent diabetes. Pancreatic extracts containing insulin capable of rescuing T1D was first reported in 1922 [15, 37]. Within one year of its original discovery, isolated insulin was used to treat diabetic patients throughout much of North America [37]. The discovery of insulin transformed our understanding and treatment of type 1 diabetes; a gruesome and fatal wasting disease accompanied by paradoxically toxic levels of carbohydrate buildup in blood and treated through a starvation diet became a manageable, chronic disease with insulin replacement therapy.

In both diseases, patients can be treated with synthetic insulin to regulate blood sugar. Type 2 diabetics can also be given other medication to suppress gluconeogenesis from the liver and may require higher doses of insulin to maintain normoglycemia to overcome insulin resistance in peripheral tissues [5]. Chronic hyperglycemia drives long-term damage to endothelial cells, resulting in microvascular complications in diabetes and also damages podocytes and the proximal tubule of the kidney, the glia of the retina, and peripheral nerves [38]. These pathologies caused by prolonged hyperglycemia are secondary to the lack of insulin action in diabetes but drive the most serious co-morbidities of the disease. Worldwide there are 422 million patients

suffering from diabetes as of 2014 [19]. Two years previously there were 2.2 million deaths worldwide caused by high blood sugar and related complications [19].

Recombinant insulin therapy is the only non-surgical method to rapidly control diabetes, either directly injected or as part of an insulin pump system [9]. While exercise and improved diet can reverse disease progression in some T2D patients [5], there is currently no therapy to reverse the course of disease in T1D as there is no way to pharmacologically restore lost mass of pancreatic β cells. Adult β cells are post-mitotic and do not replicate at a significant level to accommodate compensation for increased insulin demand [39, 40]. For this reason, as the pancreatic islet mass is lost, there is very limited capacity to increase insulin output capacity. While there is currently no way to regenerate the endogenous β cell mass in T1D, curative restoration of the β cell population has been achieved in T1D patients using cadaveric islets transplanted into the hepatic portal vein which engraft into the highly vascularized liver; a technique termed the Edmonton Protocol, combining immune suppression and large numbers of cadaveric islets [41, 42]. However, this treatment requires immune-suppression for the rest of the patient's life. For this reason, these transplants are limited to patients already on immunosuppression (often paired with kidney transplant for end stage renal failure) [41-43]. While these patients do achieve insulin independence after transplant, cadaveric islet material is a limiting resource and the obligatory immune-suppression makes this a less-than-ideal regenerative therapy.

1.4 Stem Cell-derived B Cells

It is now well established that replacement of the β cell mass in diabetic patients is sufficient to restore insulin signaling and normoglycemia in human patients using transplanted islet material, though long-term efficacy of transplanted materials may make further transplants necessary to maintain adequate islet function years after transplantation [41, 44, 45]. The scarcity of tissue and need for immune suppression makes stem cell-derived β cells (SC-β cells) an ideal cell-based therapy for T1D patients and possibly for patients with T2D. This approach uses human

pluripotent stem cells, either from human embryonic stem cells (hESCs) derived from the inner cell mass of the early blastocyst or from induced pluripotent stem cells (iPSCs) reprogrammed from adult tissue sources [46-48]. SC-β cells can provide unlimited numbers of differentiated islets and have the potential to be well-tolerated by the immune system either through use of autologous iPS cells reprogrammed from an individual in need of transplant or using genetically modified iPS cells which have been altered to become immune privileged or capable of repelling rejection from the patient's immune system [46]. This approach will be more difficult in T1D patients and may require even more drastic methods to repel the immune system. Other approaches to encapsulate stem cell-derived β cells for transplantation are also being developed; creating an immune-privileged site for the cells to remain and function normally [49]. It appears that engineered devices for immune protection will be the first tested use of SC-β cells in the clinical setting. However, it is of interest to the diabetes field to achieve a gene-edited cell source able to evade immune destruction, as it is not yet known how SC-β cells in an environment without endothelial cells, active blood flow, and innervation will function *in vivo* compared to SC-β cells with this niche after transplant. While these approaches are all under development by different groups, all SC-β technologies will depend on the ability to differentiate pluripotent stem cells into a cell type which is functionally equivalent islets faithfully, reproducibly, and using protocols with high efficacy across different pluripotent cell lines.

SC-β cells also provide a novel platform for disease modeling *ex* vivo. Study of diabetes using animal models has provided tremendous insight into the human diabetic condition and revealed multiple therapeutic targets to improve islet function. However, animal models for a human disease have also given some results that do not accurately reflect *homo sapiens* biology [50]. Some of these differences include the balance of acute versus chronic inflammation found in the diabetic pancreas [51], immunomodulatory regimens that are effective in blocking rodent but not human T1D onset [52], as well as differences in the genes regulating insulin release and glucose

responsiveness in human versus rodent β cells [53, 54]. While the contributions of animal models to diabetes research has been monumental, SC-β cells offer a complimentary approach to disease modeling and drug screening which may prove as valuable moving forward, allowing more studies to begin and end in the human species rather than identifying disease-related mechanisms which must be cross-validated between human and rodent.

Generation of adult-like tissues from human pluripotent stem cell culture has come remarkably far in the twenty years the stem cell community has been able to culture human pluripotent cells *in vitro*. Pluripotent stem cell cultures from rodent models were first established from the inner cell mass of the mouse embryo in 1981 [55, 56]. The identification of conditions required to grow the ICM-derived pluripotent stem cells in humans was some years later [47]. With the ability to culture pluripotent stem cells *in vitro*, less than a decade later a method to reprogram adult differentiated cells back to a pluripotent state was developed [48]. The ability to produce stem cell lines with diabetogenic genotypes from donors with diabetes will facilitate new platforms to study the human disease. Our laboratory and others have used this technique to generate iPS lines from diabetic and non-diabetic donors and differentiating these lines into stem cell-derived β cells (SC-β) cells [57, 58]. While we have made rapid progress toward making mature β-like cells *in vitro*, more work remains to generate SC-β cells indistinguishable from their human pancreatic counterparts.

1.5 Pancreas Development

The pancreas is derived from the endodermal germ layer in the embryo [3, 4]. Signaling from the mesoderm specifies gives rise to anterior/posterior patterns of the forming gut tube, the latter being the embryological origin of the pancreas [59]. Pancreatic buds sprout from the developing gut tube at embryonic day 9.5, induced by VEGF and FGF signaling from the developing notochord, pre-pancreatic mesenchyme, vitelline veins, and the primitive aorta [3, 60, 61]. These two buds are referred to as the dorsal and ventral pancreas, arising on opposite sides

of the gut tube. The dorsal bud develops 12 hours before the ventral structure, with the two buds eventually fusing; dorsal pancreas producing the tail and part of the head of the pancreas with ventral pancreas contributing to part of the pancreatic head only [3]. Endoderm containing the pancreatic buds as well as the surrounding regions capable of generating intestine and stomach are marked by expression of Pancreatic and Duodenal Homeobox 1 (PDX1) [3, 62]. Gut tube regions expressing this marker are capable of producing upper intestine, pancreas, and stomach outgrowths. Specification toward the pancreatic fate is achieved by induction and maintaining expression of the transcription factors, Mnx1, Hnf1β, Gata4, Gata6, and Ptf1a, resulting in pancreatic progenitor cells capable of generating all tissues within the pancreas [3, 63-67].

As the developing pancreas forms a lumen and begins to undergo branching morphogenesis, progenitor cells are localized to the tips of the branching pancreas, maintaining Pdx1 and Ptf1a expression and giving rise to all pancreatic lineages [68]. As the branching pancreas begins to differentiate, pancreatic progenitors either remain a progenitor population and lose expression of Ptf1a and retain Nkx6.1 or the opposite; forming acinar cells retaining Ptf1a but not Nkx6.1 expression [3, 4, 69]. By embryonic day 14.5, acinar fated cells are located at the tips of the branched cords of the pancreas with Nkx6.1-positive progenitor cells located within the trunk of the developing pancreas [68], that will either differentiate to remain part of the ducts or delaminate in order to form the endocrine islet compartment.

The timing of islet endocrine lineage induction is regulated by Notch signaling from the cords of the pancreatic epithelium, which occurs at a significant rate beginning at day E12.5 [3, 4]. This ensures that the progenitor cells within the trunk of the developing pancreas to not exhaust themselves in forming endocrine and duct lineages as the pancreatic mass expands [70]. A subpopulation of pancreatic progenitors begins to produce the Neurogenin3 (NGN3) transcription factor [71], which activates a subset of islet endocrine transcription factors and induces delamination of the $NGN3^{+}$ endocrine progenitors from the pancreatic cords [72, 73]. Induction of

NGN3 expression induces a quiescent state and the balance of transcription factors NEUROD1, ARX, PDX1, PAX4, NKX6.1, and HHEX determine the endocrine fate toward the alpha, β, delta, epsilon, and PP lineages [3, 74-78]. Timing of this induction also appears to bias these NGN3 progenitors toward unique fates, with early NGN3 induction before E12.5 being fated mostly toward alpha cells and E13.5 and onward fated toward β cells [72, 79]. As these cells bud off of the cord and form islets these cells are vascularized and innervated [3, 4]. The mass of β cells after endocrine induction is facilitated through β cell replication at the end of fetal development and early in perinatal life before the β cell re-enters a quiescent state for the majority of its adult life cycle [3, 73]. The regulation of endocrine induction during these steps is required for normal islet function, as reduction in islet formation during embryonic development results in a permanently reduced β cell mass, as β cells are incapable of regenerating substantial mass throughout life [80].

1.6 Differentiation of SC-β Cells

Differentiation of SC-β cells is achieved by recapitulating these processes described using a combination of small molecules and recombinant growth factors to simulate embryonic pancreas specification and differentiation. Our differentiation protocol is defined by six distinct steps of culture beginning with formation of definitive endoderm [81]. This step is achieved by a 72-hour incubation to activate Wnt and TGF-β signaling using a GSK3β inhibitor and recombinant human Activin A [82-85]. These progenitors are immunopositive for SOX17 and lose expression of markers of pluripotency. Definitive endoderm is then exposed to recombinant EGF10 (KGF) for 48 hours to induce foregut endoderm. Clusters are then exposed to stage 3 culture medium for an additional 48 hours which contains high levels of the posteriorizing factor retinoic acid (RA) and an inhibitor of sonic hedgehog (Shh) signaling for 48 hours in addition to KGF [83-87]. These cells efficiently induce expression of PDX1. Reducing RA exposure while maintaining KGF exposure and Shh inhibition for 5 days results in significant NKX6.1 expression, forming a

pancreatic progenitor population similar to bipotent trunk progenitors capable of giving rise to either duct or islet lineages [81, 88, 89]. Maintaining NKX6.1 through these stages is necessary for proper induction of mono-hormonal SC-β cells able to remain insulin-positive after transplantation. PDX1/NKX6.1 co-positive multipotent pancreatic progenitors are capable of generating human islet tissue after prolonged transplantation into the sub-capsular space of the kidney in immune-compromised animals [90], in contrast with polyhormonal cells which appear to resolve into the alpha cell fate and are used as the source of *in vitro* differentiated alpha cells in other protocols developed by other laboratories as well as our own [91]. It was later determined that these cells lack the transcription factor NKX6.1 which is necessary to repress the α cell gene expression profile driven by ARX, resulting in this continued culture in KGF stimulating medium [76, 92]. Our group and others were able to optimize these culture conditions during pancreatic progenitor induction to maintain high levels of Nkx6.1, preventing precocious endocrine differentiation into endocrine-like cells not observed during human development.

Induction of NGN3 and the endocrine lineage *in vitro* is driven by inhibition of notch and Alk5 signaling and exposure to thyroid hormone T3 [81, 89]. Resulting cells from this stage are immune-positive for Nkx6.1 and C-peptide, which we currently use to define the SC-β cells in differentiations. These cells comprise on average between 20 to 30% of the cells in culture [81, 88, 89]. These cells process and package insulin appropriately into secretory vesicles [81]. Maintenance of NKX6.1 expression during this process yields mono-hormonal insulin positive cells after differentiation which are transplantable, in contrast to the polyhormonal cells produced in earlier protocols without NKX6.1 co-expression [84]. These cells are subsequently maintained in factor-free medium without continued exposure to any signaling molecules or growth factors. These cells are stable for more than one month in culture and respond to glucose with increased insulin release compared to basal fastening secretion levels at 2.8 mM Glucose. This final culture

medium is the sixth step of differentiation and resulting cells are used for subsequent analyses or transplantation.

1.7 B Cell Mechanism of Insulin Secretion

The islet β cell secretes insulin to drive uptake of glucose in peripheral tissues [5]. This hormone's effect provides tissue with energy from dietary or liver-derived glucose to sustain cellular function and acts to reduce blood sugar levels which can become toxic to some tissues if chronically elevated, as is observed in the diabetic state. B cells maintain a negative membrane voltage potential of -70 mV, similar to that of neurons [93]. This negative membrane potential is generated through efflux of K^+ ions by ATP-sensitive K^+ channels (K-ATP channels) at the membrane [94]. As cytosolic ATP levels rise due to increased glucose metabolism, increasing the ATP/ADP ratio, these channels undergo conformational changes, inhibiting their K^+ efflux. Loss of K-ATP channel activity causes membrane depolarization of the β cell [54, 94]. This loss of polarization opens T, P/Q, and L-type calcium channels at the cell membrane and ryanodine receptor calcium-sensitive channels at the endoplasmic reticulum [54]. Increased cytosolic calcium concentration facilitates insulin containing granule exocytosis via activating SNARE proteins on these vesicles and at the cell membrane, facilitating docking and exocytosis of the insulin secretory granule's insulin content **(Fig. 1-1A-C)** [95, 96].

Insulin secretion from a healthy islet occurs in a "bi-phasic" secretion pattern, characterized by an acute peak of secretion after 5 minutes of challenge followed by a sustained second phase of release at a lower magnitude that continues until normoglycemic conditions are restored [97-100]. This biphasic pattern of secretion is thought to depend on dynamics of pre-docked, readily-releasable pools of secretory insulin vesicles that accompany the first phase of secretion [54, 93, 96], followed by more centrally localized vesicles that require further priming and reorganization of the β cells' cortical F-actin structure to facilitate exocytosis [101, 102].

Figure 1-1. Glucose stimulated insulin secretion. A) Glucose is transported into the β cell using transporters GLUT1 and GLUT2 in the β cell. **B)** Metabolism of glucose through glycolysis and the TCA cycle results in an increased ATP/ADP cytosolic ratio, inhibiting K^+ efflux from the cell and inducing depolarization. **C)** Depolarization induces opening of Voltage-dependent calcium channels at the cell membrane and Calcium-sensitive channels at the ER. Calcium influx facilitates exocytosis of insulin-containing secretory granules.

Figure 1-1 continued.

A

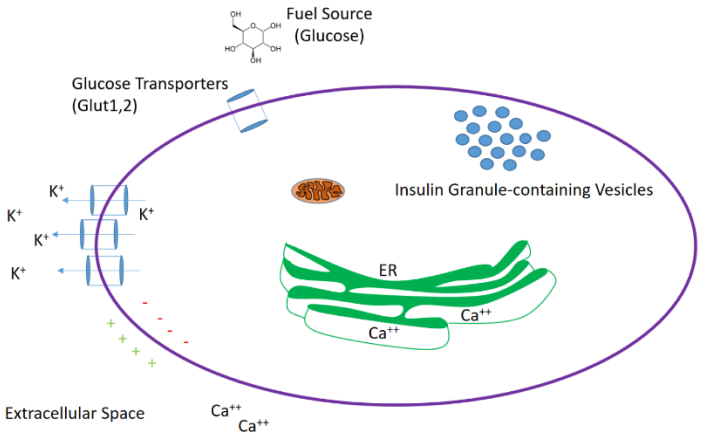

B

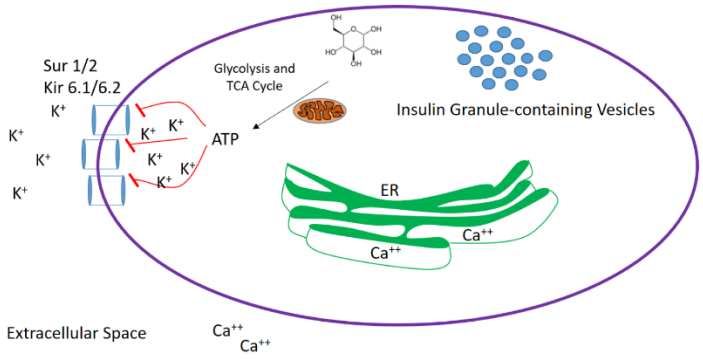

C

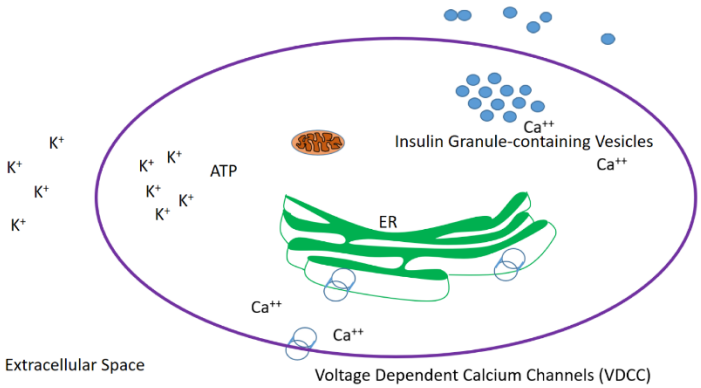

1.8 Functional Analysis of SC-β Cells

Functional insulin secretion analysis of primary and SC-β cells is performed by challenging cell clusters from fasting to fed glucose levels (most commonly 2.8 mM to 16.7 mM) and measuring insulin released into the supernatant during this time [81, 88, 89, 98]. This can either be achieved with a series of static incubations or continuous perfusion to analyze the pattern of insulin release during stimulation [103]. Other methods of analysis include measuring voltage potential changes across the cell membrane using patch-clamping or cell-permeable voltage dyes and live cell calcium flux analysis using calcium affinity dyes or genetically encoded calcium sensors [54]. One challenge in functionally testing SC-β cells is the variable number of insulin-producing cells in each cluster as well as the range of functionality observed in cadaveric human islets after prolonged cold ischemia experienced during procurement and shipping before analysis at other sites. For this reason, the term function with regard to GSIS and SC-β cells has a wide range of values associated with it. Initial reports of SC-β cells demonstrated fold changes of up to 3 after glucose challenge during static incubation in high glucose **(Table 1-1)** [81, 104, 105]. In comparison, rodent islets and insulinoma lines have reported to increase insulin release more than 20-fold after glucose challenge [106, 107]. This more similarly resembles the most healthy, functional human islets tested in the literature [98].

We know that stimulation of SC-β insulin release is lower than that in human islets, but a thorough comparison has not yet been reported to provide more detail on the dynamics of glucose sensing in SC-β cells. In addition to being a source for cell-based therapies for diabetes, SC-β cells offer a significant improvement over human cadaveric islets for disease modeling and drug screening *in vitro*. Proliferation of the endogenous β cell population, which occurs at a much higher rate in rodents than humans [27, 108], is driven by chronic glucose exposure. Glucose sensing also drives hypertrophy of the human islet β population to compensate for increased insulin secretion demand as insulin resistance progresses [25, 27]. Studying replication and other

adaptations to demand for more insulin release will require appropriate glucose sensing in SC-β cells toward identifying novel drivers of β cell replication. Fully functional SC-β cells will be crucial for accurate disease modeling and as a readout for stress-induced dysfunction for T2D and possibly T1D modeling [109]. Stress of continuous hypersecretion of insulin and its mediator, the unfolded protein response will require massive insulin release induced by chronic hyperglycemic conditions for T2D disease modeling and drug screening [110-112]. Without appropriate glucose sensing and correct magnitude of GSIS, this stress will be insufficient for *in vitro* studies. In addition, loss of β cell identity has been used as a way to measure and chronical β cell disease states [113, 114]. The inappropriate or lacking expression of maturity-related genes will also hinder their use as a disease modeling platform if a true unstressed, mature, healthy state is not the starting point in these experiments. Further understanding of maturation-associated gene expression and a better understanding of SC-β cell functionality is paramount to their success both as a research tool using human islet-like tissue as well as a source of islet material for curative cell therapy in T1D.

Table 1-1. Protocol Modifications and GSIS Outcome in SC-β Cells.

Author (Lab)	Year	Functional Assays	Fold-change Insulin Secretion	Protocol Characteristics
D'Amour (Baetge)	2006	Static (sequential)	< 2	Mostly Poly-hormonal
Rezania (Keiffer)	2014	Static (sequential) Dynamic perifusion	< 2 < 2	AXL Inhibitor Increased MAFA
Pagliuca (Melton)	2014	Static (sequential)	~ 2.5	High Nkx6.1 Expression
Nostro (Keller)	2014	Static (sequential)	< 2	High Nkx6.1 Expression
Russ (Hebrok)	2015	Static (sequential)	~ 2	High Nkx6.1 Expression
Yoshihara (Evans)	2016	Static (sequential)	~ 2.5	Lentiviral ERRg Expression
Talavera-Adame (Dafoe)	2016	Static (sequential) Dynamic perifusion	~ 5 < 2	Endothelial cell coculture Increased UCN3
Millman (Melton)	2016	Static (sequential)	< 2	Type 1 Diabetes iPS Cells
Ghazizade (Chen)	2017	Static (sequential)	~ 4	Rho Kinase Inhibition
Velazco-Cruz (Millman)	2018	Static (sequential) Dynamic perifusion	~ 4 ~ 4	Simplified Basal Media
Nair (Hebrok)	2019	Dynamic perifusion	~ 3	Sorted INS::eGFP Cells

[57, 81, 84, 88, 89, 104, 105, 115-118]

1.9 B Cell Metabolism

B cell secretion of insulin is directly coupled to glucose metabolism to ensure appropriate and rapid response to changes in glycemic levels over time [54, 94, 96]. While insulin acts as a growth factor during embryonic and perinatal development [119, 120], its central role throughout life is the maintenance of energy homeostasis in tissues other than the islet. B cells express unique enzymes for glucose metabolism which enable intracellular glucose to act as a cellular rheostat to appropriately couple extracellular glucose levels to the release of insulin [121, 122].

The first step of glucose sensing in the β cell is transport of D-glucose into the intracellular space. While most peripheral tissues express glucose transporters dependent on insulin signaling for their localization to and activity at the plasma membrane, β cells express transporters that function independent of insulin signaling, GLUT-1 and slightly lower levels of GLUT-2 [123, 124]. These transporters are constitutively localized to the plasma membrane and have a low k_m affinity for glucose [123] resulting in significant transport as glycemic levels rise. Both channels ensure constant β cell uptake of glucose, regardless of extracellular glycemic conditions, to facilitate rapid response to changes in glucose levels. Cytoplasmic glucose pools are then freely metabolized, with downstream metabolic flux directly coupled to extracellular blood sugar, causing rapid changes in β cell energetics reflecting real time changes in blood glucose dynamics from fasting to fed states. Initial reports of SC-β cell differentiation indicate appropriate expression of *GLUT1* and *GLUT2* in differentiated cells [81, 104], ensuring physiological glucose transport.

Generation of Glucose-6-phosphate (G6P) is the first rate-limiting step of glycolysis in the β cell. Its generation is dependent on activity of the Hexokinase. Most hexokinase enzymes' (HK1-3) activity are maximal at glucose concentrations less than 2 mM and are inhibited by increased G6P levels in the cytoplasm [125, 126]. In contrast, β cells only express Hexokinase 4, also known as glucokinase (GCK). GCK is different from the rest of the hexokinase family, as it has a lower affinity for glucose, resulting in a higher Michaelis-Menten (K_m) constant of 10 mM (150 mg/dL)

as opposed to sub-1mM Km values of the rest of the HK family [127, 128]. GCK activity is also insensitive to G6P accumulation, allowing sustained enzymatic flux until the extracellular glucose concentration is lowered [126, 127]. Expression of HK4 allows glycolytic flux to occur at physiological glucose levels when insulin becomes necessary. Inappropriately high levels of hexokinase activity at low glucose could result in hypoglycemic episodes as described above. Forced expression of other hexokinase enzymes will cause insulin release at low blood sugar which is detrimental or glycemic regulation [125, 129]. Appropriate expression of both glucose transporters and hexokinases have been confirmed in multiple differentiation protocols including our own to generate SC-β cells, suggesting that the unique characteristics of glucose uptake and initial metabolism are recapitulated *in vitro* [81, 89].

Abnormal metabolic gene expression abrogates the β cell's ability to maintain normoglycemia, and genes which are otherwise ubiquitously expressed outside of the islet but interfere with β cell glucose sensing, are described as "disallowed genes" [121, 122]. These genes regulate activities including lactic acid fermentation and transport activity, fatty acid synthesis and metabolism, as well as lesser understood processes including Galactose Mutarotase which interconverts glucose anomers. Inappropriate expression of disallowed genes can have detrimental outcomes on patients, such as those who inappropriately express lactic acid transporters. This is observed in patients with familial exercise-induced hypoglycemia [130], in which insulin secretion is metabolically dysregulated, resulting in dangerous drops in blood sugar during intense exercise caused by lactic acid production inappropriately stimulating insulin secretion [131].

With glycolytic rate dependent upon extracellular glucose concentration, glucose-derived pyruvate is able to drive oxidative mitochondrial metabolism at a higher rate as the islet β cell is exposed to hyperglycemic conditions [132]. Efficient use of glycolysis-derived pyruvate for oxidative phosphorylation of ADP in the mitochondria is ensured through tight suppression of

disallowed genes in the lactic acid fermentation pathway [121, 122]. ATP production is the initiating step in β cell insulin secretion and depolarization as detailed earlier. The islet is a highly vascularized functional unit within the pancreas and receives a rich supply of oxygen to maintain O_2-consuming oxidative phosphorylation, with ten times the vascular density of the surrounding acinar tissue [6], guaranteeing enough oxygen tension to support mitochondrial activity at all times. SC-β cell mitochondria have not been well-characterized to date, though increased activity has been recorded in several reports after high glucose challenge [104, 105, 133]. The first examination of SC-β cell mitochondrial activity regulating insulin secretion suggests that enrichment of β cell mass after differentiation improves GSIS phenotypes *in vitro,* through improvement of mitochondrial function, as measured by oxygen consumption rate (OCR) [105]. However, this report does not exclude the possibility that OCR profiles improve after eliminating non-SC-β cells and there is no direct mechanism given for reported improvements in mitochondrial activity. Nevertheless, mitochondrial dynamics in SC-β cells may be key toward generating more functional cells *in vitro* and the SC-β field is beginning to focus on this organelle's role in maturing GSIS profiles during differentiation.

In addition to ATP, other signals generated from glucose breakdown are characteristic of and required for functional insulin secretion. Islet mitochondria maintain tremendous spare respiratory capacity to drive oxidative phosphorylation [132]. Continuous mitochondrial activity to drive ATP synthesis from pyruvate requires replenishment of the TCA cycle intermediates, as these metabolites are continuously cycled into and out of the mitochondria and used for biosynthetic processes [134]. A pre-existing pool of oxaloacetate (OAA) to combine with pyruvate-derived Acetyl-coenzyme A must be maintained to produce citrate as the first step of the TCA cycle [135]. Replenishment of these pools is facilitated by a family of processes which drive "reverse" metabolism of carbon chains to refill these pools, a series of processes collectively referred to as anaplerosis [134], balancing continuous loss of TCA cycle metabolites from the

mitochondria, termed cataplerosis. One of the most important cycling reactions in the islet to maintain oxidative phosphorylation and GSIS is pyruvate breakdown to produce oxaloacetate through the enzyme pyruvate carboxylase (PC) [135]. PC is abundant in mice and slightly lower in rats and human islet protein lysates [136, 137], though inhibition of PC activity is able to significantly reduce glucose responsiveness in the islet [138]. Anaplerotic cycling of the islet doesn't just facilitate insulin secretion through ATP generation but also produces secondary signals that are required for GSIS. Oxaloacetate in the mitochondria is also the substrate for mitochondrial phosphoenolpyruvate (PEP) generation from the mitochondrial PEPCK-M enzyme [139]. While cytoplasmic generation of PEP from pyruvate is also a disallowed process in the islet, as it would reverse glycolytic flux and is mostly associated with gluconeogenesis in the liver [139], mitochondrial PEP generation is a necessary step for GSIS, as it acts as a sensor for mitochondrial GTP generation [140]. Other metabolite cycling pathways active in the islet include citrate/isocitrate cycling and malate/pyruvate cycles [135]. Islet β cells have tremendously high levels of these cycles and inhibition of these processes can be detrimental for mitochondrial respiratory capacity and the ability of the islet to undergo maximal GSIS [135]. In fact, glucose stimulated changes in metabolism of the islet more dramatically increase anaplerotic cycles than "forward" TCA cycle reactions [135, 139, 141, 142]. These processes have not yet been examined in SC-β cells in any report to date.

1.10 Other Signals in Insulin Secretion

In addition to direct control over insulin secretion, metabolic amplifying signals are able to fine-tune release of insulin from the β cell. Amplifying pathways converge on cytoplasmic calcium flux in the islet, increasing insulin exocytosis per cell and fortifying cellular insulin content [54, 96]. Metabolic flux in response to high glucose provides ATP as a substrate for adenylate cyclases at the cell membrane, generating cyclic AMP (cAMP) which allosterically activates protein kinase A (PKA) [143]. PKA lowers the ATP threshold of the KATP channels at the cell membrane by

increasing ATP affinity and slows cytoplasmic calcium reuptake [93], increasing β cell insulin secretion magnitude and duration. Increased generation of cAMP is also stimulated by the activity of Glucagon-Like Peptide 1 (GLP-1) signaling through its receptor, GLP1R [144]. GLP-1 signaling activates adenylate cyclase, increasing PKA activity and stimulating Insulin secretion. Long term activity of this signal is also able to increase Insulin synthesis and storage through calcium-stimulated PKC activity. These pathways are therapeutically targetable through the small molecule incretin drugs which act through the GLP1R receptor, either extending the circulating lifetime of GLP1 by inhibiting its degradation by DPP-4 [145], or by mimicking GLP1 and directly stimulating GLP1R [146]. While these signals serve to increase insulin release, their effects are still glucose-dependent. They increase both basal and stimulated insulin secretion in islets, still requiring glucose stimulation for maximal secretion of the insulin hormone. Other ATP-independent signals that can amplify insulin release in the islet include secondary metabolites from glucose metabolism such as reduced NAD(P)H and other intermediate metabolites including malonyl-CoA and glutamate [147-149].

1.11 B Cell Metabolism in Diabetic Dysfunction

B cell glucose sensing underlies the ability to undergo GSIS and regulate glucose homeostasis within the body. In both T1D and T2D, β cell mass decreases over time as cells are either killed by autoimmune destruction or succumb to cell stress induced by compensating for increased insulin demand [27]. Processes regulating islet dysfunction may contribute to both forms of diabetes, as hypersecretion stress underlies β cell death in T2D and manipulating islet stress in T1D can have striking impacts on timing on diabetes onset [150]. In addition, insulitis observed in human T1D is much less acute and occurs at varying speeds throughout the pancreas [51]. As islet mass decreases due to autoimmune destruction the remaining β cells may be under similar hypersecretion stress observed in T2D, though our inability to track loss of islet mass in T1D in humans makes this a difficult hypothesis to test [27]. Insulin secretion profiles in individuals

with impaired fasting glucose levels in T2D show significant loss of acute insulin in the first phase of secretion [151]. This can also be observed *in vitro*, as brief culture of islets in high glucose overnight can raise basal secretion while diminishing glucose-induced rises in insulin release [152]. Prolonged exposure to hyperglycemic conditions also leads to β cell exhaustion and degranulation of the β cell [153], reflecting decreased insulin content. Simultaneously, gene expression profiles of dysfunctional islets appear to revert to a more "immature" state. This includes loss of developmentally activated genes including UCN3, MAFA, and dysregulation of the metabolic sensor FoxO1, inducing nuclear translocation and suppression of islet-specific genes [109, 114]. As gene expression changes during diabetes-induced dysfunction, metabolism in the β cell also becomes dysfunctional. B cells in partial pancreatectomy rats lose expression of GLUT2, GCK, PC, and other enzymes involved in metabolic flux and cycling which may further explain the loss of glucose responsiveness in diabetes [154]. In this same study, disallowed genes including LDH and regulators of lipid metabolism are also up-regulated, suggesting a loss of β cell-specific metabolism tightly controlling insulin release. Prolonged, overstimulated metabolism also induces mitochondrial dysfunction [155]. Mitochondria from diabetic islets exhibit hyperpolarization in some studies [156], which can induce uncoupling protein expression to alleviate this prolonged polarization at the cost of decreased ATP output [155, 157, 158] . Other work has also identified reduced capacity for increased respiration after glucose challenge [159], as well as the overproduction of reactive oxygen species from hyperactivated mitochondria, disrupting normal metabolism [156]. Dysfunction of islet GSIS is tightly linked with metabolism and even protective mechanisms of prolong β cell survival can be detrimental to function.

1.12 Maturation of SC-β cells

Early analysis of the maturity of stem cell-derived β cells revealed that these cells are similar to fetal, immature β cells compared to adult human cadaveric islets [86]. This is still true with regard to newer differentiation protocols as the induction of developmental maturation-

associated genes still remains elusive . As islets mature after birth, GSIS profiles improve, characterized by a sharper threshold for glucose stimulation of Insulin secretion and a higher magnitude of insulin release after glucose challenge [107, 160]. In the mouse this perinatal time period occurs in the first two weeks of development [107, 160-163], correlating with expression of several β cell genes including the transcription factor MafA and a peptide co-secreted with insulin, Ucn3 [107, 160]. The transcription factor MafA drives β cell-specific gene expression [164, 165], and its activation slightly improves GSIS from SC-β cells and activates higher levels of insulin expression [89, 164, 166]. Loss of MafA does slightly reduce functionality in rodent islets but does not fully ablate GSIS [3, 161]. This could in part be due to expression of its paralog MafB, which is redundant in binding sites and nearly identical in peptide sequence. Ucn3 is a secreted peptide involved in paracrine regulation of insulin release, suppressing δ cell release of somatostatin, itself a negative regulator in insulin secretion within the islet [167, 168]. SC-β cells express significantly less of each gene compared to human islets [81, 89, 104, 105]. Following initial reports of glucose responsive SC-β cell generation, multiple groups have also sought to increase expression of these maturation-associated genes with some limited success [116, 166]. The goal of these studies has been to create more functional SC-β cells. Other genes have also been identified correlated with function of islets including *ESRRg, SIX2,* and *SIX3* [116, 169]. Some correlation has been shown with functionality of SC-β cell differentiation and expression of *MAFA* and *ESRRG*, though in both cases glucose responsiveness was not profiled in depth, and in both cases GSIS profiles were similar to other reported protocols without specific activation of either transcript [89, 116].

1.13 Need for Functional SC-β Cells

SC-β cells are an unlimited source of islet-like tissue and may be able to replace or supplement human islet tissue for transplantation in diabetic patients. The ability to build transgenic reporters in SC-β cells may streamline drug discovery for replication and insulin

secretion capacity, and the rates of replication of pluripotent stem cells far surpass human β cell lines [170], making their expansion and use in high-throughput assays much more tractable. However, for cell therapy, disease modeling, and drug discovery potential of SC-β cells to be reached, these cells must be properly glucose-responsive, as insulin secretion and the limited capacity for β cell replication are both glucose-dependent processes [54, 108]. Without the full capacity to sense and response to glucose *in vitro* SC-β cell potential to replace and build upon cadaveric and murine islet sources will be handicapped.

Our ability to derive patient-specific iPSCs will also complement the ability to generate SC-β cells for disease modeling of these complex diseases. Incomplete understanding of the genetics underlying susceptibility to both T1D and T2D makes patient-specific SC-β cell lines the ideal source of human islet tissues to study autoimmune rejection of the islet. We may soon be able to generate complementary immune cells matched to the SC-β cells produced, creating completely *in vitro*, high throughput models of autoimmune β cell rejection which has not yet been accomplished and will provide a groundbreaking new tool to further study human β cell rejection *in vitro*. While disease modeling of T2D may be more straightforward, appropriate glucose and lipid metabolism, sensing and insulin secretion responses will be paramount to building an accurate model to study SC-β cell dysfunction in response to glucose toxicity as well as screen for compounds that can rescue SC-β cells in these stress conditions. As function correlates with health of the islet [45], we may also find that more functional SC-β cells provide a better starting point for T1D autoimmune modeling as these platforms are generated.

1.14 Summary

SC-β cells represent an opportunity to replace and supplement human islets for cell-based therapies in diabetic patients and current human cadaveric and murine islet models of disease and platforms for drug discovery. These cells are currently limited by their physiological response to glucose and capacity to undergo GSIS *in vitro* and we do not yet understand how these cells

perform after transplantation to regulate glycemic levels in diabetic patients. We must now apply our knowledge of islet biology to SC-β cells to better understand their similarities and differences with the human islet to further improve these cells *in vitro* and fully harness their potential in diabetes treatment, disease modeling, and drug discovery.

Chapter 2: Metabolomic Profiling of SC-β Cell Glucose Sensing

Copyright Disclosure:

This chapter is adapted from the following manuscript for submission:

Jeffrey C. Davis, Tiago C. Alves, Aharon Helman, Jonathan C. Chen, Jennifer H. Kenty, Rebecca L. Cardone, David R. Liu, Gordon C. Weir, Susan Bonner-Weir, Richard G. Kibbey, and Douglas A. Melton. "Functionally Mature Glucose Response in Stem Cell-Derived β Cells is Inhibited by a Bottleneck in Glycolysis"

2.1 Introduction

β cells in the pancreatic islets of Langerhans regulate blood sugar levels by secreting the peptide hormone insulin, which then drives glucose uptake in peripheral tissues to preserve normoglycemia [171]. Islets secrete insulin in response to rises in circulating glucose levels by coupling insulin secretion to increased glucose metabolism [54]. Patients lacking sufficient insulin due to the autoimmune destruction of the islet β cell in Type 1 Diabetes (T1D) [51], or due to β cell dysfunction in Type 2 Diabetes (T2D) [5], are treated with administration of exogenous insulin; a lifesaving therapy but one that incompletely recapitulates the functional glycemic control of the islet [9]. Transplantation of human cadaveric islet tissue successfully restores glycemic control in T1D patients, but at a cost of immune suppression to prevent allo-rejection [42, 43]. Transplantation is also limited by a scarcity of healthy islet tissue [172]. Both of these challenges can be solved through the use of SC-β cells in place of cadaveric islets. To fully and safely replace human islets for T1D cell-based therapies, SC-β cells must fully recapitulate the process of glucose stimulated insulin secretion (GSIS) to maintain normoglycemia as well as *bona fide* islets.

Initial reports of differentiating insulin-producing cells from pluripotent stem cells resulted in very little glucose responsiveness [83, 84]. As protocols were developed to produce more functionally mature cells *in vitro*, SC-β cells were shown to undergo successful GSIS responses in multiple publications, reproducibly exhibiting higher secretion of insulin after glucose exposure *in vitro* [81, 88, 89]. Recently reported protocol modifications to improve SC-β cell function have

utilized small molecule screening [118], activated genes up-regulated during development of mature functional islets [116], or improved culture conditions for differentiation [104, 105]. These studies used slightly modified culture media formulations to improve SC-β cell function *in vitro*, but none have achieved a GSIS response equivalent to that of cadaveric islets. In none of these studies has the metabolomic landscape of SC-β cells been fully examined. Thus, we do not understand the relationship between differential gene expression or media modifications and the improvements in GSIS phenotype, nor have we resolved if any of these modifications robustly or stably modify the outcome of SC-β cell glucose responsiveness after transplantation. To approach this level of understanding a more thorough interrogation of the biochemical pathways that couple Insulin secretion to glucose metabolism would be instructive.

In this report, we examine glucose responsiveness in SC-β cells and identify the biochemical processes that may be lacking or deficient, preventing a fully islet-like response to glucose challenge *in vitro*. We demonstrate that SC-β cells are capable of an insulin secretion phenotype *in vitro* that is indistinguishable from fully functional human islets. We report on an unexpected and novel bottleneck in glucose metabolism that limits glucose responsiveness in SC-β cells. The glycolytic "housekeeping" enzyme, GAPDH, exhibits reduced activity in SC-β cells, restricting their GSIS phenotype. Bypassing this bottleneck in glucose sensing fully rescues insulin secretion during nutrient challenge. Correcting this error of metabolism will lead to the generation of fully functional SC-β cells *in vitro*.

2.2 Glucose Stimulated insulin Secretion in Stem Cell-Derived β Cells and Healthy Human Islets

SC-β cells respond to glucose *in vitro* and secrete insulin corresponding to level of glucose challenge [81, 88, 89]. These differentiated clusters contain 20-40% SC-β cells, which are defined by expression of the transcription factor Nkx6.1 and the processed C-peptide fragment of insulin [81], but also contain other endocrine populations including alpha and delta cells at lower frequencies (Veres *et al*, accepted). We analyzed a large cohort (n = 74) of differentiations using

cells with multiple genetic backgrounds, and cadaveric human islets as controls, to establish a more complete record of SC-β cell *in vitro* function. On average, cadaveric human islets display a much larger magnitude of insulin secretion in response to glucose **(Fig. 2-1A)** when compared to SC-β cells **(Fig. 2-1B)**. While different SC-β cell batches exhibit variable glucose responsiveness, compiling data across a wide range of differentiations results in a statistically significant difference in glucose response. Presented as a stimulation index, or fold-change in insulin secretion during glucose challenge, human islet response to glucose challenge is approximately 12-fold higher than basal secretion, whereas SC-β clusters respond with an average of 2.4-fold higher secretion. Notably, the response to membrane depolarization with KCl is not different, indicating that SC-β cells have the capacity for a more complete response. Direct depolarization using 30 mM KCl results in similar magnitudes of maximal insulin release **(Fig. 2-1C, D)** in human islets and SC-β cells of 20-30-fold over basal insulin release. While differing in glucose response, SC-β cells and human islets retain similar overall insulin content **(Fig. 2-1E)**. Dynamic perfusion reveals similar bi-phasic insulin secretion patterns in both cell types, though the magnitude of SC-β response is roughly 10% of that observed in human islets, similar to static incubation **(Fig. 2-1F,G)**. These findings replicate previous reports of a muted insulin secretion in response to glucose challenge with a variety of protocols [57, 81, 88, 89, 104, 105].

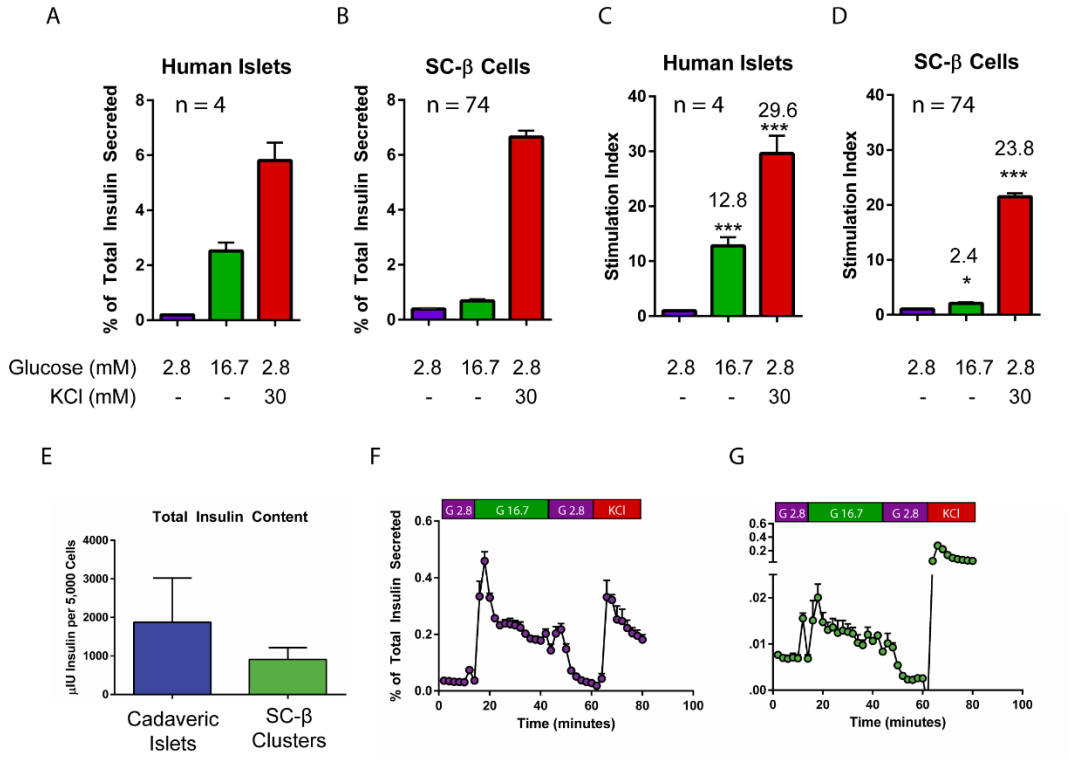

Figure 2-1. Insulin secretion profiles in SC-β cells. A) Glucose response profile of human cadaveric islets and **B)** SC-β cells challenged with low glucose (2.8 mM) high glucose (16.7 mM) or KCl (30 mM) in low glucose buffer for 60 minutes. **C)** Stimulation index of cadaveric islets and **D)** SC-β cells after glucose or KCl challenge. Stimulation indices are indicated above each column. **E)** Total insulin content profile of human cadaveric islets and SC-β cells. **F)** Dynamic perifusion insulin secretion profile of human islets and **G)** SC-β cells. (* $p < 0.01$, *** $p < 0.0001$ using a paired T-Test)

2.3 insulin Secretion Capacity

Because the magnitudes of insulin release after KCl depolarization are similar in human islets and SC-β cells **(Fig. 2-1A,B)**, we asked whether the smaller SC-β GSIS response is due to a deficiency in glucose metabolism to generate ATP-induced depolarization, or the inability of SC-β cells to appropriately undergo membrane depolarization following a glucose challenge. We perifused SC-β clusters and cadaveric human islets with glucose followed by modifiers of KATP channel activity and cAMP/PKA-mediated amplification of insulin release [143]. As expected, human islets responded at similar magnitudes to high glucose and tolbutamide challenge with a return to baseline secretion after diazoxide exposure as has been previously reported [98]. Further exposure to forskolin revealed a significant increase in insulin release in islets **(Fig. 2-2A)**. SC-β cells exhibited a weaker response to glucose than human islets with a slight reduction in insulin release after diazoxide exposure. However, tolbutamide challenge induced a similar magnitude of insulin release to human islets. Further potentiation of insulin release after forskolin exposure also resulted in a similar magnitude of insulin release of 0.1% of insulin content per minute in both cell types **(Fig. 2-2B)**. These results demonstrate that SC-β cell KATP channels are functional and regulate (re)polarization in a time period and magnitude similar to human islets.

2.4 Live Cell Labeling of Zinc Content to Isolate SC-β Cells

Clusters of differentiated SC-β cells are heterogenous [81, 88, 89]. As a result, some physiological measurements of SC-β cells other than insulin secretion require enrichment of the SC-β cell population. We devised a method to isolate SC-β cells using zinc content-based sorting. We use the live cell dye (TSQ) as its excitation/emission spectrum is in the UV/Violet range, allowing for combinations of other more common spectra at longer wavelengths [173]. TSQ^{High} cells are observable by flow cytometry and the size of this population closely resembles the total size of the $insulin^{+}$ population within a differentiation **(Supplemental Fig. I-2A)**. Using this approach, it is possible to enrich the endocrine SC-β population from differentiations in different

pluripotent cell lines as well as human islets **(Supplemental Fig. I-2 B)**. Live cell experiments in this report use both the HUES8 hES and 1016 iPS-derived SC-β cells to allow applicable findings from genetically distinct cell sources using the same differentiation protocol.

2.5 Glucose Uptake and Oxidative Phosphorylation

To investigate glucose metabolism in SC-β cells we first measured their capacity to transport glucose across the cell membrane. Using the fluorescent glucose analog 2-NBDG, flow cytometric analysis of glucose uptake appears similar in the TSQ^{High} population of SC-β cells to that of human islets **(Fig. 2-2C)**. We sorted and reaggregated SC-β cells to quantify glucose metabolism using oxygen consumption rate (OCR) as a live-cell readout of ATP synthesis and observe a glucose-dependent increase in OCR in both human islets and SC-β cells **(Fig. 2-2 D,E)**. In contrast, we observe a difference in maximal OCR capacity after decoupling of the inner mitochondrial membrane using carbonyl cyanide 4-(trifluoromethoxy)phenylhydrazone (FCCP). While human islets maintain a spare respiratory capacity for OCR more than one hour after exposure to FCCP, SC-β cells are unable to maintain fully uncoupled OCR and rapidly lose electron transport chain activity after decoupling. These results suggest the capacity to generate ATP from glucose may underlie differences in SC-β cell and human islet GSIS.

To determine whether SC-β cells have the proper mitochondrial complement for a sustained increase in OCR we quantified mitochondria in SC-β cells and human islets with both flow cytometry using the MitoTracker Green FM dye and real time RT-PCR analysis of mitochondrial mass **(Fig. 2-2F, Supplemental Fig. I-2C)** [174]. In both assays, SC-β cells contain equal or higher amounts of mitochondrial mass per cell compared to human islets. Thus, glucose transport into the cell and mitochondrial mass of SC-β cells are similar to human islets, though SC-β cells may have compromised capacity to maintain maximal respiration.

2.6 ATP-Independent insulin Secretion Pathway

β cell potentiation of insulin also occurs through pathways other than KATP channel-mediated depolarization. This is driven by products of glucose metabolism other than ATP itself and is referred to as the ATP-independent pathway [175]. To assess this process in SC-β cells we perifused SC-β cells or human islets with 100 μM tolbutamide to maintain SC-β cell depolarization in the presence of 2.8 mM glucose. After 20 minutes glucose levels were increased in the presence of constant tolbutamide. In human islets, a significant amount of insulin is released after glucose addition to tolbutamide **(Fig. 2-2G),** as metabolism of glucose further potentiates Insulin release independent of KATP channel activity. In contrast, SC-β cells did not increase insulin secretion **(Fig. 2-2H)**. This supports the hypothesis that glucose metabolism is deficient in SC-β cells, as both KATP-dependent and –independent glucose induced insulin release are diminished in SC-β cells. The metabolism of glucose itself is the process inhibiting full GSIS in SC-β cells.

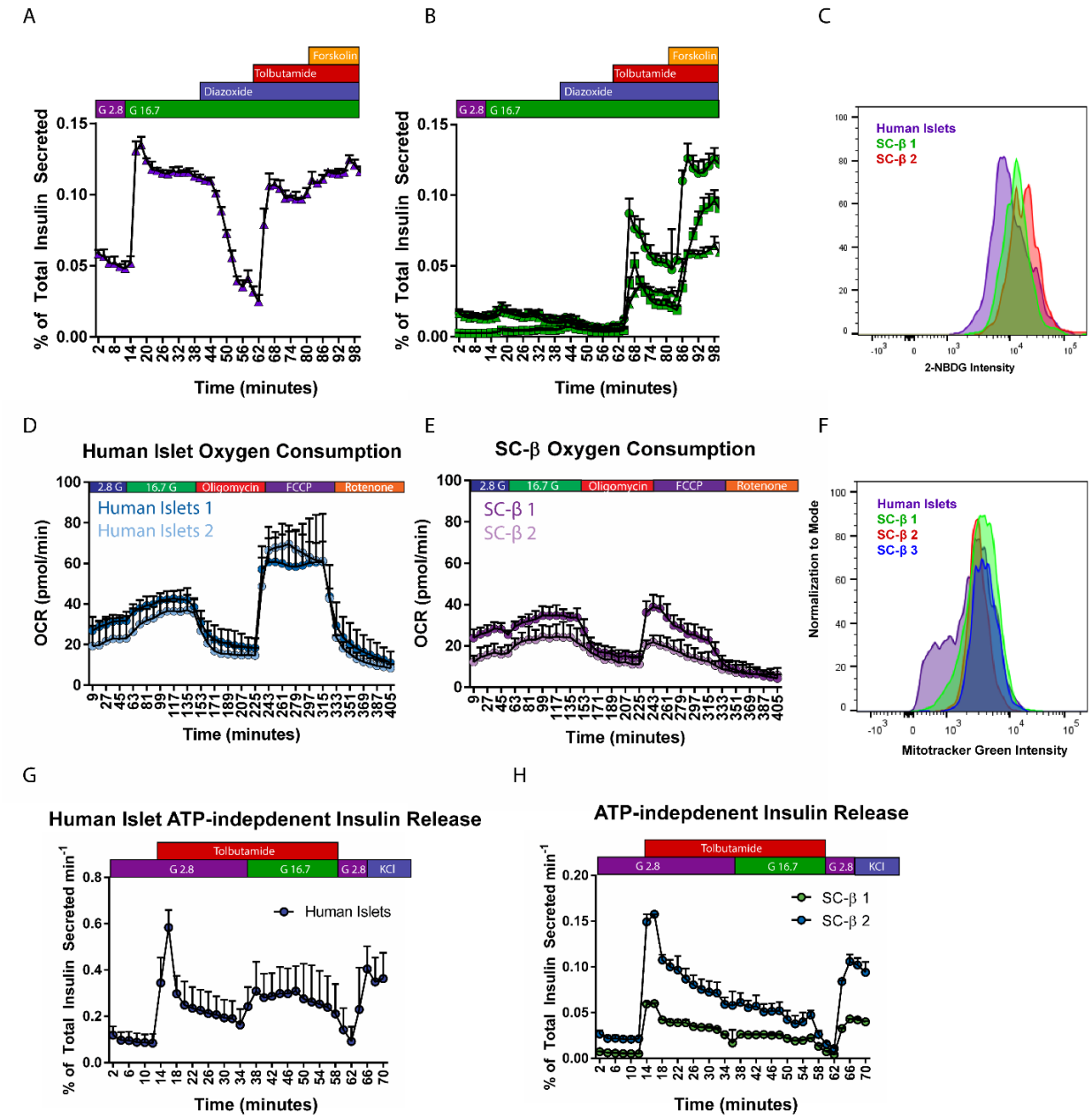

Figure 2-2. Analysis of SC-β cell secretory machinery. A) Dynamic perifusion of human cadaveric islets or **B)** SC-β cells with insulin secretion modifiers. **C)** Uptake of fluorescent glucose analog 2-NBDG after 15-minute incubation in TSQ^{+} cells of human cadaveric islets and SC-β cells. **D)** Oxygen consumption profile of human cadaveric islets and **E)** SC-β cells. **F)** Mitotracker Green dye uptake in human cadaveric islets and SC-β cells. **G)** ATP-independent insulin secretion in dynamic perifusion of human islets or **H)** SC-β cells.

2.7 MIMOSA Metabolomic Analysis

After demonstrating SC-β cells may not be able to metabolize and sense glucose as well as islets, we sought to characterize glucose metabolism in SC-β cells using an unbiased approach. To quantify the metabolism of glucose underlying GSIS we utilized the recently reported Mass Isotopomer Multi Ordinate Spectral Analysis (MIMOSA) technique pairing ^{13}C glucose tracing and mass spectrometry [176] to track flux through glycolysis and the TCA cycle. Utilizing TSQ-enrichment of SC-β cells as described earlier, reaggregates of 5,000 cells were cultured after sorting for 72 hours. Resulting enriched SC-β clusters contained majority SC-β cells in addition to a smaller population of poly-hormonal cells. Clusters comprised of more than half SC-β cells and of this size are similar to the composition of unsorted human islets which were used as controls [6, 50]. Clusters enriched to this level also resemble other recent reports to purify and reaggregate differentiated cells to improve GSIS phenotypes *in vitro* [105]. Cells were incubated in 9 mM glucose and 4 mM glutamine for 3 hours in base DMEM medium to establish steady state metabolism in a stimulatory concentration of glucose before exposure to the same medium with ^{13}C-labeled glucose for time points of 1, 2.5, 5, 15, and 180 minutes **(Fig. 2-3A)**. We chose these conditions because 9 mM glucose is sufficient to induce maximal glucose metabolism and insulin release in mature islets while avoiding induction of glucose detoxification pathways [177], and is the concentration previously established for metabolomic flux analysis in β cells using MIMOSA [176]. 4 mM glutamine also facilitates glucose metabolism and TCA cycle activity without directly stimulating insulin secretion independent of glucose [178]. Analyzing ^{13}C accumulation as a function of atomic percent enrichment (APE), we first quantified enrichment of labeled glycolytic intermediates. Accumulation of ^{13}C in dihydroxyacetone phosphate, glycerol-3-phosphate, and phosphoenolpyruvate (PEP) derived from 2-Phosphoglycerate (PEP M+3) occurred at similar rates over the first 15 minutes of exposure in cadaveric islets and SC-β cells **(Fig. 2-3B-D)**.

2.8 Mitochondrial Metabolism

Major differences in ^{13}C enrichment between SC-β cells and human islets appeared in mitochondrial metabolite pools involved in anaplerosis and cataplerosis. As the TCA cycle produces NADH from pyruvate metabolism, intermediates in the cycle are also used in other processes in the mitochondria and in the cytoplasm [135]. Anaplerosis is the process of "refilling" metabolites of the TCA cycle to sustain mitochondrial metabolism, maintaining a balance between their loss (cataplerosis) for non-metabolic processes and replenishment to sustain TCA cycle activity. ^{13}C accumulation in malate from pyruvate-derived oxaloacetate (Malate M+3) and subsequent PEP derived from oxaloacetate (PEP M+2) was much slower in SC-β cells than human islets **(Fig. 2-3E,F)**. Mitochondria-derived PEP drives GSIS in the islet, and loss of its production is incompatible for successful GSIS [140, 141]. Further examination of PEP levels in SC-β cells revealed that the total PEP metabolite pool derived from both glycolysis and oxaloacetate was also much smaller in SC-β cells than human islets **(Fig. 2-3G)**. Normalizing the calculated PEPCK-M enzymatic activity to the PEP pool size reveals even lower flux PEPCK-M activity when compared to human islets **(Fig. 2-3H)**. Decreased PEPCK-M activity is not due to a lack of its expression, as both PC and PEPCK-M are highly expressed in SC-β cells and human islets **(Fig. 2-3I)**. These reactions ensure sufficient TCA cycle intermediate concentrations to maintain continuous activity within mitochondria. In rodents, PEPCK-M-derived PEP accounts for as much as 40% of the pyruvate pool during high glucose challenge and loss of either PEPCK-M or the GTP-specific isoform of Succinyl CoA-Synthetase (SCS-GTP) abrogates GSIS [140]. This lack of PEPCK-M activity is incompatible with robust GSIS and likely the most significant cause of decreased glucose responsiveness in SC-β cells, both by slowing the TCA cycle and disabling GTP sensing.

2.9 Dilution of ^{13}C signal in Citrate

^{13}C label accumulation in TCA cycle metabolites was similar between SC-β cells and human islets in all pools except for citrate, which had a significantly lower APE in SC-β cells. This lower enrichment indicates that a significant amount of citrate may be excluded from the mitochondria of SC-β cells, as we do not observe dilution of label in the subsequent steps of the TCA cycle **(Fig. 2-3J)**. Mitochondrial PEP and malate are used for antiport with citrate in the cell [140]. The observed decrease in PEP and Malate replenishment might account for the decreased citrate labeling and movement observed in these experiments **(Fig. 2-3K)**. Slowed or inhibited citrate metabolism might also contribute to lower metabolic flux and dampened GSIS driven by a lack of PEPCK-M activity.

Figure 2-3. MIMOSA metabolomic profiling of SC-β cells. A) Outline of experimental protocol for metabolomic profiling using MIMOSA. **B)** Atomic percent enrichment (APE) of ^{13}C in dihydroxyacetone phosphate, **C)** glycerol-3-phosphate, and **D)** phosphoenol pyruvate. **E)** APE of malate (Purple) and PEP M+2 (Green) in human islets and **F)** SC-β cells. **G)** glycerol-3-phosphate and PEP pool size in Human islets (purple) and SC-β clusters (green). **H)** Adjusted PEPCK-M activity to **I)** PEP metabolite pool size. Western blot for Pyruvate carboxylase and PEPCK-M enzyme expression. **J)** APE of ^{13}C in citrate metabolite pool after 180-minute exposure. **K)** Summary of results from MIMOSA metabolomic profiling.

Figure 2-3 continued.

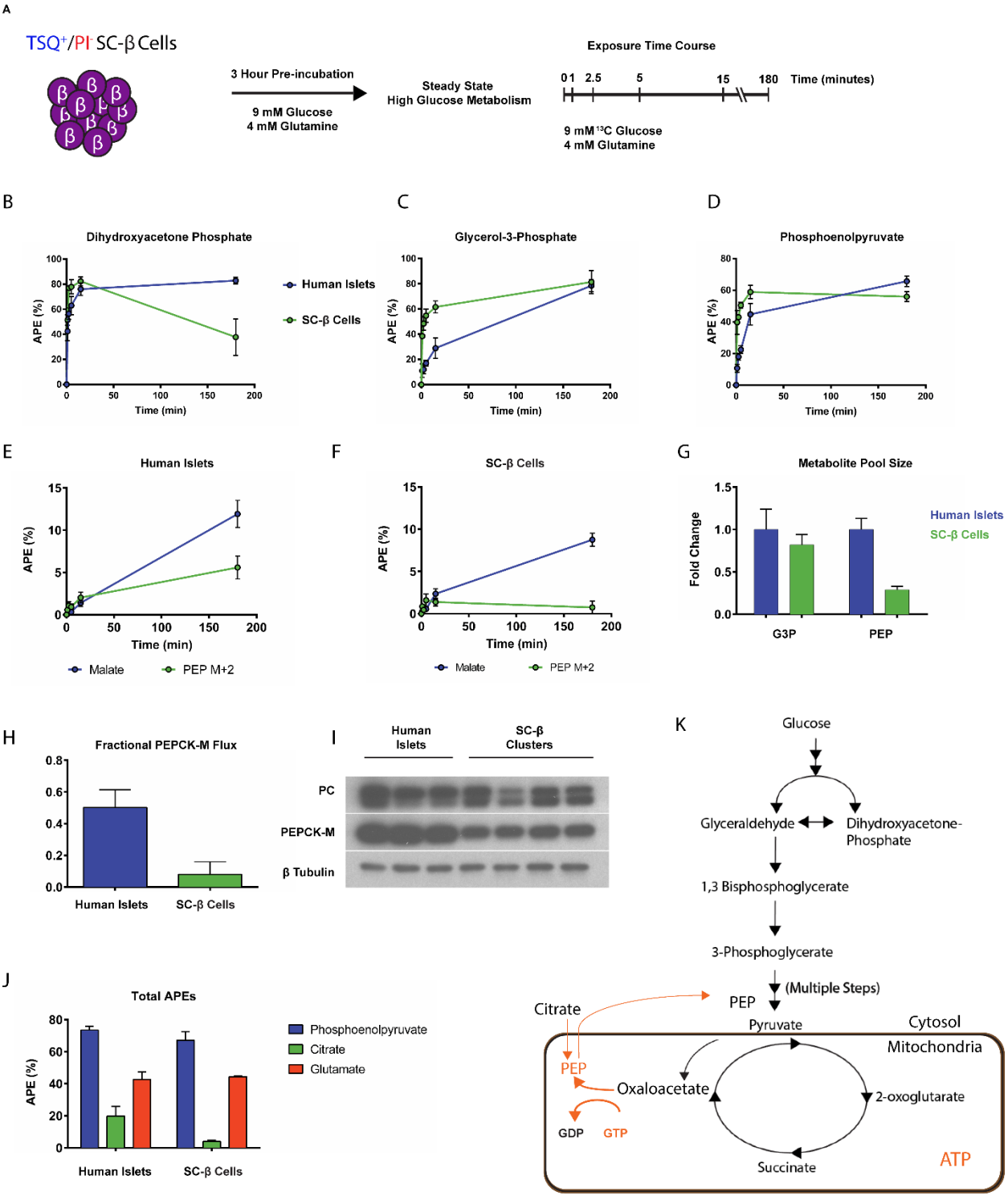

2.10 TCA Cycle Metabolites as Secretagogues

PEPCK-M activity depends on flux of mitochondrial GTP derived from the enzymatic reaction of Succinyl CoA Synthetase (SCS-GTP) [140]. Loss of this enzyme inhibits PEPCK-M activity as GTP is no longer generated from the TCA cycle. Cell-permeable forms of metabolites utilizing methyl ester groups to facilitate diffusion across the membrane have been valuable tool compounds to study effects of specific metabolic intermediates on GSIS [179-181]. We activated PEPCK-M and PEP cycling to drive the TCA cycle by exposing SC-β cells to mono-methyl succinate [181] to ask if stimulating mitochondrial activity could activate PEPCK-M and induce insulin secretion. Strikingly, in contrast to high glucose, methyl succinate exposure resulted in ATP-dependent insulin secretion at the same level as KCl exposure in SC-β cells and human islets **(Fig. 2-4A, Supplementary Fig. I-4A)**. We also probed SC-β response to other TCA cycle metabolites including methyl-pyruvate [180], ketoisocaproic acid [182], and β-hydroxybutyrate **(Fig. 2-4B and Supplementary Fig. I-4B,C)** . In all cases we insulin release at a similar magnitude to KCl positive controls in both SC-β cells and cadaveric islets. These results demonstrate stimulation of the TCA cycle and PEPCK-M activity can successfully achieve islet-like levels of insulin release in SC-β cells. This also confirms that PEPCK-M itself is not inhibited but rather lacking sufficient substrate to generate PEP within the mitochondria.

2.11 A bottleneck in Glycolysis Limits GSIS

Because we were able to induce robust insulin secretion with all mitochondrial substrates tested we worked forward through early glycolysis, using the non-polar metabolites glyceraldehyde and dihydroxyacetone: cell-permeable fuel sources that contribute to metabolism at the steps of glyceraldehyde-3-phosphate and dihydroxyacetone phosphate, respectively **(Fig. 2-4C, Supplementary Fig. I-4C)** [179, 183]. These two intermediates are produced after the six-carbon chain of fructose 1,6 bisphosphate is cleaved into two, 3-carbon chains by aldolase [184]. In both cases we observed no insulin secretion response in SC-β cells at the same magnitude of

high glucose, but full insulin secretion response in cadaveric human islets at the level of KCl. These results support earlier observations of glucose uptake in SC-β cells, as glucose is capable of getting into the SC-β cell but does not fully stimulate insulin release, as bypassing glucose uptake and early processing by GCK does not enhance insulin secretion.

Following these results, we exposed SC-β cells and human islets to glyceric acid, the non-phosphorylated form of 2- and 3-phosphoglycerate and the immediate downstream metabolite from glyceraldehyde-3-phosphate metabolism. Strikingly, SC-β cells secreted insulin at the same magnitude as KCl depolarization, identical to the response observed in cadaveric human islets **(Fig. 2-4D)**. To further validate this result, we also exposed SC-β cells to cell-permeable methylated forms of 2- and 3- phosphoglycerate. These compounds were synthesized in-house as described previously for methyl-2-phosphoglyceric acid [185]. Methyl-2 and methyl-3 phosphoglycerate both stimulated insulin release at a magnitude indistinguishable from KCl challenge **(Fig. 2-4E, Supplementary Fig. I-4D)**. These results demonstrate the ability of SC-β cells to sense and respond to changes in metabolic flux and point to the metabolism of glyceraldehyde-3-phosphate as the defect preventing full GSIS in SC-β cells **(Fig. 2-4F)**.

Figure 2-4. Some cell-permeable intermediates drive insulin secretion in SC-β cells. Intermediate metabolite insulin secretion responses for cadaveric human islets and SC-β cells. **A)** Mono-methyl succinate response profiles in human islets (left) and SC-β cells (right). **B)** Response profiles of methyl-pyruvate, **C)** glyceraldehyde, and **D)** glyceric acid in cadaveric human islets and SC-β cells. **E)** SC-β response to methyl-3-phosphoglyerate (m-3PG). **F)** Schematic representation of metabolite effects on SC-β cell insulin secretion with successful metabolic handing of metabolites in blue and inability to respond in SC-β cells in red.

Figure 2-4 continued.

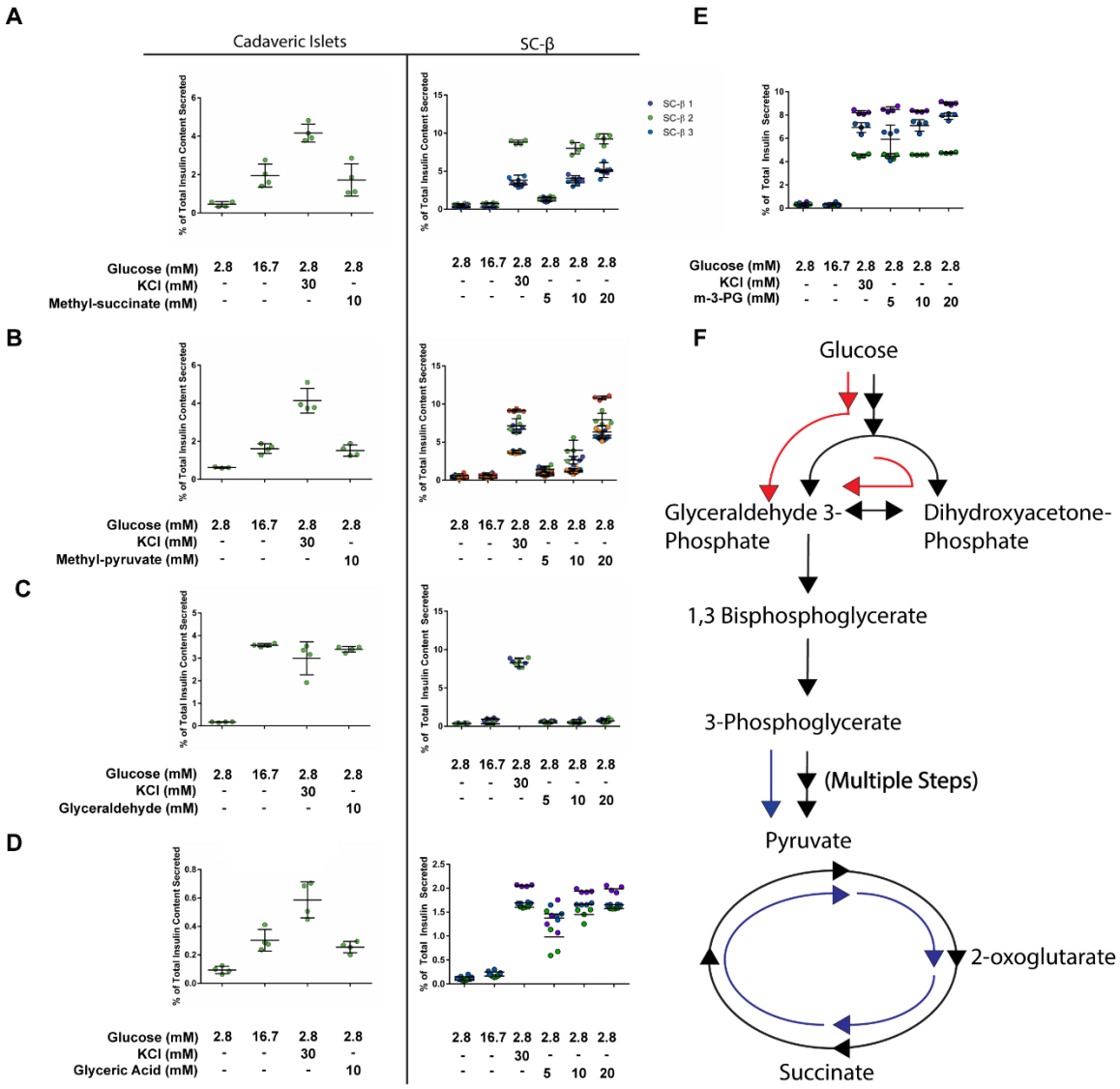

2.12 Insulin Secretion Improves to a Full Response after 3-PG Exposure to SC-β Cells

Glyceric acid and metabolites downstream of the GAPDH/PGK1 axis stimulate insulin release at the level of human islets. To ensure that SC-β cells secrete insulin in an appropriate pattern after exposure to glyceric acid we performed dynamic perifusion of SC-β cells with 10 mM glyceric acid and glyceraldehyde **(Fig. 2-5A)**. Secretion occurred in a bi-phasic manner and exhibited both a first and second phase of insulin release, an activity not previously obtained by any other *in vitro* manipulation of SC-β cells [81, 88, 89, 104, 105]. The peak of first phase of insulin release after glyceric acid challenge matched the magnitude of KCl challenge, in contrast to glyceraldehyde exposure.

We next sought to demonstrate the mechanisms controlling insulin release after exposure to intermediate metabolites. We first demonstrated insulin secretion induced by glyceric acid challenged is induced by its metabolism. Inhibition of ATP Synthase and production of ATP/ADP flux necessary for β cell depolarization using Oligomycin A was sufficient to ablate insulin secretion after glyceric acid challenge in low glucose **(Fig. 2-5B)**. We previously suggested the lack of GSIS is partially caused by a lack of ATP-independent insulin release after glucose challenge in SC-β cells **(Fig. 2-2H)**. This same experiment using glyceric acid robustly induces insulin secretion in the presence of tolbutamide, demonstrating metabolism of 3-PG produces both ATP-dependent and ATP-independent signals that drive GSIS *in vitro* (**Fig. 2-5C)** [175]. We then tested whether insulin secretion is facilitated through cytosolic calcium flux with exposure to glyceric acid. TSQ-sorted and reaggregated SC-β cells were immobilized in matrigel and exposed to the live cell cytosolic calcium indicator Fluo-4. Clusters were imaged for 5 minutes before and after challenge with 16.7 mM glucose, 30 mM KCl, or 10 mM m-3PG. **(Fig. 2-5D-F)**. As expected, SC-β cells demonstrated a smaller calcium flux in glucose compared to that of KCl challenge. In contrast, we observed a significant calcium flux after exposing SC-β cells to m-3PG. Calcium fluxes propagated as waves across SC-β clusters after m-3PG, suggesting SC-β clusters formed

interconnected organoids after enrichment and re-aggregation, which may underlie improvements in GSIS after reaggregation reported recently **(Supplemental Movie files 2-5A-C)**.

Figure 2-5. Metabolic stimulation of glycolysis drives physiological insulin secretion in SC-β cells. A) Dynamic perifusion of SC-β cells with 10 mM glyceric acid (green) or 10 mM glyceraldehyde (purple). **B)** Insulin secretion is stimulated by glyceric acid and its effect is ablated by inhibition of ATP Synthase using Oligomycin A. **C)** ATP-independent insulin secretion is also stimulated in SC-β cells after bypassing GAPDH activity. **D)** Calcium flux in TSQ-enriched SC-β cells after high glucose, **E)** low glucose with 30 mM KCl, or **F)** 10 mM 3-PG. **G)** Images from Fluo-4 signal during fasting (top row) and 20 seconds after exposure with the indicated KRB solution (bottom row).

Figure 2-5 continued.

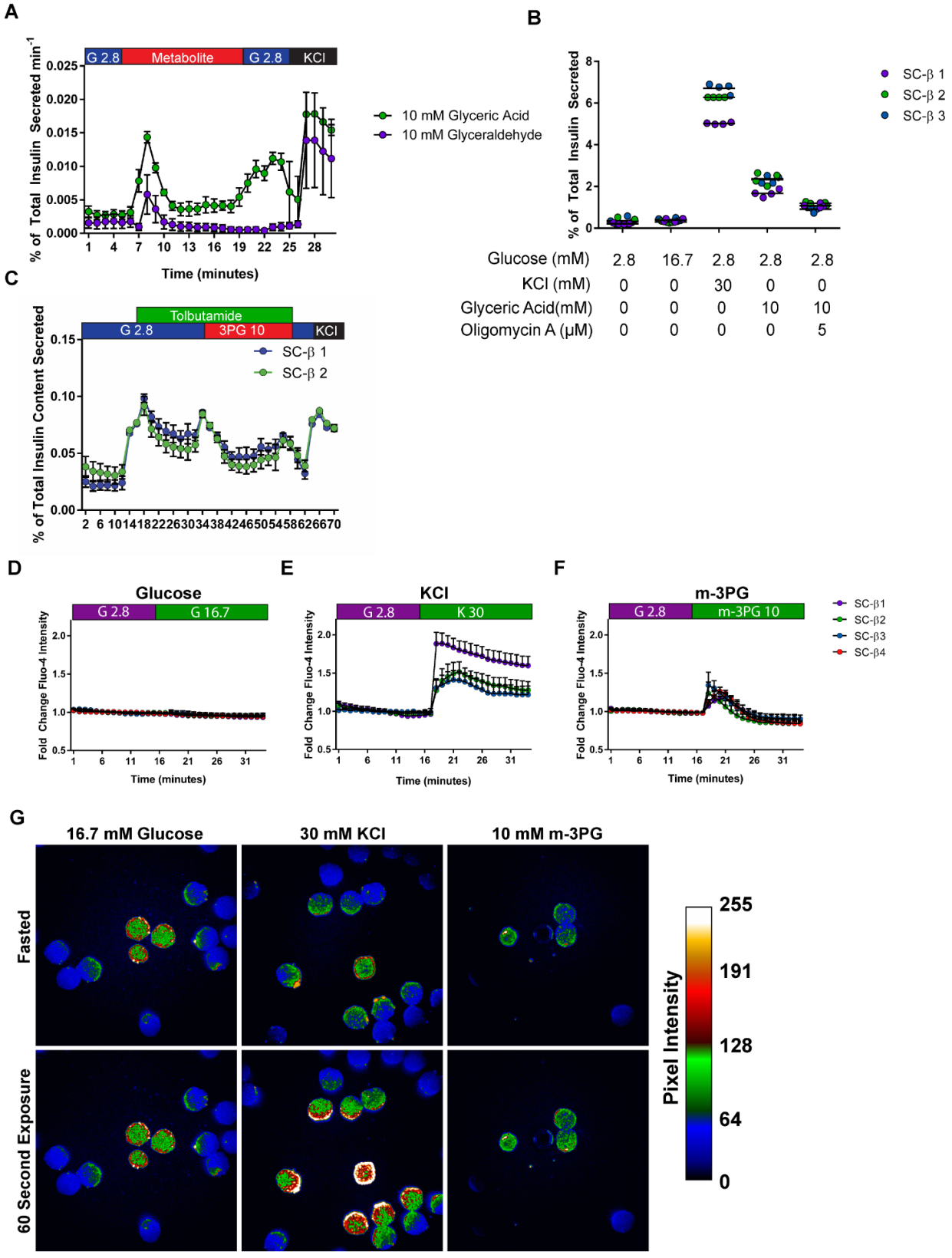

2.13 GAPDH Activity is Reduced in SC-β Cells

These results show that bypassing the GAPDH/PGK1 enzymatic complex results in full insulin secretion, to the same magnitude as the positive control KCl and observed in healthy human islets. Both GAPDH and PGK1 proteins are expressed at identical levels between SC-β cells and human islets, suggesting the inhibition of this enzymatic complex is not due to a lack of enzyme expression **(Fig. 2-6A)**. GAPDH is known to act in a tetramer composed of two dimers which loosely associate with PGK1 [186, 187], converting glyceraldehyde-3-phosphate to 3-phosphoglycerate through its short-lived, unstable 1,3 bisphosphoglycerate intermediate. Human islets, undifferentiated pluripotent stem cells (hES), and SC-β cells were briefly exposed to the cell-permeable protein cross-linking agent disuccinimidyl suberate (DSS) and lysates were analyzed by western blot. Islets and hES cell lysates contained active GAPDH multimers which were present at much lower levels in differentiated SC-β cells **(Fig. 2-6B)**. Lysates from the same cell types were collected and tested for GAPDH enzymatic activity. In agreement with the loss of GAPDH active dimer/tetramer conformation, GAPDH enzymatic activity was less than half of that of hES and cadaveric human islets **(Fig. 2-6C)**.

Cells were collected at various timepoints during the six-step differentiation protocol to determine when the active form of GAPDH is lost. The results suggest that the active GAPDH tetramer is in decline early in the differentiation protocol, after induction of definitive endoderm (stage 2) and is further diminished in the following stages **(Fig. 2-6D)**. GAPDH inhibition has also been reported to occur simultaneously with its translocation to the nucleus in some contexts of cell stress and glucotoxicity in the retina. We analyzed GAPDH localization throughout differentiation to determine if loss of GAPDH functional dimerization is accompanied by changes in its cellular compartmentalization. Strikingly, GAPDH localization became nuclear in a significant fraction of SC-β cells after induction of insulin expression **(Fig. 2-6E,F, Supplementary Fig. I-6A)**. However, this timing does not appear to correspond with the loss of functional GAPDH

dimerization, though it does suggest GAPDH may be actively modified or regulated during the process of pancreatic differentiation *in vitro*. We and others have determined that omitting serum from culture medium when differentiating SC-β cells improves GSIS profiles [104]. We determined that improved GSIS profiles with removal of serum from culture medium does affect GAPDH dimerization *in vitro* at a detectable level **(Supplementary Fig. I-6B,C)**.

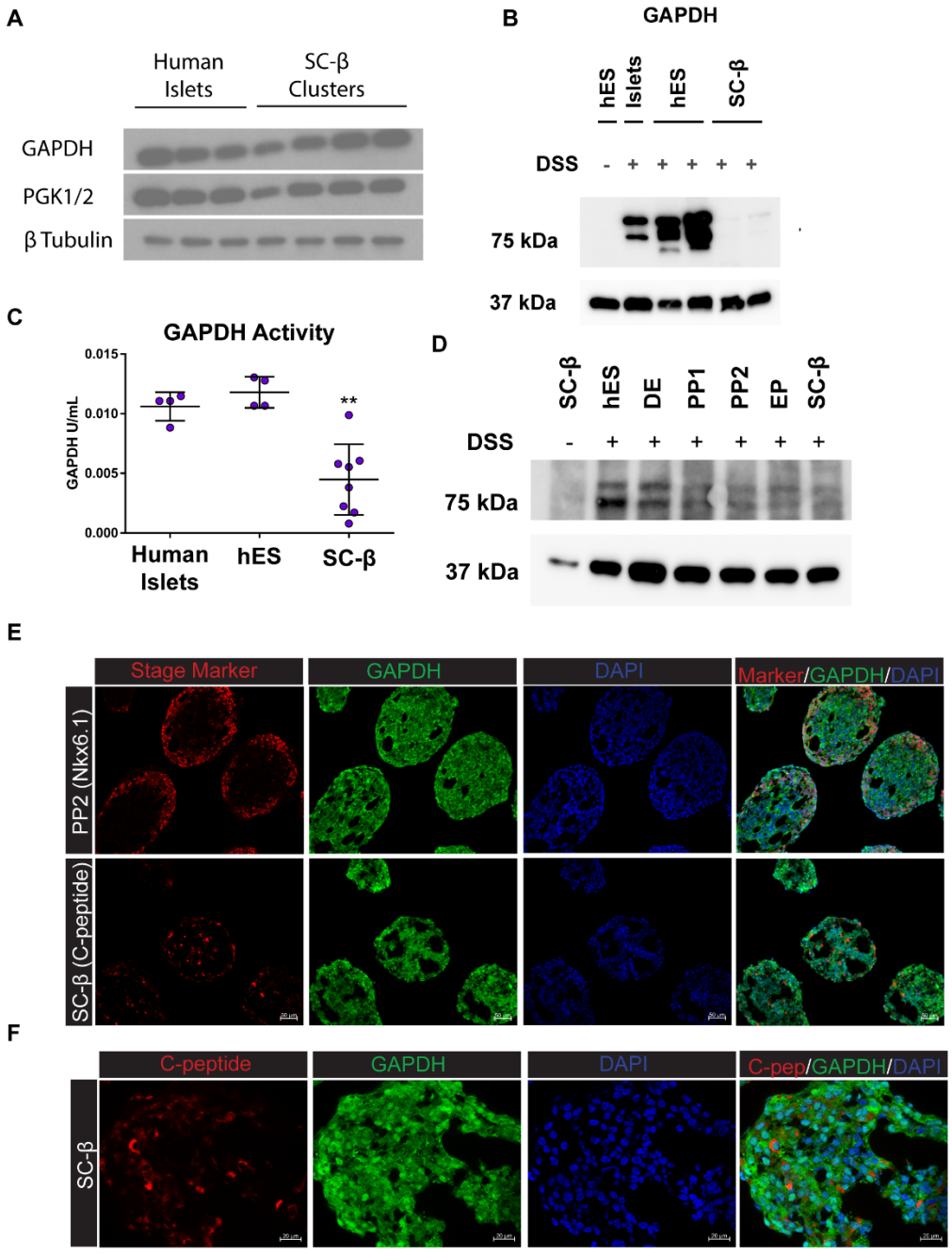

Figure 2-6. Activity of GAPDH is perturbed in SC-β cells. A) Western blot of lysates from differentiated SC-β cells and human islets for GAPDH and PGK1. **B)** Lysates from DSS-crosslinking in primary islets, hES cells and differentiated SC-β cells. **C)** GAPDH enzyme activity in human islets, hES cells, and differentiated SC-β cells. **D)** Western blot of lysates from DSS-crosslinked samples at each step of SC-β cell differentiation. **E)** Immunofluorescence images of GAPDH localization before and after endocrine induction in SC-β cells. **F)** Higher magnification of SC-β cell cluster GAPDH localization. (** indicates $p < 0.005$ using a paired T-test.)

2.14 GAPDH Localization in Primary Islets

Correlation with changes in subcellular localization of GAPDH during stem cell differentiation *in vitro* led us to ask whether changes in the active forms of GAPDH are also found *in vivo*. Surprisingly, we observed mixed localization between the nucleus and cytoplasmic compartments in normal mouse, rat, and human islets **(Fig. 2-7A)**. GAPDH localization to the nucleus has also been reported to occur in the retina of diabetic mice [188-196]. we analyzed pancreatic islets from diabetic rats 4 weeks after partial pancreatectomy or sham surgeries. We did not observe an increase in nuclear GAPDH in insulin-expressing cells after onset of hyperglycemia **(Fig. 2-7B)**. The nuclear translocation and enzymatic inhibition of GAPDH has been reported to occur through post-translational modifications near the GAPDH active site including Lysine Acetylation and S-nitrosylation of cysteine [188, 190, 197, 198]. We performed mass spectrometry on GAPDH immunoprecipitated from islets of healthy donors and SC-β cells **(Supplementary Fig. I-7A-C)**. These modifications were detected at low abundance in SC-β cells and human islets alike, suggesting that enzymatic inhibition of GAPDH in SC-β cells and its nuclear translocation is not mediated by mechanisms described in the retina or apoptosis in stressed cell lines through Lysine acetylation or cysteine S-nitrosylation. The timing of nuclear translocation in SC-β differentiations occurs much later than the observed loss of tetrameric GAPDH. However, due to the surprising nature of this localization pattern we asked whether GAPDH is localized to the nucleus at the time of endocrine induction in the mouse pancreas, as we observe GAPDH at the onset of endocrine differentiation. We were able to find insulin-expressing cells with both nuclear and cytoplasmic GAPDH at this time point **(Fig. 7-C)**.

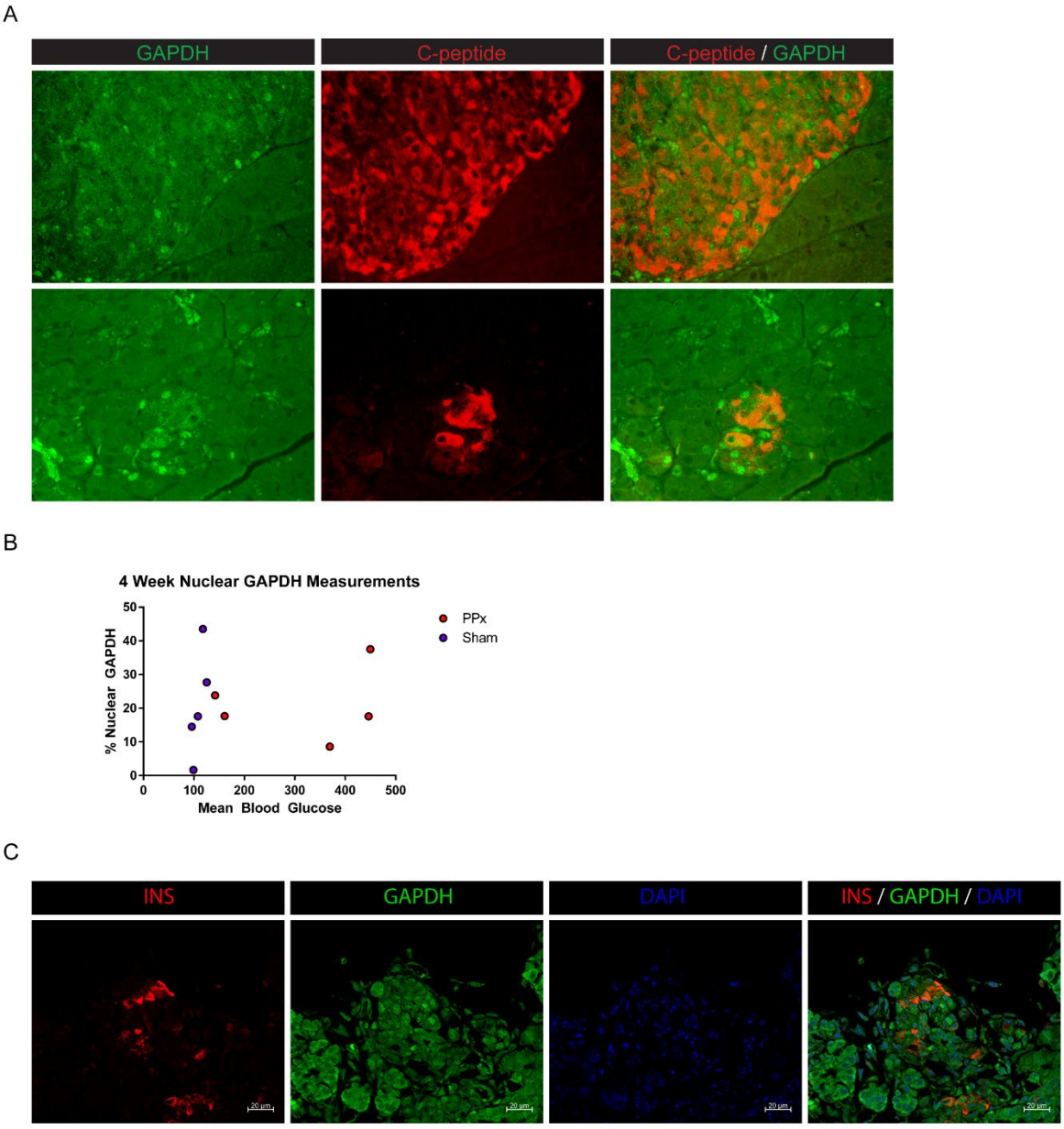

Figure 2-7. Localization of GAPDH in Primary Islets. A) GAPDH localization in healthy rat pancreata after sham surgery. **B)** Quantification of nuclear GAPDH in sham and partial pancreatectomy (PPX) rats 4 weeks after surgery plotted against resting blood glucose levels. **C)** Immunofluorescence for GAPDH in pancreata of mice at embryonic day 15.

2.15 Discussion

Insulin secretory capacity is an essential characteristic of the islet and has rightfully been profiled in nearly all reports of insulin-producing cells differentiated from stem cells. While this process has been characterized during *in vivo* development and in adult human islets, reports of SC-β cell glucose sensing and regulation of insulin secretion do not achieve the magnitude or quantitative levels found in their *in vivo* islet counterparts. We demonstrate here that the insulin secretion capacity of SC-β cells is very similar to healthy human islets. SC-β cells have the ability to regulate de- and re-polarization, releasing more than 10% of their insulin content over 60 minutes after direct depolarization with KCl or by manipulating KATP channel activity. This indicates that the muted ability of SC-β cells to secrete insulin in response to glucose is a metabolic failure, not a defect in the cell's secretory machinery. Furthermore, maximal insulin release after challenge with metabolic intermediates in both human islets and SC-β cells occurs at a similar magnitude to KCl.

Recent publications toward physiological glucose sensing in SC-β cells have sought to understand how changes in culture and differentiation conditions affect the GSIS phenotype *in vitro*. These experiments hint at improved glucose metabolism and have even pointed to mitochondrial activity as a component of improved *in vitro* function [105], but to date a direct mechanism for improved function has remained elusive. Our approach to measure and compare glucose metabolic flux in SC-β cells to human islets revealed a lack of PEPCK-M activity in differentiated cells. Slow TCA cycle flux slows this reaction which can be rescued by using cell-permeable metabolites. This slowed PEPCK-M activity prevents a necessary mitochondrial GTP sensing mechanism from coupling increased glucose metabolism to PEP cycling; a process which has only recently been described as an obligate component of β cell glucose responsiveness [139-141]. Increased cytosolic ATP/ADP ratios derived from oxidative phosphorylation are the dogmatic signal derived from mitochondrial activity in high glucose conditions that drive

depolarization and insulin release, and this flux is unquestionably important as loss of mitochondrial activity abrogates GSIS in the islet. This work reminds us that other signals derived from the mitochondria also play fundamental roles in the GSIS mechanism and also require our attention as we study and fine-tune glucose response in SC-β cells toward the most functionally mature, differentiated cells attainable outside of the body.

GAPDH regulation of glucose metabolism is not a well-studied topic. Other glycolytic enzymes including Fructose 1,6-bisphosphatase and hexokinase are more commonly regarded as regulators of cytoplasmic metabolism [199]. The islet β cell has unique metabolic properties, down-regulating enzymes nearly ubiquitously expressed in other tissues and expressing other glycolytic enzymes that play a more regulatory role than in other tissues [121, 122], such as Glucokinase with an uncharacteristically high k_m and agnostic to rises in glucose-6-phosphate [128, 200], as well as increased expression of G6PC2 which further regulates the first glycolytic intermediate pool of the β cell [201]. It may well be that GAPDH also plays a more central role in regulating β cell metabolism than other tissues. Glycolytic enzyme “moonlighting” has also become more appreciated in the last decade, with multiple enzymes playing non-metabolic roles in other cellular compartments [202-204]; GAPDH is also among this list with roles in cell biology ranging from transcriptional regulation to endocytic cycling to apoptosis. The metabolically coupled β cell may also be using GAPDH in yet unexplored mechanisms to regulate functional activity and further link glucose metabolism with β cell physiology. GAPDH has already been implicated in diabetic dysfunction of the retinal glia [189, 192]; it is possible different PTMs or binding partners in the β cell are changing its function through mechanisms not yet observed in the islet.

SC-β cell *in vitro* physiology is also important for use of SC-β cells in screening platforms toward discovery of new insulinotropic factors and compounds to stimulate β cell proliferation. Insulin secretion as well as replication are dependent upon and stimulated by glucose sensing

[108]. To produce the most translatable results from these cells, improved glucose sensing will recapitulate an important aspect of β cell physiology and life cycle. Our findings may suggest metabolic intermediates can recapitulate some aspects of β cell physiology and could be used with current protocols to stimulate glucose-induced proliferation, glucotoxicity, or insulin secretion toward discovery of new anti-diabetes therapies.

Bypassing GAPDH activity using cell-permeable metabolites results in bi-phasic insulin release including a second phase of secretion which has not been previously observed in stem cell-derived β cells. In addition, both the magnitude and fold-change of insulin secretion in both the first and second phases of release is equal to that of a KCl challenge. This is important, as it demonstrates that metabolizable substrates for SC-β cells produce insulin release at the level of healthy islets and that their capacity to sense metabolic flux is intact. SC-β cell GSIS is limited by a bottleneck in metabolism of glucose itself that is not yet fully functional in SC-β cells. Protocols to achieve physiological GSIS must solve this deficiency, determining what is inhibiting the GAPDH enzymatic complex in these cells and how this process can be manipulated toward more glucose responsive SC-β cells *in vitro*.

Chapter 3: *in vivo* Maturation of SC-β Cells

Copyright Disclosure

Portions of this Chapter are adopted from the following publication in preparation for submission:

Jeffrey C. Davis and Maria Ryaboshapkina, Aharon Helman, Edwin Rosado-Olivieri, Suraj Menon, Mårten Hammar, Björn Tyrberg, and Douglas A. Melton. "Mechanisms Governing SC-β Cell Maturation *in vivo*"

3.1 Introduction

The current standard of therapy for T1D patients is insulin replacement therapy, delivered either via injection through syringe or a subdermal pump device. While the discovery and use of insulin has transformed diabetes from a fatal wasting syndrome to a manageable chronic disease, long-term morbidity due to incomplete glycemic control still results in patients suffering from increased rates of diabetic nephropathy (25.9%), neuropathy (18.0%), and cardiovascular disease (22.3%) among other complications [205]. A more complete and physiological control of glycemic level has been achieved by transplanting human cadaveric islets in patients with "brittle diabetes," characterized by poor control of sugar levels with insulin injections and high risk of hypoglycemic episodes with insulin therapy [42]. The transplantation of human cadaveric islets into the hepatic portal vein using a glucocorticoid-free immunosuppressive regimen, termed the "Edmonton Protocol", has resulted in insulin independence in patients since its initial report in 2000 with minimal hypoglycemic episodes and excellent glycemic control [43]. The initial report demonstrated efficacious islet function 12 months after transplantation and later follow-up studies reported similar results. To date, little is known about the processes maintaining islet function after transplant. Remodeling of the graft's niche and interactive signals to and from the islet must be necessary to maintain function in transplanted islets, as cadaveric islets are not stable during long term culture *in vitro* [206]. Transplantation of islet tissue is also known to improve function and health in dysfunctional tissues, as our laboratory has previously demonstrated that islets that

have lost functionally mature status *in vitro* after prolonged culture can be rescued and mature islet gene expression markers rescued after transplantation under the kidney capsule for several weeks [114]. Transplantation of stem cell-derived β (SC-β) cells has also been demonstrated to mature differentiated cell types [92, 107]. Initial reports of insulin-producing cells from stem cells were achieved through transplantation of pancreatic progenitor cell types which underwent differentiation into β-like cells *in vivo* after 16 weeks [83]. We have also demonstrated that expression of mature islet gene expression, which has not yet been achieved through *in vitro* differentiation alone, is induced after transplantation [107].

For stem cell-derived β cells to replace human islets as a cell therapy for diabetes, we need to understand much more about the process of transplantation and engraftment that regulate long-term survival, and which may affect functionality in a positive or negative way. We have previously reported that SC-β cells continue to function after transplantation [81], and we and others have observed that SC-β cell functionality is improved after transplantation [105], though we do not understand what processes regulate this improved GSIS phenotype. It is possible that these processes guide developmental maturation pathways which have not yet been activated *in vitro*, as we have previously reported that SC-β cells are more similar to fetal than adult human islets. Improvements in our differentiation protocol have yielded cells more similar to human islets, but the lack of full GSIS response *in vitro* suggests that other processes may still be missing from these protocols that are induced during maturation *in vivo*. The genes we and others have identified as missing in SC-β cells are developmentally regulated and linked to functional GSIS. These genes include expression of MAFA and UCN3, which are up-regulated during perinatal islet development as GSIS responsiveness improves [107, 160], and are also up-regulated when dysfunctional islets are transplanted under the kidney capsule of healthy mice [114]. As diabetic islets become dysfunctional, they de-differentiate, losing expression of markers of maturity in the adult islet that regulate islet function [109, 114, 207]. Understanding the

processes driving SC-β cell maturation *in vivo* may contribute to protocols yielding more reproducibly functional SC-β cells *in vitro* with a more robust response to glucose without the need for transplantation. These studies may also shed light on signals that maintain islet healthy lost in diabetes but restored after transplant into the kidney.

Transplantation of SC-β cells exposes them for the first time to a niche containing endothelial, neuronal, and mesenchymal signaling. Endothelial cell signaling to islets is necessary for normal islet development and a high degree of vascularization is a hallmark of pancreatic islets [60, 208-210]. Islets are also regulated by the sympathetic nervous system, as insulin release is suppressed by epinephrine and activated upon feeding by the parasympathetic nervous system [8, 211, 212]. Mesenchyme is less well-understood in adult islet biology, though early pancreatic mesenchyme is able to maintain proliferation of islet pancreatic progenitors *in vitro* [213], and recent reports indicate mesenchymal interactions with the islet may regulate islet function [214-216]. Our laboratory has demonstrated that allowing pancreatic progenitors to mature *in vivo* induces expression of UCN3, a maturation-associated gene not currently induced during *in vitro* differentiation [107]. This same marker is lost in diabetes but rescued after transplant in healthy mice [114]. Transplantation into the kidney capsule niche facilitates signaling pathways that can induce functionally mature gene expression after transplantation. This may also be true in differentiated SC-β cells. Here we have profiled gene expression associated with *in vivo* maturation of SC-β cells as GSIS profiles of transplanted cells improve over time, identifying several potential markers of maturing SC-β cells, including Islet Amyloid Polypeptide (IAPP).

Using co-expression network analysis, we have also identified several signaling pathways that are up-regulated after transplantation that correlate with islet function in publicly available datasets. Manipulating these pathways had a modest effect on GSIS *in vitro* and identifies several genes that may be drivers of the *in vivo* maturation process that warrant further study in SC-β cells.

3.2 In vivo Maturation of SC-β Cells

We sought to profile changes in transcription which accompany improved functionality of SC-β cells after maturation *in vivo*. To accomplish this, we differentiated a constitutive eGFP-expressing induced pluripotent stem (iPS) cell line 1016 using the protocol developed by our laboratory [81]. This line generated SC-β cells with an average efficiency of 15% Nkx6.1/C-peptide co-positive cells (**Fig. 3-1A**, **Supplemental Fig. II-1A**). Glucose responsiveness *in vitro* was profiled using dynamic perfusion and revealed a limited secretion response at differentiation stage 6 and robust insulin secretion response after KCl challenge (**Fig. 3-1B, Supplemental Fig. II-1B**), similar to previous reports from our and other laboratories [81, 89]. Differentiated SC-β cells were transplanted under the kidney capsule of immune-compromised SCID-Beige mice for a duration of 6 weeks to facilitate maturation of the grafts. Transplants were functionally monitored by measuring human serum Insulin after overnight fast and 30 minutes after an intraperitoneal injection of glucose. To score graft function, we quantified the stimulation index, or fold-change in insulin secretion after glucose injection, 2, 4, and 6 weeks after surgery **(Fig. 3-1C, Supplemental Fig. II-1C**). Stimulation indices rose on average over the course of transplantation, but significant heterogeneity was observed between animals. *In vitro* functional analysis revealed that SC-β cells were not fully induced to secrete insulin in response to glucose in contrast to KCl challenge. Analysis of basal and stimulated insulin release revealed that functional maturation *in vivo* was governed by increased Insulin release after challenge rather than reduced basal secretion at fasting (**Fig 3-1D,E**).

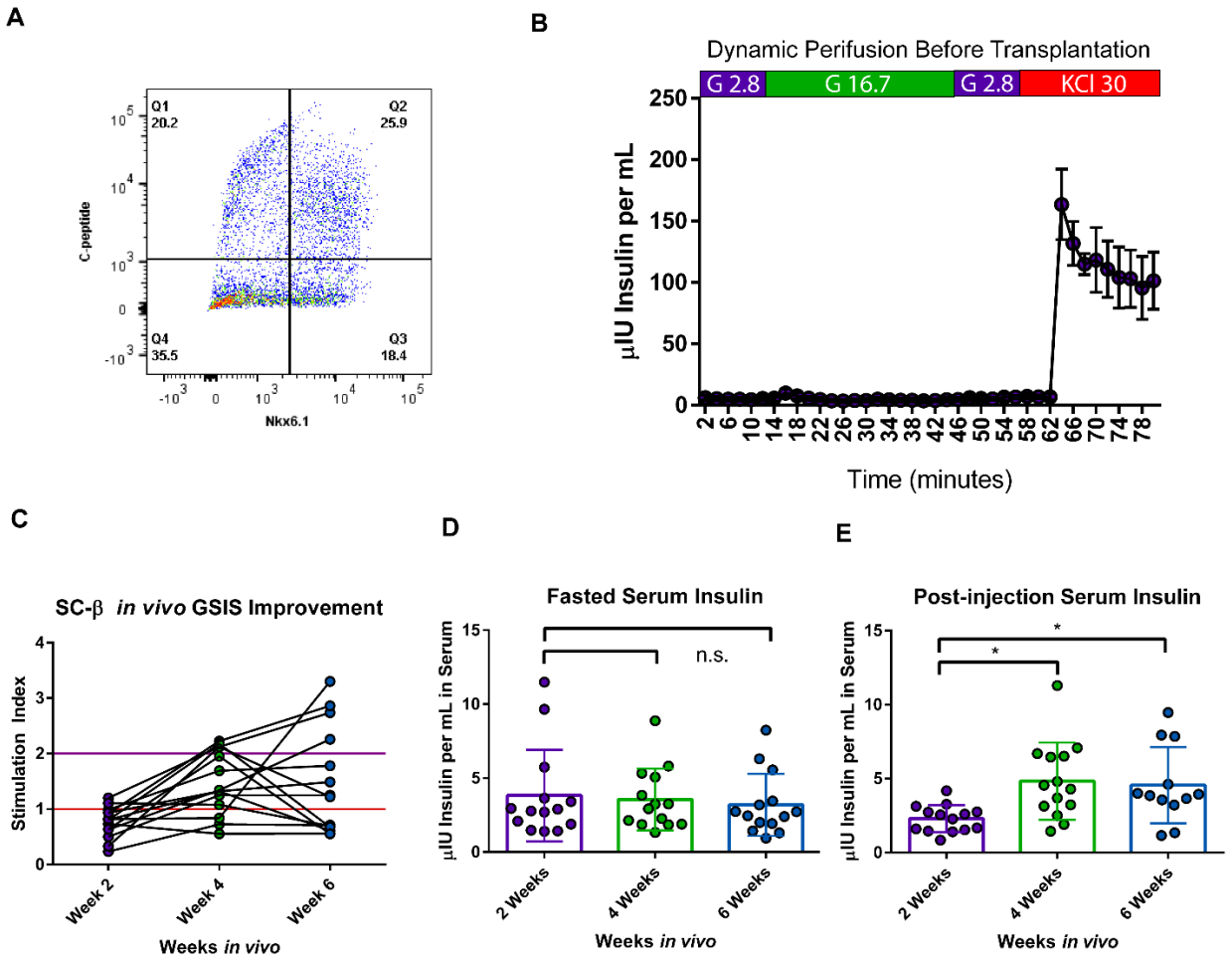

Fig 3-1. SC-β Cell Glucose Responsiveness before and after transplantation. A) Flow cytometry of differentiated 1016 iPS AAVS1-eGFP expressing SC-β cells. **B)** Dynamic perfusion of SC-β cells before transplantation showed a small increase in Insulin release after glucose challenge. **C)** GSIS profile of transplanted SC-β cells over a 2 months period. Each point represents a single animal. Connected dots are the same mouse over time. **D)** No change in fasted insulin release was observed over time. **E)** Stimulated Insulin release increased during the period of *in vivo* maturation.(* denotes $p < 0.05$ using a paired T-test.)

3.3 Enrichment of SC-β Cells using Zinc Sorting

Constitutive expression of eGFP was used to sort differentiated human cells from the tissue of the kidney graft. However, differentiations of SC-β cells are heterogeneous and contain other cell types including undifferentiated progenitors and non-β cells [81, 89, 105]. To specifically isolate SC-β cells before and after transplantation, the cells were incubated in live cell dye N-(6-Methoxy-8-quinolyl)-p-toluenesulfonamide (TSQ) which binds to intracellular zinc, preferentially labelling islet endocrine cells which use zinc to package insulin into its hexameric crystalline structure [173, 217, 218]. Recovery of enriched SC-β tissue after transplantation has not yet been reported, likely due to the difficulty of re-isolation caused by fibrosis and build-up of scar tissue around the transplants. Using a combination of physical and chemical disruption we were able to retrieve a limited number of cells (5,000-15,000) after isolation and sorting which were GFP-positive/TSQ-positive/PI-negative, i.e., live human, zinc-containing cells **(Fig. 3-2A,B)**. These cells were lysed for RNA collection and subsequent global assessment of gene expression by RNA-sequencing. A sample of each graft was preserved for histological analysis. In order to compare gene expression to functional human islet β cells, we also collected cadaveric islet tissue from four non-diabetic human sources also using TSQ sorting as well as uptake of the fluorescent glucose analog 2-NBDG to further enrich the β cell population from other endocrine subtypes **(Fig. 3-2C)**.

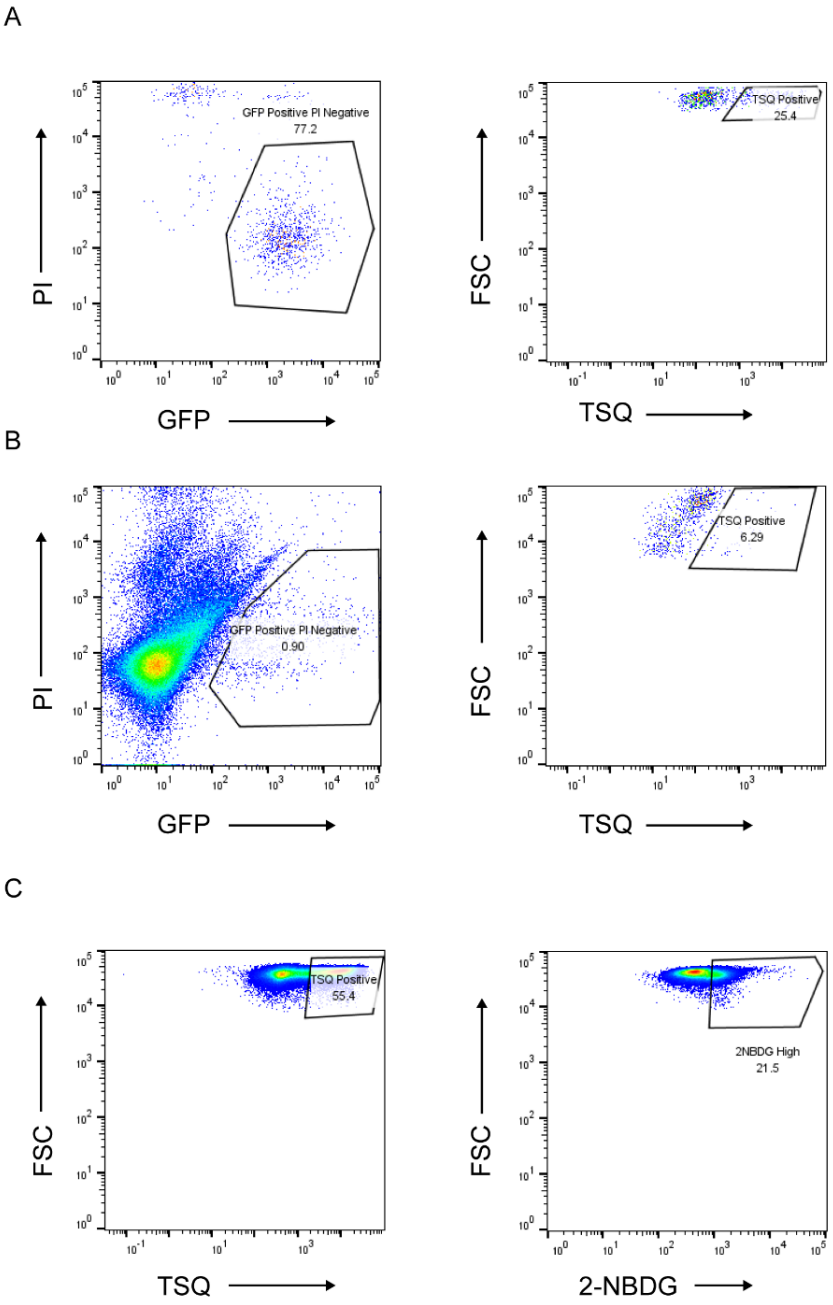

Figure 3-2. Isolation of SC-β cells and human islets using 1016 eGFP expressing iPS line in combination with TSQ live cell zinc enrichment. A) Isolation of GFP^{+} TSQ^{High} SC-β cells before transplantation and **B)** after transplantation. **C)** Isolation of Human islet β cells using zinc content (left) and 2-NBDG uptake (right).

3.3 SC-β Cell Transplants Resolve Endocrine Identity and Increase Expression of Maturity Markers

First, we investigated the expression of selected marker genes and proteins to confirm that maturation of the transplants was successful. SC-β cells resemble immature islet β cells when compared to human fetal and adult cell types [86]. We performed immunofluorescence staining on SC-β cells and the isolated grafts after *in vivo* maturation. Expression of the maturation marker UCN3, normally induced during perinatal islet development, was still limited in SC-β cells but improved after 6 weeks of *in vivo* maturation **(Fig 3-3A)** [107, 168, 219]. Poly-hormonal cells also resolved into either single hormone-positive α or β cells in this time window after transplantation **(Fig 3-3B)**.

Insulin gene expression remained similar after transplantation **(Fig 3-3C)**. This was also true of the other islet endocrine hormones Glucagon *GCG*, Pancreatic Polypeptide *PP*, and Somatostatin *SST*, which is attributable to the mixture of polyhormonal non-SC-β cells present in differentiations [81]. Interestingly, the β cell hormone Islet Amyloid Polypeptide (IAPP) and α/β hormone Adenylate Cyclase Activating Polypeptide 1 (ADCYAP1) were some of the most strongly induced genes after transplantation [220, 221]. We also examined genes associated with β cell functional maturation in perinatal development. As expected, expression of *MAFA* and *UCN3* were both up-regulated after transplantation **(Fig 3-3D)**. We also observed increased expression of *SIX2*, which has recently been correlated with maturation of developing β cells [169] in humans. In summary, *in vivo* maturation of SC-β cells involved expression of insulin and additional β cell hormones, while maturation of transplanted non-SC-β, poly-hormonal cells involved suppression of insulin expression and resolving into other islet endocrine lineages.

Fig 3-3. Maturation of SC-β cells after transplantation. A) Immunofluorescence staining before and after transplantation revealed increased expression of maturation marker UCN3 in insulin-expressing cells after maturation. **B)** Polyhormonal cells resolved into insulin or glucagon expressing cells after 6 weeks *in vivo* maturation. **C)** Hormone expression of *GCG* and *INS* remained similar after transplant but expression of other β cell hormones *IAPP* and *ADCYAP1* increased after maturation. **D)** Expression of developmentally-regulated β cell transcripts including *MAFA*, *UCN3* and *SIX2* were up-regulated after transplantation.

Figure 3-3 continued.

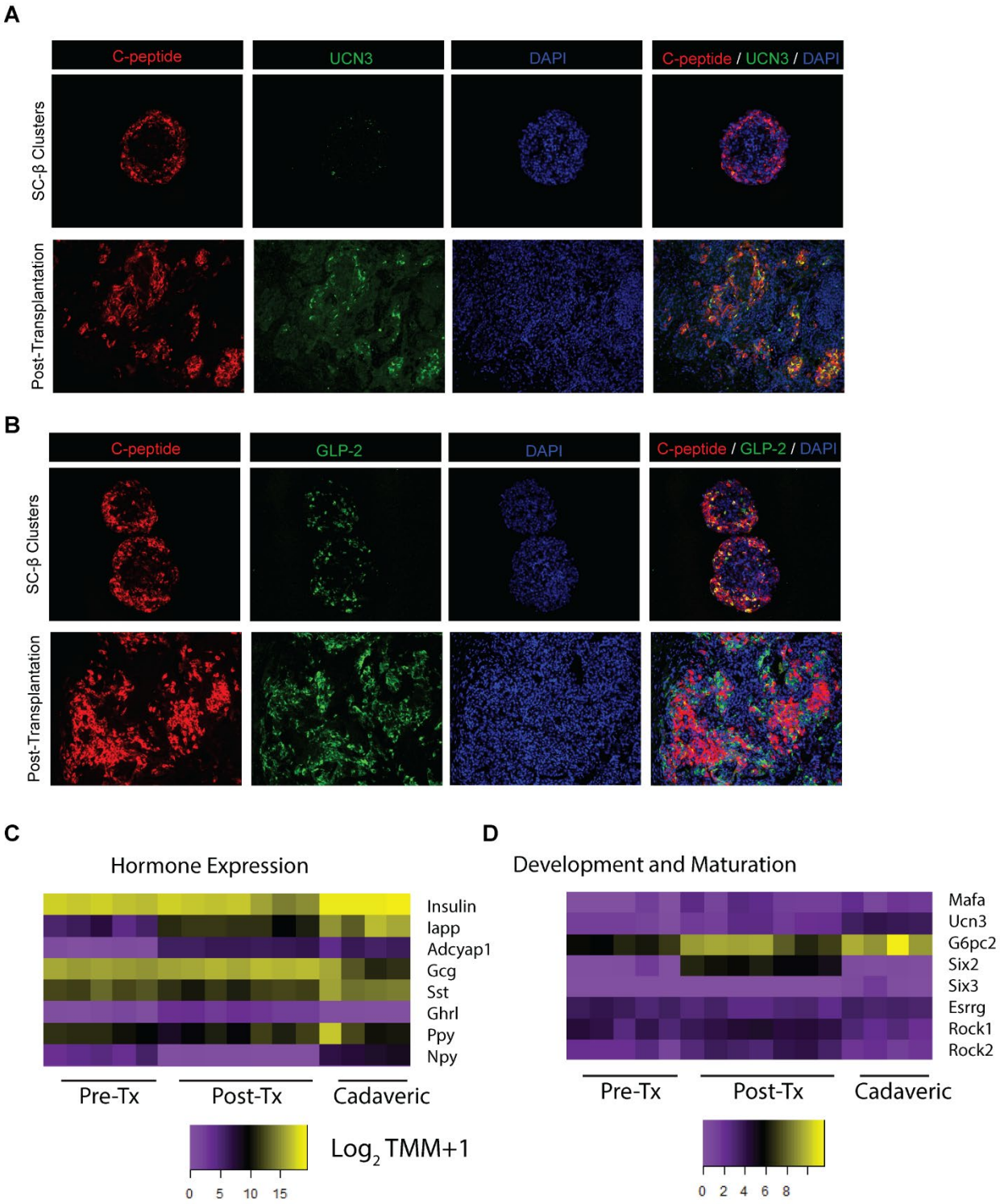

3.4 Disallowed Gene Expression

Expression of maturation-associated genes is improved after transplantation of SC-β cells. These genes play functional roles in glucose sensing and β cell function. In addition to up-regulating tissue-specific gene expression, developing islets must also silence genes that would disrupt physiology of the β cell, but which are nearly ubiquitously expressed in other tissues, referred to as “disallowed” genes [121, 122]. This group of genes was first identified by searching for genes that are uniquely silenced in β cells, with the assumption that specific down-regulation of genes might have a functionally relevant effect in the islet to preserve control of glucose homeostasis. We examined a list of 38 disallowed genes in the islet before and after transplantation as well as in cadaveric human islets **(Fig. 3-4A)** [121]. Most disallowed genes were expressed at low levels in SC-β clusters after TSQ sorting followed by RNA extraction, though we did observe elevated expression of Carbonic Anhydrase 2 (CA2) and Monoglyceride Lipase (MGLL). Both of these genes regulate lipid metabolism; inappropriate dependence upon β oxidation and metabolism of lipids can decouple release of insulin from the β cell-specific metabolism of glucose. We and others have observed that removal of fetal bovine serum from culture conditions in the final stage of differentiation significantly improves GSIS profiles of SC-β cells [88, 104]. Serum contains a rich mixture of lipids. Removing other fuel sources from SC-β medium could improve their ability to metabolize solely glucose for GSIS. We analyzed cellular lipid content using the live cell lipid dye, BODIPY-490/513 in TSQ-positive cells in human islets and SC-β cells. Strikingly, SC-β cell BODIPY labeling was much stronger in medium containing 10% FBS compared to BSA-supplemented basal medium **(Fig. 3-4B,C)**. SC-β cells cultured in BSA-supplemented media more closely resembled the lipid content of healthy cadaveric human islets cultured with serum supplementation. We also observed strikingly high levels of Lactate Dehydrogenase (LDH) expression in SC-β cells as well as human islets in this analysis. LDH activity uncouples glycolytic flux from TCA cycle stimulation, though our previous work did not suggest that pyruvate metabolism was disrupted in SC-β cells [222], and significant lactate

generation was not present. To be sure LDH activity does not affect SC-β cell glucose sensing we analyzed GSIS in SC-β cells pre-incubated for 72 hours with the inhibitor of LDH, sodium oxamate at three doses **(Fig. 3-4D)** [223]. We did not observe an improvement in insulin secretion after oxamate exposure. Curious why LDH expression was observed in SC-β cultures, we performed immunofluorescence on fixed SC-β clusters to assess whether LDH localized with C-peptide-positive cells. LDH signal did not co-localize with C-peptide, with the strongest staining occurring in non-SC-β cells **(Fig. 3-4E)**. We expect that LDH signal in the RNA Seq experiment may have originated in non-insulin expressing cells that represent approximately 20% of the TSQ-sorted cells *in vitro*. LDH expression in sorted islets may have been derived from islet α cells, which do express LDH at a much higher level than the β cell population [224]. While disallowed gene expression may indicate altered lipid metabolism in SC-β cells, this defect is avoided by changing culture medium and may underlie recently reported improvements in SC-β cell function achieved through changes in cell culture medium. It does not appear that changes in disallowed gene expression underlie improvements in GSIS after maturation *in vivo.*

Figure 3-4. Disallowed gene expression in SC-β cells. A) Analysis of RNA Seq before and after transplantation and in human islets comparing disallowed gene expression. **B)** BODIPY live cell assay in TSQ-positive SC-β cells in base medium containing 10% FBS and **C)** in base medium with BSA supplemented for FBS. **D)** GSIS analysis after sodium oxamate exposure in SC-β cells. **E)** Immunofluorescence staining for LDH enzyme expression in insulin-positive cells after differentiation.

Figure 3-4 continued.

A

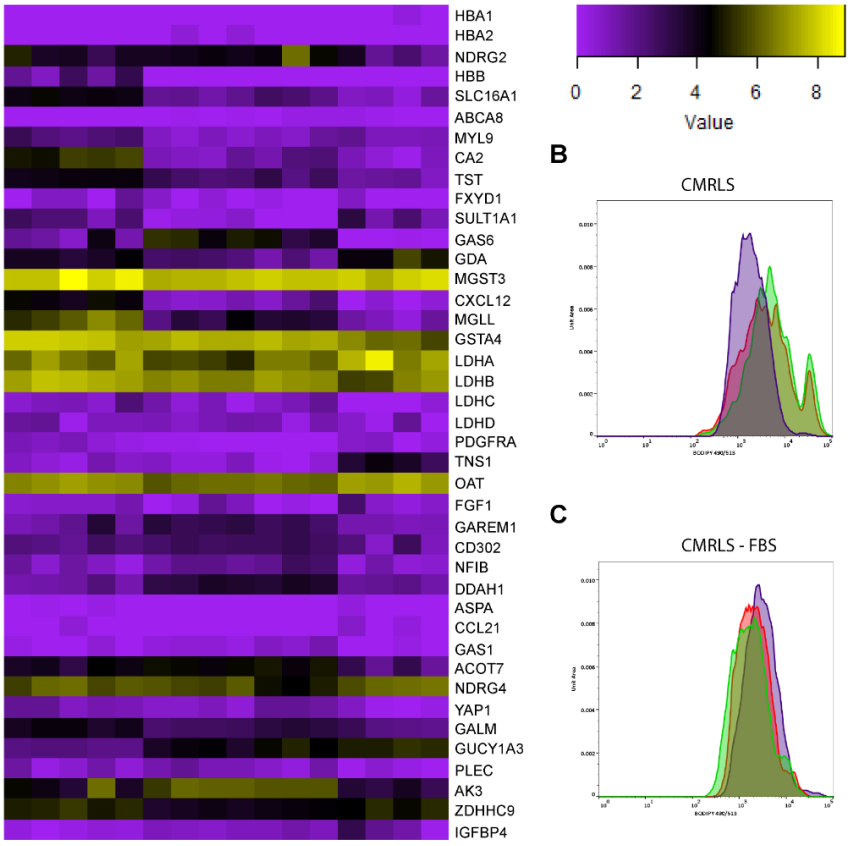

B

C

D

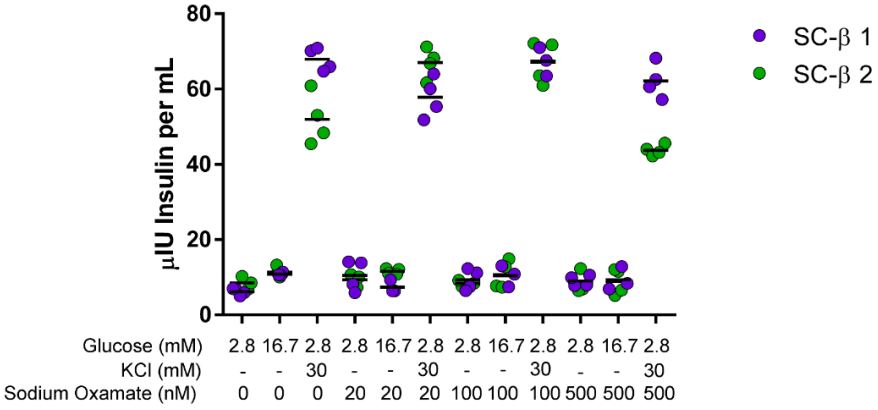

E

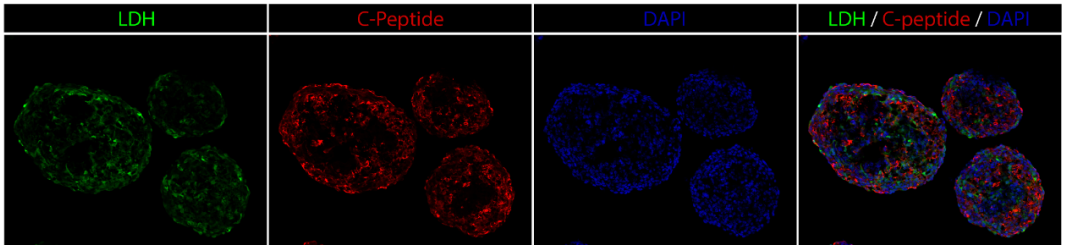

3.5 Co-expression network analysis

We aimed to further dissect mechanisms underlying the improvement in GSIS. We have previously shown that SC-β clusters are a complex population consisting of β cells, α cells and minor cell populations such as pancreatic progenitor cells and confirmed the β and α cell populations persist after transplantation. Therefore, we decided to integrate our RNA-sequencing data with published bulk islet and FACS-sorted β cell data sets to analyze biological materials of comparable composition. We constructed a co-expression network from a large bulk islet RNA-sequencing data set from 89 donors from a publicly available human islet expression analysis previously published by the Groop lab [225] containing gene expression data from normal, pre-diabetic, and diabetic islets, using the MEGENA algorithm [226] to obtain an islet-specific gene expression "pathway map." We then overlaid gene expression signatures from the *in vivo* maturation experiment and compared these results with previous studies of islet functionality including analysis of human fetal islet development [86], islets exposed to experimental hyperglycemia after transplantation [110], and a broad study of islet ability to successfully engraft and rescue diabetes in animals after transplantation [227].

Co-expression networks built using MEGENA represent communities of genes which demonstrate similar variation in transcript expression patterns observed between biological replicates. Genes in a module may participate in a common biological process or pathway, share upstream regulators, be expressed in a specific cell type, or encode structural components of a subcellular organelle or protein complex. Co-expression modules may deviate from canonical pathway definitions and capture tissue-specific aspects that are not reflected in pathway database annotations that often represent an "average" over multiple model systems. One can think of the resulting graph as a representation of correlations between genes rather than all correlations that pass a certain false discovery rate threshold. The MEGENA algorithm was selected because it

leads to well-defined modules and establishes relationships between the modules through clustering.

3.6 Candidate modules for improvement in GSIS

The resulting network generated by the MEGENA algorithm included 17,829 genes forming 538 significant modules that were hierarchically organized in ten branches. Modules c1_8 **(Supplemental Fig. II-3A)** and c1_21 **(Supplemental Fig. II-4A)** were highly enriched for genes up-regulated during *in vivo* maturation and fetal islet development **(Supplemental Fig. II-3B,C, Supplemental Fig. S4B,C)** [86], diabetic versus nondiabetic islets **(Supplemental Fig. II-3D, Supplemental Fig. II-4D)** [228], and successful islet transplantation outcome **(Supplemental Fig. II-3E, Supplemental Fig. II-4E)** [227]. Genes in modules c1_8 and c1_21 were enriched in key processes of β cell function **(Supplemental Table II-1)**, including processes that are unlikely to be fully sustained outside of the *in vivo* environment including cell-to-cell communication and innervation-dependent electrophysiological processes. Gene ontology cellular component enrichment analysis indicated that both modules c1_8 and c1_21 were enriched in gene products localized to the synapse, vesicles, and to a lesser extent the endoplasmic reticulum and cell membrane.

We also examined composition of modules c1_8 and c1_21 to see if they included well-established genes implicated in β cell function. We identified six markers with strong preferential expression in healthy adult β cells from single-cell transcriptomics studies of human islets **(Table 3-1)** [229, 230]. Four out of six mature β cell markers were member genes of c1_8 and c1_21. *CDKN1C* and *MAFA* had comparable expression with FACS-sorted β cells already at stage 6, while up-regulation of the other markers was consistent with maturation *in vivo*. Modules c1_8 and c1_21 also incorporated crucial diabetes and GSIS genes **(Supplemental Table II-2)**.

Table 3-1. Validation candidate modules for relevance to β cell biology.

		Log_2FC (FDR)	
Gene	**Module hierarchy**	**β cells vs stage 6**	**Post *in vivo* maturation vs stage 6**
INS	c1_2,c1_16,c1_134,c1_384	1.7 (0.0045)	not DE
ADCYAP1	c1_8,c1_66	5.7 (0.0013)	6.2 (7.3e-05)
HOPX	c1_8,c1_67,c1_277	3.4 (0.0013)	3.9 (0.0020)
IAPP	c1_8,c1_66	9.6 (0.0009)	5.7 (0.0037)
CDKN1C	c1_2,c1_28,c1_182	not DE	not DE
MAFA	c1_2,c1_21,c1_155	not DE	2.7 (0.0475)

3.7 Interaction with the in vivo environment

in vivo maturation induced expression of genes implicated in regulation of insulin secretion, cAMP-mediated signaling, and calcium signaling, as determined by PANTHER overrepresentation test [231]. *in vivo* maturation up-regulated receptors of incretin hormones/gastrointestinal polypeptides, neurotransmitters, and hormones such as growth hormone (*GHR*), thyroid hormone (*THRA*) and somatostatin (*SSTR3*).

GABA receptor *GABRB3* was an up-regulated hub gene in submodule c1_66 of module c1_8. Hub genes are strongly correlated components of a submodule that are likely to drive expression of other module genes or play a regulatory role within the module's activity [226]. Also, GABA-ergic synapse biology was 3.1-fold overrepresented among GO Cellular Component terms in module c1_8 according to PANTHER overrepresentation analysis. Thus, we identified GABA signaling as candidate inducer of functional maturation **(Fig. 3-5A)**. Gene expression in submodule c1_66 was anti-correlated with higher HbA1c in islets from deceased donors **(Supplemental Fig. II-5A)** and a large fraction of genes in this hub exhibited differential expression during human islet development **(Supplemental Fig. II-5B)**. In addition to GABRB3 being a hub gene in submodule c1_66, other components of GABA signaling as well as synthesis were also differentially expressed during the *in vivo* maturation process **(Supplemental Fig. II-5C)**. GABA is produced by the islet β cell and is stored in separate secretory vesicles from insulin, released in a pattern dependent upon Ca^{2+} influx [232]. To test whether manipulation GABA and growth-hormone-receptor signaling pathways could potentiate GSIS, SC-β cells were cultured for 72 hours with GABA followed by challenge in low (2.8 mM) or high (16.7 mM) glucose Kreb's Ringer Buffer solution with 30 mM KCl in low glucose as a positive control (**Fig 3-5B**). Treatment of cells with GABA resulted in a positive but not statistically significant trend for STIM index with GABA treatment when each batch was normalized to untreated controls **(Fig. 3-5C)**. GABA's effect on islets has been previously reported to suppress basal Insulin release. As SC-β cells

regulate basal secretion more appropriately than in high glucose conditions [233], it is possible that GABA-reinforced suppression of basal insulin release has a more pronounced effect *in vivo* after acquisition of a more glucose-responsive state.

Fig 3-5. GABA as candidate inducer of maturation. A) *GABRB3* was up-regulated in the *in vivo* maturation experiment and was a hub in submodule c1_66 in c1_8; Submodule c1_66 contained key β cell genes (enlarged) and was enriched in differentially expressed genes up-regulated in the *in vivo* maturation experiment. **B)** GSIS performed on SC-β cells after 72-hour exposure to GABA. **C)** STIM indexes of all replicates after GABA pre-incubation.

Figure 3-5 continued.

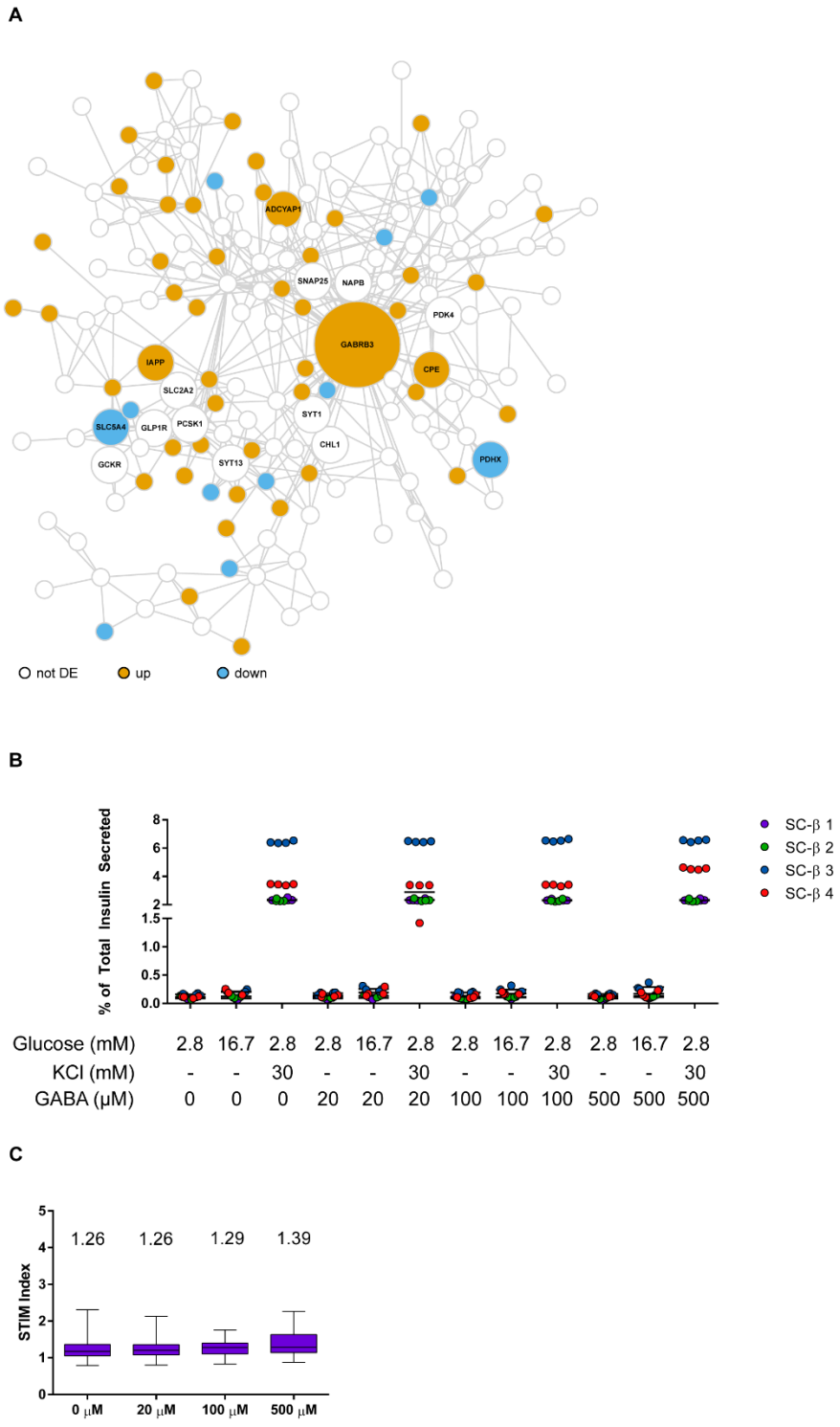

In addition to GABA receptor signaling, receptor-type protein tyrosine phosphatases *PTPRN2* and *PTPRA*, down-stream targets of JAK/STAT signaling, were up-regulated in the *in vivo* maturation experiment and were hub genes in submodules c1_409 of c1_21 and c1_291 of c1_8, respectively **(Fig 3-6A,B)**. Both of these submodules were also anti-correlated with diabetic islet state and insulin content of islets **(Supplemental Fig. II-6A,B)**. In addition, JAK/STAT signaling as well as Growth Hormone signaling, an inducer of the JAK/STAT cascade, were both up-regulated during *in vivo* maturation **(Supplemental Fig. II-6C)**. To determine if recombinant human Growth Hormone (hGH) could potentiate GSIS, SC-β clusters were cultured in hGH for 72 hours before GSIS challenge. Treatment with hGH did increase GSIS stimulation after 72 hours in 100 ng/mL by an average of 40% (**Fig 3-6C**), which was statistically significant when all data was converted into STIM indices and analyzed together **(Fig. 3-6D)**. In summary, *in vitro* GSIS could not implicate GABA signaling as a component of *in vivo* maturation and functional improvement of SC-β cell grafts. In contrast, activating hGH and signaling did have a statistically significant effect on STIM index, suggesting that supplementation of the final stage of SC-β culture with rhGH could have a modest effect on GSIS.

Fig 3-6. JAK/STAT signaling as candidate inducer of maturation. A) *PTPRN2* was a hub in submodule c1_409 in c1_21. Submodule c1_409 was enriched in differentially expressed genes up-regulated in the *in vivo* maturation experiment. **B)** *PTPRA*, another member of the protein tyrosine phosphatase family and a known modulator of GSIS [234], was a hub in submodule c1_291 in c1_8. **C)** GSIS performed on SC-β cells after 72-hour exposure to recombinant hGH. D**)** STIM indexes of all replicates after hGH pre-incubation. (* denotes $p < 0.05$ normalized using mixed effect modeling.)

Figure 3-6 continued.

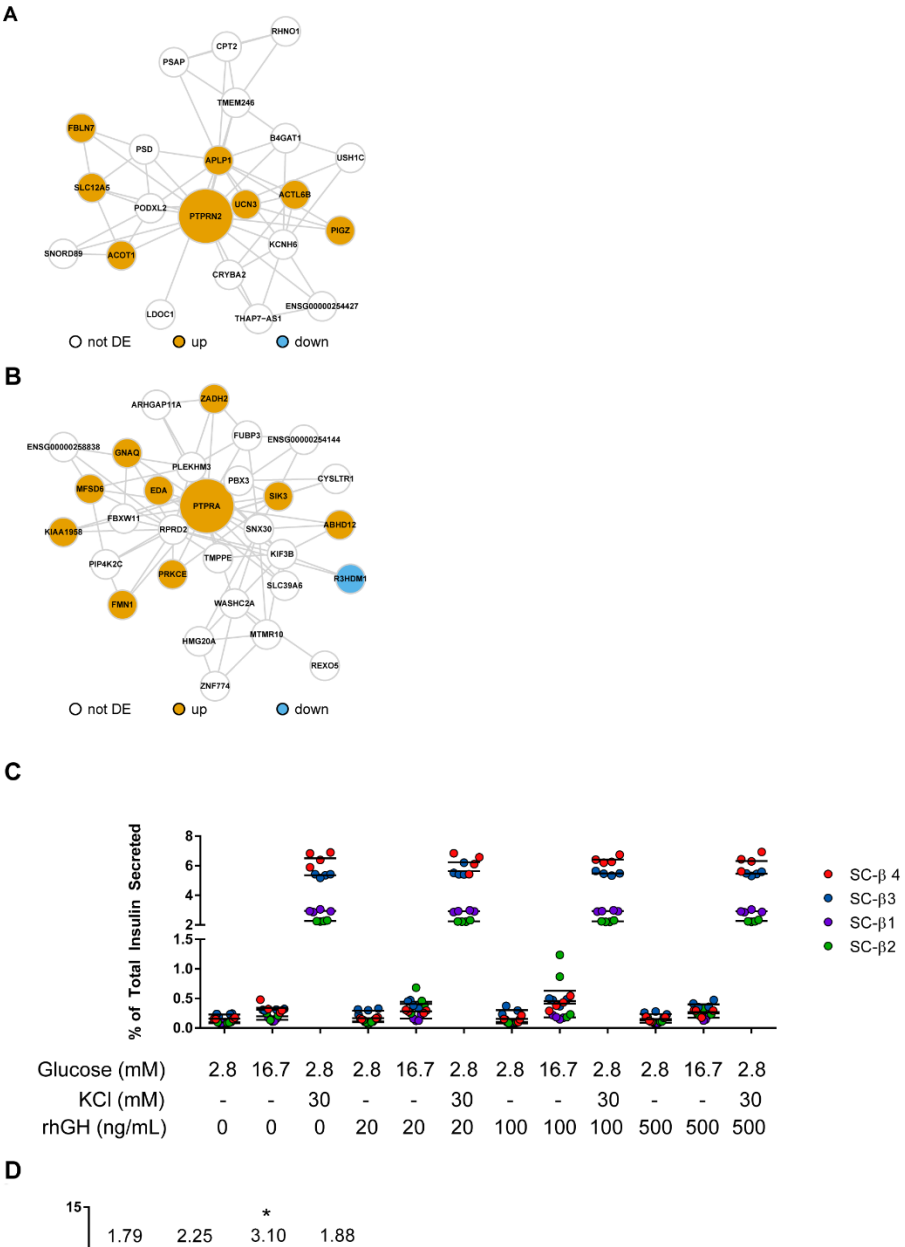

3.8 Endothelial Cell Interactions

Next, we investigated differentially expressed transcripts encoding secreted proteins. These signals may provide insight as to what processes are induced to sustain and mature SC-β cells after transplant. Up-regulated genes from the *in vivo* maturation experiment encoding secreted products were enriched in gene ontology terms related to formation of blood vessels (e.g., angiogenesis, endothelial cell migration) and new nerve endings (axon guidance, neuron projection guidance, gliogenesis), but also processes that could elicit formation of a fibrotic capsule around the grafts (complement activation, regulation of inflammatory response, and extracellular matrix organization). Notably, *VEGFA*, *VEGFB* and *VEGFC* were among the up-regulated secreted products and we found extended evidence for SC-β cell – endothelium cross-talk **(Fig 3-7A, B)**. VEGFA-mediated vascularization is crucial for sustained glucose induced insulin secretion *in vivo* [235], and islets lacking dense vasculature exhibit reduced GSIS phenotypes [208]. While vascularization and oxygen delivery are obligate processes for graft survival *in vivo* [236], signaling from blood vessels regulates pancreas specification during early fetal development [60], and islet vasculature is dynamically regulated by and exerts control over insulin secretion from the islets in high and low glucose [237]. Other reports have also suggested that co-culture with endothelial cells may improve expression of islet genes including UCN3 and insulin in other differentiation protocols [117], and thus may functionally improve SC-β cells. We co-cultured SC-β cells for 72 hours with 3 different ratios of endothelial cells using human umbilical vein endothelial cells (HUVECs) to simulate vascularization of the graft. After 72 hours of co-culture, GSIS was analyzed in reaggregated SC-β clusters containing HUVECs. Surprisingly, HUVECs co-culture resulted in a dose-dependent decrease in insulin secretion in response to glucose **(Fig. 3-7C),** though no single treatment was statistically significant on its own. Normalized to control SC-β clusters, GSIS with endothelial cell co-culture was reduced by as much as 50% **(Fig. 3-7D)**. This is surprising, as previous reports have suggested that endothelial cell co-culture is a way to improve SC-β maturation, but our results suggest that

functionality may be inhibited by endothelial cells without an islet-specific identity. It remains possible that some positive effects are induced by endothelial cells, regardless of their tissue of origin, but functional maturation does not appear to be a benefit that is universally achieved using unspecified endothelial cells.

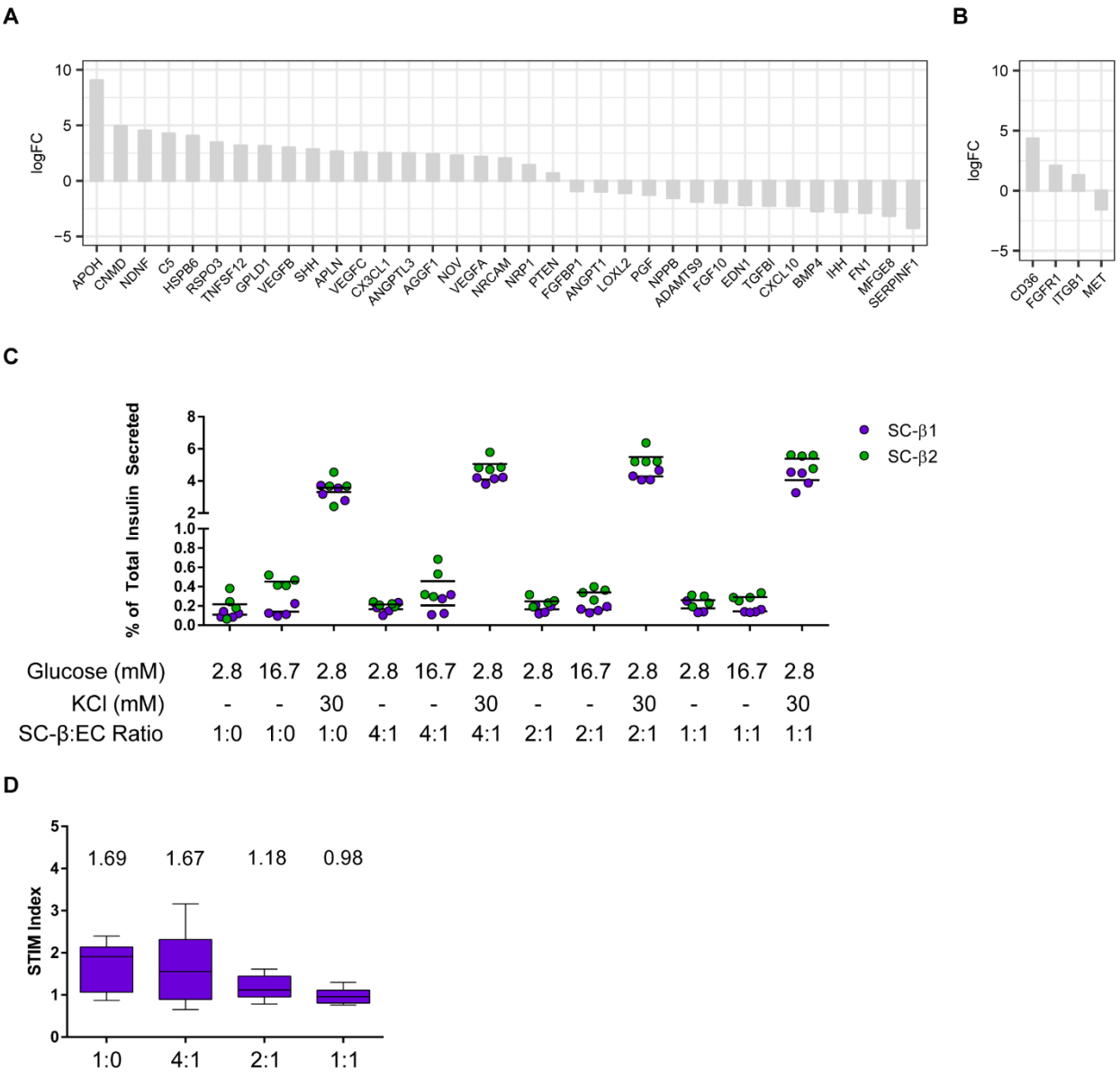

Fig 3-7. SC-β cell–endothelium cross-talk. A) Differentially expressed genes the *in vivo* maturation experiment that encoded pro- and anti-angiogenic secreted factors and **B)** receptors of secreted or extracellular matrix factors originating from endothelial cells [238]. **C)** Co-culture with HUVECs reduced glucose responsiveness in SC-β cells. **D)** STIM index reduced below baseline level at higher EC:SC-β ratios.

3.9 Future work for improvement of the SC-β cell differentiation protocol

Finally, we sought candidate transcriptional regulators for improvement of SC-β differentiations. We specifically identified hub nodes: genes that are densely interconnected with their neighbors and positioned between different components of the network. Modulating hubs and genes located between multiple modules could trigger dramatic changes in phenotype, possibly facilitating the shift from immature SC-β cells to adult β cell-like gene expression.

We examined hub nodes and genes with high interconnectivity between modules c1_8 and c1_21. We further required the genes to have unequal mRNA expression in stage 6 cells and FACS-sorted adult β cells ("immature genes") and to be differentially expressed in the *in vivo* maturation experiment (to undergo "maturation"). We identified 28 genes satisfying these criteria **(Supplementary Table II-3)**. 8 candidates were supported by related phenotypes in published animal and cell culture studies. *DACH1* is a transcription factor with an established role in endocrine cell development and perinatal increase of β cell mass [239] and is associated with risk of developing type 2 diabetes in human [240]. Drosophila homolog of *NUDT3* is involved in insulin secretion and signaling [241]. *MAPK10* is implicated in GLP-1 mediated antiapoptotic pathway in β cells [242]. *RCAN2* is a regulator of calcium signaling [243], while *CNTN1* [244], *NMNAT2* [245], and *PRUNE1* [246] play roles in neurogenesis and may also be functionally important for β cells.

Other genes in this table encode proteins without any known connection to β cell biology and would be of interest to study, as they correlate both with SC-β maturation after transplantation and are highly expressed in healthy human islets. As SC-β differentiation protocols are improved and progress is made toward generation of functionally mature cells *in vitro*, these genes could be used as markers to identify potentially important regulators of this process and give some clue as to how protocol improvements are mechanistically affecting GSIS.

3.10 Discussion

This study is a first step toward characterizing the processes regulating maturation of SC-β cells and their fate after transplantation. While the stem cell field has focused its attention on the *in vitro* functionality of these cells, their ultimate potential as a curative therapy for T1D will be limited by their ability to thrive and function after transplant. Functional studies *in vitro* are relatively straightforward, but analysis of *in vivo* function is much more difficult. Grafts behave much more variably after transplantation, and the time required to acquire a more functional GSIS profile also appears to vary between experiments. Here we chose 6 weeks to balance time allowed for maturation with practicality of study duration. In the timescale of curative transplantation this represents only the very beginning of a transplanted SC-β cell's lifespan in a patient.

Assays to compare function both *in vitro* and *in vivo* are not currently standardized. We can detect relative improvements in function after transplantation, but the noise and detection limit for GSIS *in vivo* make this phenomenon challenging to measure in detail. Function of human islets appear similar to that of SC-β cells after transplantation. While we assume here that both are indistinguishable in function because they behave as healthy human islets, difference in transplantation site and host species could also cause both tissues to assume a GSIS phenotype in between healthy islets and SC-β cells *in vitro*.

Analysis of the most differentially expressed genes before and after transplantation identified both ADCYAP1 and IAPP secreted peptides as potential markers of *in vivo*-matured SC-β cells. It is interesting that two β cell-specific peptide hormones are so highly up-regulated. Induction of IAPP expression will be necessary for disease modeling *in vitro*, as its ability to aggregate and contribute to β cell dysfunction through the production of insoluble amyloid fibrils will be a desirable strength of human SC-β cells to recapitulate this human-specific aspect of T2D stress, as rodent islets do not contain an amyloidogenic IAPP peptide sequence [247]. ADCYAP1 biology is not well-characterized, but its ability to stimulate cAMP signaling and potentiate Insulin

release could undoubtedly improve *in vitro* GSIS profiles [248]. Indeed, cAMP signaling is a gene ontology term enriched in SC-β cells after transplantation, and autocrine signaling through ADCYAP1 may play a role in this pathway.

Our approach to use co-expression network analysis was able to identify pathways that may play a role in maturing SC-β cells, though their manipulation using the addition of single factors may limit our ability to untangle any synergistic or combinatorial effects that multiple signals may have in concert. Growth hormone as a component of the *in vivo* niche that improves GSIS is intriguing, as GH signaling has previously been suggested to inhibit islet function *in vivo* [249]. However, this effect was observed when cells were producing very high levels of GH, expressed at the level of insulin in the β cell. In addition, exposure to recombinant GH may have different effects than production of the active peptide within the cell. Follow-up experiments to demonstrate that the hGH effect is through the GHR will be necessary. GABA is also an interesting pathway, as β cells are able to produce GABA and its secretion may play a role in normal β cell homeostasis.

Hub genes identified in this study may be useful tools toward identifying other factors to recapitulate the *in vivo* environment to mature SC-β cells. As opposed to transcriptomic studies, this small list of less than 50 genes could be used for staining or qPCR-based screens to mature cells *in vitro*. One caveat of this approach is that these genes have not yet been confirmed to be mechanistically important for β cell physiology. We have utilized this study to search for functionally important genes that regulate GSIS *in vitro*. However, we have also demonstrated that maturation of SC-β cells *in vivo* induces a more complete repertoire of β cell hormone expression and resolves mono-hormonal and poly-hormonal gene expression profiles of differentiated cells. Genes and pathways investigated here may also be important in these processes or others of which we do not yet know of. Examining hub genes may be an efficient way to test these possibilities, as their interconnectedness to gene expression modules may

increase the convergence of pathways regulating cell identity with only a few candidate transcriptional regulators.

An equally important topic to focus on is the down-regulation of genes and processes that may inhibit graft function or survival. In particular, modulators of inflammation and scar tissue formation could be inhibiting survival of transplants. This would be interesting to investigate in grafts that have better or worse functional outcome. However, in order to have higher confidence in these experiments it would be valuable to establish a more detailed functional profile of transplants as discussed above. One possible method would be to utilize hyperglycemic clamp studies, though these are time consuming and technically challenging. Ultimately *in vivo* maturation is still a difficult phenomenon to study and further work to improve our tools to characterize the process may greatly improve our ability to understand the fate of transplanted SC-β cells.

Chapter 4: IAPP is a Marker of Mature SC-β Cells

4.1 Introduction

Limited SC-β cell functionality remains a hurdle to generating islet-like cells *in vitro* from pluripotent stem cells. We have determined that metabolic regulation of glucose processing is dysfunctional in the SC-β cell, and that this deficiency is partially rescued after transplantation. Using a guilt-by-association bioinformatic approach we have identified a number of genes that appear to correlate with islet functionality, health, and *in vivo* maturation of SC-β cells. Of this list, Islet Amyloid Polypeptide (IAPP) is particularly interesting; this peptide hormone is co-secreted with Insulin from the islet β cell [220, 250-256], and is expressed specifically in β cells of the adult islet [250]. *IAPP* is up-regulated approximately 30-fold after transplantation of SC-β cells during their functional maturation *in vivo*, suggesting that cells expressing this peptide have a more mature peptide secretion profile. IAPP-expressing SC-β cells may also more stringently regulate their basal insulin secretion, as IAPP negatively regulates Insulin release [250, 251, 255, 256]. This expression pattern after transplant is also observed with the β cell peptide hormone Adenylate Cyclase Activating Polypeptide (ADCYAP1), a less-characterized α and β cell hormone that activates Adenylate Cyclase activity, amplifying stimulated insulin secretion [221, 257, 258]. These results suggest that as SC-β cells mature *in vivo* they attain a more complete hormone secretion repertoire. How this relates to functional maturation is not understood, as IAPP and ADCYAP have not been described in a developmental or maturation context in the islet and represent unexplored potential markers of maturing SC-β cells. To date, two studies have identified IAPP as potentially important in SC-β cell biology. IAPP is known to be expressed at low levels in previous iterations of SC-β cell differentiation protocols [86], and has been observed to slowly increase in expression over time in differentiated SC-β cells using single cell-RNA sequencing approaches (Veres *et al*, accepted), a discovery made in parallel while analysis of *in vivo* maturation was performed in our laboratory.

IAPP, also known as Amylin, is an 89 kD peptide hormone processed to 37 amino acids and secreted by the islet [259, 260]. It belongs to the calcitonin peptide related family, which also includes adrenomedullin, α/β calcitonin gene related peptide (CGRP), intermedin, and calcitonin [250, 261]. IAPP secretion is thought to regulate satiety and gastric emptying, playing a complementary role to insulin in peripheral tissues [250, 251, 253, 255, 262-265]. Islets secrete insulin and IAPP at a 100:1 ratio; both peptides are packaged in the same vesicles and undergo post-translational modification [250, 260]. IAPP is cleaved into separate domains through prohormone convertases 2 (PC2) and 1/3 (PCSK1/3), similar to the processing of insulin and resulting in a peptide hormone of similar size.

In peripheral tissues, the IAPP ligand binds to the calcitonin receptors. The affinity of these receptors for IAPP is modified by receptor activity-modifying proteins (RAMPs) [250, 266-268]. It is not well understood how these combinations direct IAPP responsiveness, and there are currently no known agonists/antagonists of calcitonin receptor signaling that affect IAPP activity. In the brain, IAPP synergizes with leptin signaling in the hypothalamus to induce satiety [250, 255, 262, 264, 269, 270]. Developmentally, IAPP expression appears to coincide with insulin production in the fetal islet β cell population and may also be expressed in other hormone-expressing cell types during initial endocrine induction of α cells [271], which are the first endocrine cells produced by NGN3-positive endocrine progenitors [79]. This is in contrast with our observations that SC-β cell IAPP expression appear to lag behind insulin and glucagon expression, suggesting that SC-β cell differentiation *in vitro* may be missing some inductive cues to induce full islet gene expression which is rescued after transplantation.

In addition to the possibility that IAPP may be a marker of more mature SC-β cells as suggested by our earlier work, this peptide hormone is particularly interesting for its poorly understood role in islet pathology in type 2 diabetes [250, 252, 272]. IAPP is the first described amyloidogenic peptide, with its aggregates discovered in plaques assumed to be caused by

insulin aggregation in the pancreata of diabetic patients [273-275]. IAPP aggregation occurs through a similar mechanism observed in other amyloidogenic diseases including Alzheimer's and Parkinson's disease [272]. Misfolded, toxic intracellular oligomers of IAPP are capable of driving cell stress and apoptosis in the β cell and may significantly contribute to the pathology of type 2 diabetes [250, 276, 277]. This process is poorly studied, as rodent IAPP does not form amyloid fibrils due to lack of conservation of the amyloidogenic peptide sequence [247, 250, 278]. As IAPP may be an important component of T2D pathogenesis, appropriate expression of IAPP in SC-β cells is desirable toward a platform to study the disease *in vitro*. Its potential as a marker of maturing SC-β cells as observed *in vivo* may also prove a useful tool for protocol development and toward screening to generate more mature SC-β cells *in vitro*. Here we have explored the dynamics of IAPP expression in SC-β cells using gene targeting to generate a dual insulin and IAPP fluorescent reporter model and identified key differences in the IAPP-expressing population during differentiation of SC-β cells.

4.2 Generation of ANGIs Reporter Line in 1016 iPS Background

Maturation of SC-β cells *in vivo* is accompanied by changes in gene co-expression networks corresponding to β cell function and regulation of calcium homeostasis and exocytosis. One of the genes associated with these coexpression networks is the β cell-specific hormone Islet Amyloid Polypeptide (IAPP) **(Fig. 4-1 A)**. Another β cell hormone, Adenylate cyclase activating polypeptide 1 (ADCYAP1) is also up-regulated, indicating that the β cell hormone repertoire is expanded upon functional maturation *in vivo*. Until now, the SC-β field has characterized multi-hormone expressing populations based on the assumption that mixed hormone expression profiles indicate incomplete differentiation or sub-populations with a preference toward one lineage over time [81, 83-86, 91]. To complement this approach, we sought to determine if SC-β cells expressing IAPP in addition to insulin represent a more mature sub-population of SC-β cells

and whether IAPP-only expressing cells also exist *in vitro.* We took a gene targeting approach to create a dual IAPP/INS reporter line in the 1016 iPS background.

Using a homology-based insertion sequence, an mCherry coding sequence was inserted in-frame behind the preserved coding sequence for the *INS* gene, creating a single peptide coding sequence separated by the self-cleaving P2A motif [279]. This targeting vector was termed Insulin Red Nucleus, or IRN **(Fig. 4-1B, Supplemental Fig. III-1A)**. After PCR validation of the knock-in clone, cells were differentiated in a planar 2-D format, resulting in epifluorescence in the mCherry channel without signfiicant backgorund in the empty eGFP channel **(Fig. 4-1C)**. Sorting based on mCherry fluorescence resulted in significantly higher Insulin mRNA, as validated by Real Time RT-PCR **(Fig. 4-1D)**.

After confirmation of successful targeting of the *INS* locus, a second homology-based template was generated to insert a 3x NLS-flanked eGFP coding sequence behind the *IAPP* coding sequence, also separated by a P2A self-cleaving signal. This second vector was termed Amylin Nuclear Green, or ANG **(Fig. 4-1E, Supplemental Fig III-1B)**. Efficiency of targeting was strikingly high (100% of more than 10 tested clones) **(Fig. 4-1F, Supplementary Fig. III-1C)**, as confimred by PCR of genomic DNA from clones spanning the 5' and 3' ends of the transgene into the gene locus outside of the homology vector. The resulting dual-reporter iPS line was named Amylin Nuclear Green in IRN, abbreviated ANGIs [ang-g*uh* s].

Figure 4-1. Transgene targeting in 1016 iPS cells. A) RNA Seq expression analysis of islet endocrine hormone expression after transplantation reveals maturation-associated changes in β cell-specific gene expression. **B)** Targeting vector construct design for Insulin Red Nuclear (IRN) knock-in. **C)** SC-β differentiation of 1016 IRN reporter line results in mCherry signal from clusters without fluorescence in eGFP (empty) channel. **D)** Real Time RT-PCR on cDNA from unsorted and mCherry positive and negative cells after sorting reveals significant differences in *INS* transcript. **E)** Targeting vector construct for Amylin Nuclear Green (ANG) knock-in reporter. **F)** PCR validation of 5' and 3' transgene knock-in for double IRN and ANG targeting resulting in ANG in Amylin Nuclear Green in IRN background (ANGIs).

Figure 4-1 continued.

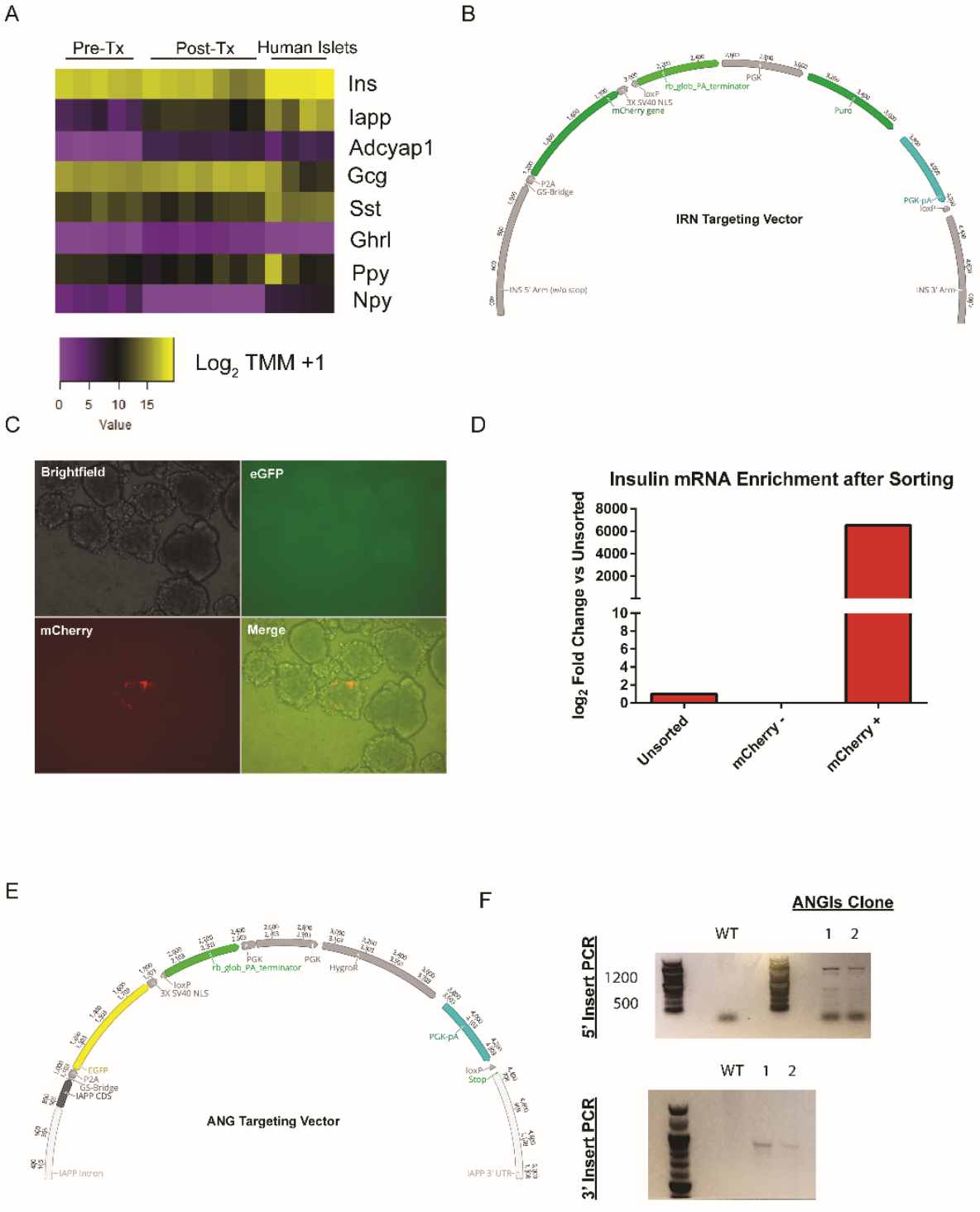

4.3 ANGIs Differentiation Dynamics

In order to prevent possible artifacts due to results from a single clone when characterizing IAPP expression, experiments were performed in two separate clonal lines, referred to as clone 1 and clone 2. Differentiation the ANGIs lines in 3D suspension resulted in the expected Insulin::mCherry signal at the end of endocrine induction in stage 6 day 1, but very little eGFP fluorescence was observed. eGFP signal accumulated over 50 days of differentiation in stage 6 media without additional factors **(Fig. 4-2A)**. Measurement of the mCherry-positive sub-population revealed an increasing fraction of eGFP signal within the insulin-producing cells of the differentiation, plateauing at approximately 30% of mCherry cells after 50 days **(Fig. 4-2B)**. We have previously observed that extended culture of SC-β cells over time results in a decrease in population size of NKX6.1/C-PEP co-positive cells. It is in this range of declining population size that we observed an increase in eGFP signal. After 50 days of differentiation SC-β cells were sorted into mCherry only and mCherry, eGFP co-positive populations and RNA was collected. Real Time RT-PCR on cDNA from these populations revealed faithful reporter activity of the *IAPP* locus, as eGFP-expressing cells contained more than 100-fold higher *IAPP* transcript than eGFP negative cells in both clones tested **(Fig. 4-2C)**. Analysis of fixed sections from the ANGIs differentiations revealed differential localization of eGFP and mCherry signals and confirmed the ratios of mCherry and eGFP-expressing cells observed via flow cytometry, with most eGFP signal present in cells co-positive for mCherry **(Fig. 4-2D)**. While both the mCherry and eGFP transgenes contained flanking nuclear localization signals, we did not observe mCherry in the nuclear compartments, but rather appearing within insulin secretory vesicles in differentiated cells. Using structured illumination super-resolution microscopy, mCherry signal appears localized to vesicles located outside of the nucleus while eGFP is properly localized **(Fig. 4-2E)**. It is possible that the P2A self-cleaving peptide is not functioning properly when fused to insulin, resulting in a fusion protein packaged as Insulin, as we know Insulin is properly packaged in SC-β cells using

electron microscopy [81] and staining for both INS and CGA proteins in fixed ANGIs cells at stage 6 reveal nearly identical localization patterns **(Supplemental Fig. III-2)**.

Figure 4-2. ANGIs transgene expression profile after SC-β induction. A) Differentiation of 1016 ANGIs line results in significant mCherry signal after endocrine induction with increased eGFP signal with continued culture in stage 6 media. **B)** eGFP expression in the mCherry-positive sub-population increases with time in stage 6 of the SC-β protocol in ANGIs dual reporter cells. **C)** Real Time RT-PCR of cDNA generated from mCherry-positive, eGFP-negative/positive ANGIs SC-β cells in both clone 1 and clone 2 used for these studies. **D)** Epifluorescence in cryosections of differentiated ANGIs 1016 cells at stage 6 day 19. **E)** Structured Illumination Microscopy (SIM) superresolution image of an mCherry/eGFP co-positive SC-β cell

Figure 4-2 continued.

A

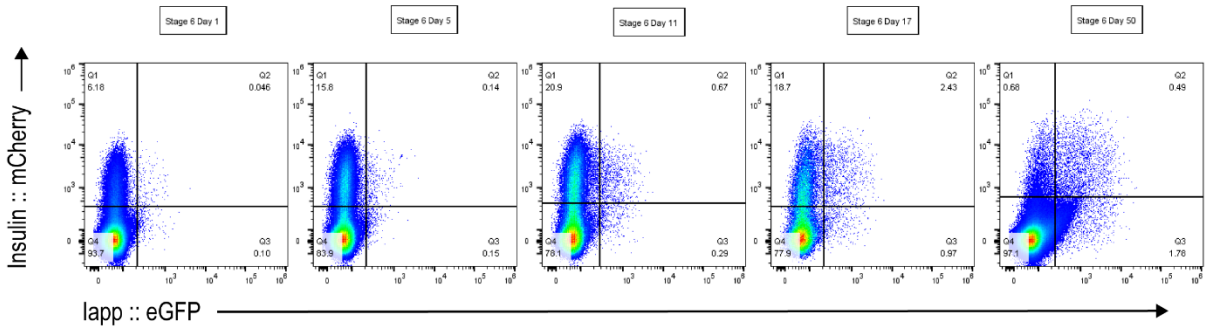

B

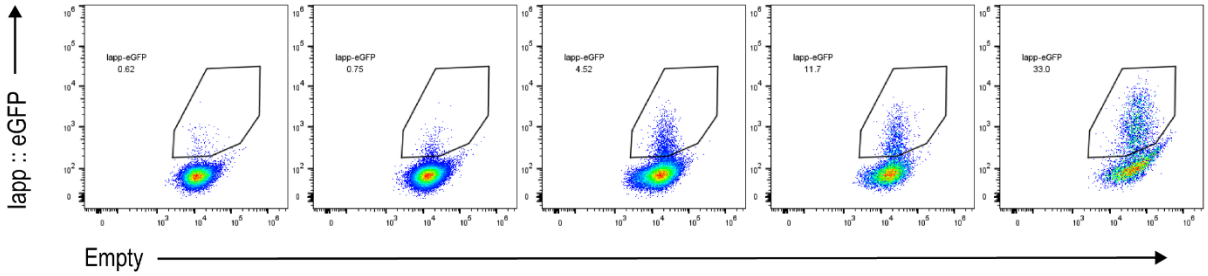

C

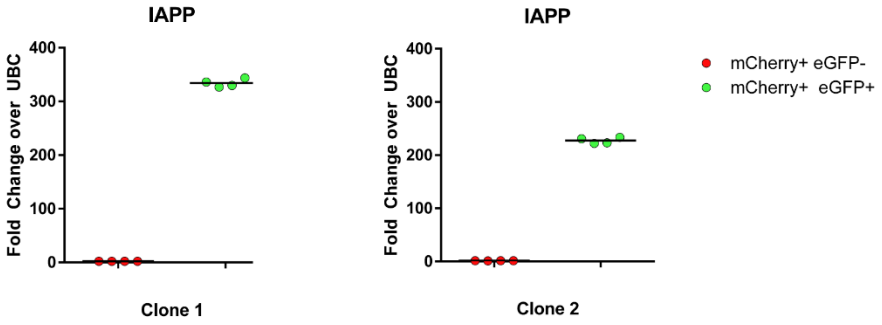

D

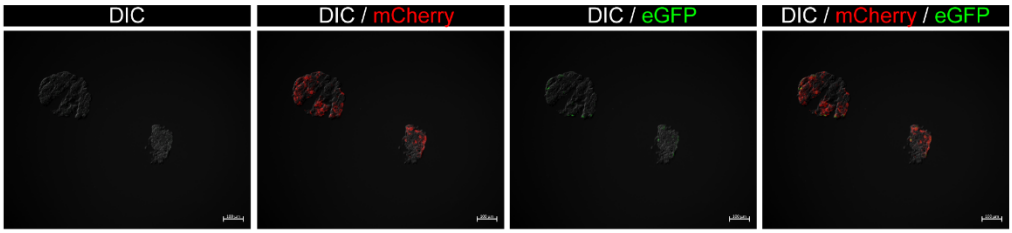

E

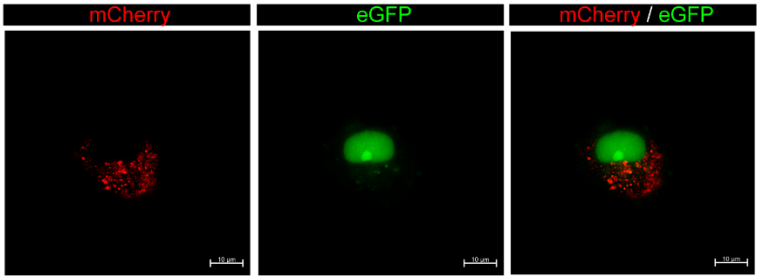

4.4 Enrichment of ANGIs Sub-populations

Sorting ANGIs SC-β cells between eGFP positive and negative subpopulations of the mCherry positive cells followed by reaggregation resulted in pure clusters with epifluorescence profiles as expected **(Fig. 4-3A)**. It has recently been reported that reaggregation of purified insulin-expressing cells results in a more mature GSIS profile than heterogenous clusters as a result of mitochondrial maturation of an unknown mechanism [105]. To determine if SC-β cells expressing IAPP have a different insulin secretion profile from those that do not, as well as to attempt to recapitulate this finding, we exposed both sets of mCherry-positive reaggregates to a single static GSIS assay. When normalized to total insulin content, both populations of SC-β cells exhibited similar insulin secretion proifiles as described for unsorted cells, with some glucose stimulation, but to a much lower degree than observed with KCl challenge or of the response observed in healthy cadaveric human islets **(Fig. 4-3B)**. It was notable that IAPP-expressing cells exhibit a lower basal insulin secreiton profile and a higher degree of insulin released after KCl compared to non-expressing cells, possibly as a result of more complete regulation of cytosolic calcium levels as suggested by our work with *in vivo* maturation, or due to autocrine signaling through the IAPP/calcitonin receptor axis [256]. When comparing raw insulin secretion values, however, it was apparent that SC-β cells expressing IAPP are capable of secreting insulin at an order of matnigude higher level than in non-IAPP expressing cells **(Fig. 4-3C)**. As proportional insulin release is similar between populations, IAPP-expressing cells also contain appriximatley 10-times higher levels of Insulin per cell compared to that of mCherry-only population **(Fig. 4-3D)**. While we do observe higher levels of insulin secretion regulatory genes after transplantation, insulin expression itself does not appear to change. To determine if insulin expression is higher in the IAPP-positive population we compared *INS* mRNA levels from sorted cells **(Fig. 4-3E)**. Strikingly, expression of the *INS* gene is also ten times higher in IAPP-expressing SC-β cells in both clones. Thus, in addition to more complete control of basal Insulin secretion levels, IAPP-

expressing SC-β cells also contain and produce approximately an order of magnitude more insulin than non-IAPP expressing cells.

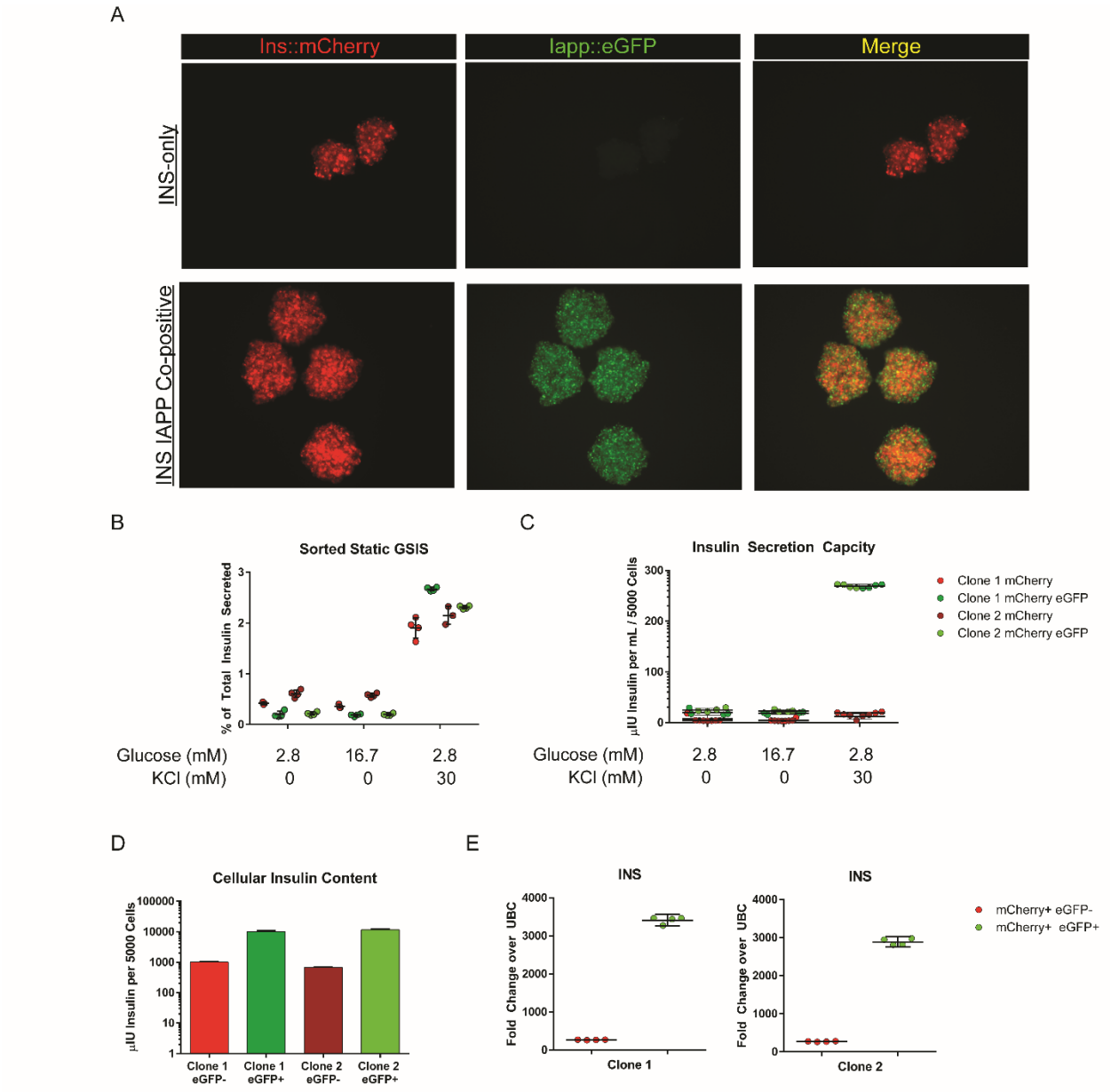

Figure 4-3. Insulin secretion capacity in IAPP-expressing SC-β Cells. A) Both clones 1 (shown here) and 2 of the ANGIs reporter line were sorted and reaggregated in 5,000 cell clusters after sorting. **B)** Sorted reaggregates were assayed for glucose responsiveness after reaggregation. **C)** Raw insulin secretion data from static GSIS analysis reveals significantly higher levels of insulin secreted by IAPP-expressing SC-β cells. **D)** Total cellular insulin content in IAPP expressing cells from clones 1 and 2 both reveal an order of magnitude higher insulin content in IAPP-expressing SC-β cells. **E)** Real Time RT-PCR of cDNA from sorted ANGIs clones reveals more than 10-times higher expression of *INS* mRNA in IAPP-expressing SC-β cells than IAPP-negative cells.

4.5 In vivo maturation of ANGIs SC-β Cells

Our initial observation that IAPP expression is associated with maturation was in the context of transplantation **(Fig. 4-1A)**. Continued culture of IAPP expressing SC-β cells *in vitro* reached a plateau of less than half of the mCherry-positive population. To determine if this was also the case *in vivo*, both ANGIs clones were differentiated and transplanted under the kidney capsule of SCID-Beige mice for 10 weeks **(Fig. 4-4A,Supplemental Fig. III-4)**. Grafts continued to demonstrate improved GSIS over time with a high degree of variability as we observed previously in Chapter 3. Serum insulin levels continued to rise as expected from week 1 **(Fig. 4-4B, Supplemental Fig. III-4)** to week 9 **(Fig. 4-4C, Supplemental Fig. III-4)**. After *in vivo* maturation, mice were sacrificed and transplants were dissociated and ANGIs SC-β cells were analyzed by FACS. Strikingly, while cells at the time of trasnplantation contained less than 10% eGFP expression within the mCherry population, 10 weeks *in vivo* resulted in nearly 100% expression of eGFP within the Insulin::mCherry positive sub-population, indicating that *in vivo* maturation produces a fully mature IAPP expression profile in SC-β cells within 10 weeks, as opposed to the partially mature IAPP expresion profile *in vitro* after prolonged culture **(Fig. 4-4D)**. Analysis of all differentiations from both clones before and after transplantation revealed remarkably similar results **(Fig. 4-4E)**.

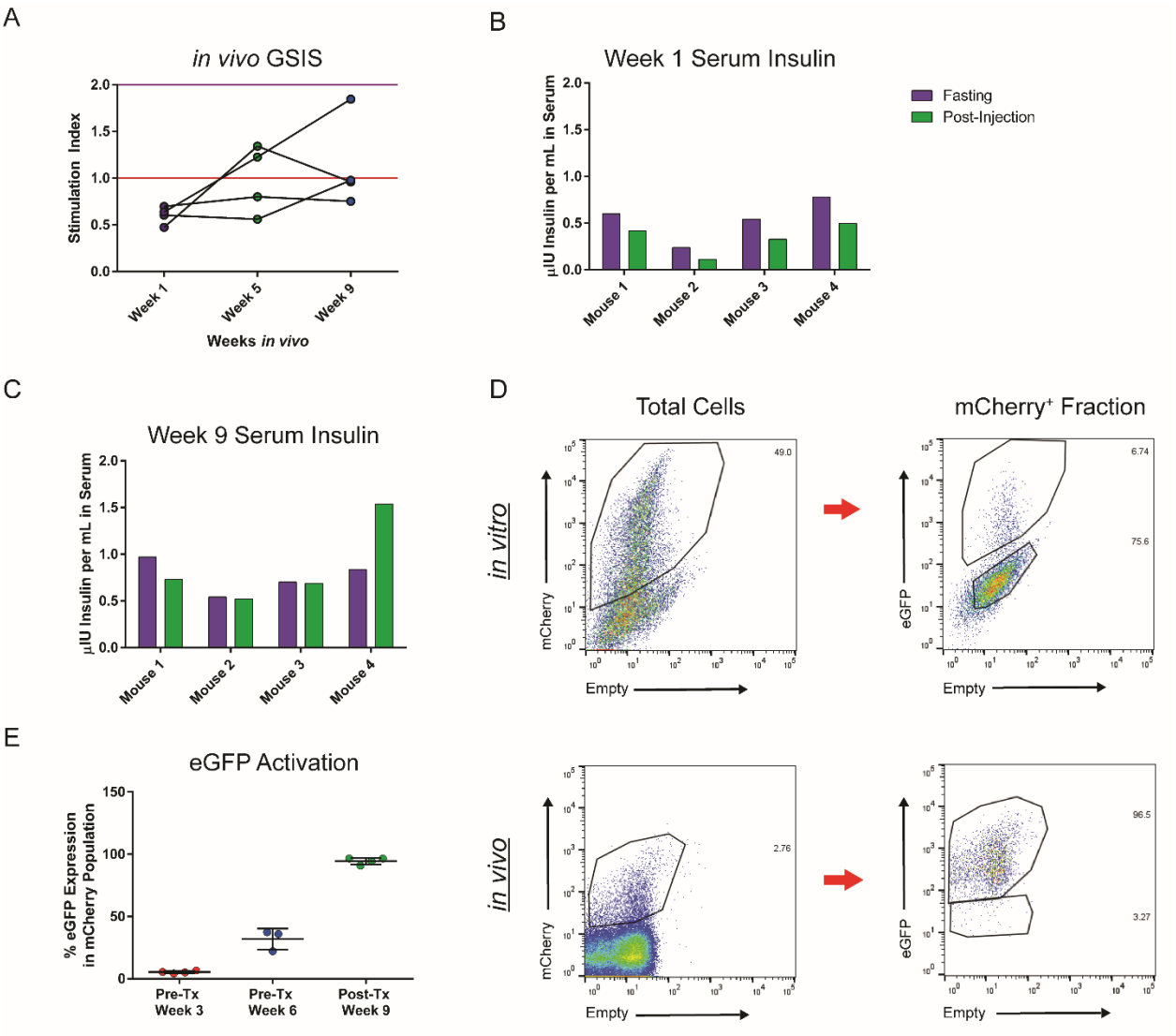

Figure 4-4. *in vivo* maturation of SC-β cells results higher IAPP expression post-transplantation. A) STIM index of a cohort of SC-β transplanted SCID-Beige mice with SC-β cells derived from Clone 1 of the ANGIs dual reporter line. **B)** Serum levels of human insulin before and after intra-peritoneal glucose injection one-week **C)** and nine weeks after transplantation. **D)** Flow cytometry on dissociated cells before transplantation (top row) or dissociated grafts after transplantation (bottom row). **E)** Comparison of data from both ANGIs clones 1 and 2 during differentiation *in vitro* and after *in vivo* maturation reveals near complete maturation of IAPP expression after 9 weeks of transplantation.

4.6 Gene Expression in ANGIs Subpopulations

RNA Seq analysis was performed on sorted ANGIs subpopulations from both clones at the same time as reaggregation for functional testing. Remarkably few genes (84) were differentially expressed ($P < 0.001$ and fold-change > 2) between the mCherry positive cells that were eGFP positive/negative after two weeks in stage 6. Of the differentially expressed genes, we observed IAPP as expected. We also observed *PCSK1* up-regulation, indicating that insulin processing may also be more efficient in the IAPP-expressing subpopulation to facilitate higher insulin expression. We also observed increased *HOPX*, a transcription factor present in our *in vivo* maturation dataset and identified as a differentially expressed gene missing *in vitro* and up-regulated during human fetal pancreatic development **(Fig. 4-5A)** [86]. Genes down-regulated transcripts included *GHRL*, *GCG*, and *DPP4*, a transcript expressed from the opposite strand of the *GCG* locus **(Fig. 4-5B)** in α cells, which functions to degrade the incretin hormone GLP-1 and is the target of some anti-diabetes drugs [280]. Analysis of islet endocrine hormones revealed higher expression of both *IAPP* and *INS* in the $eGFP^+$ subpopulation, as well as decreased expression of all other islet hormones except for *ADCYAP1,* which was not expressed at a higher level in IAPP-positive cells, suggesting that its up-regulation is specific to the *in vivo* maturation process **(Fig 4-5B)** and not a characteristic of $IAPP^+$ cells *in vitro*. Analysis of other differentially expressed transcripts potentially related to islet function ($P < 0.05$) identified other genes including the lncRNA *PLUTO*, expressed from the *PDX1* locus in the opposite direction from the *PDX1* promoter region. *PLUTO* is implicated in facilitating PDX1 transcription factor activity and is lost in diabetic islets [281]. We also identified downregulation of the vesicular glutamate transporter *SLC17A6* **(Fig. 4-5C)** [282]. Both of these genes may be facilitating increased insulin transcription and packaging in the SC-β cell. We also observed decreased expression of *CCND2*, whose expression is low in non-replicating β cells, as well as a member of the disallowed monocarboxylate transporter protein family *SLC16A7*, which is characteristic of α cells but not functional β cells [121]. Lastly, we examined expression of transcription factors responsible for

guiding islet endocrine lineages during development **(Fig. 4-5D)**. Interestingly, we did not observe significantly different expression of β cell lineage genes including *NKX6.1* or *PDX1* which would differentiate between α and β cell subpopulations. We did, however, observe much less expression of the α cell-specific transcription factor *ARX* in IAPP-expressing cells, which supports observed decreases in *GCG* and *DPP4* expression [76]. Together, these results suggest that the IAPP-expressing subpopulation of SC-β cells may be more β cell-like in nature. This is supported by decreased expression of other islet endocrine lineage markers and lower expression of transcription factors that drive other lineages during pancreatic development. In addition, these cells also express higher insulin as well as the insulin processing enzyme PCSK1, suggesting a higher capacity for generating and storing insulin.

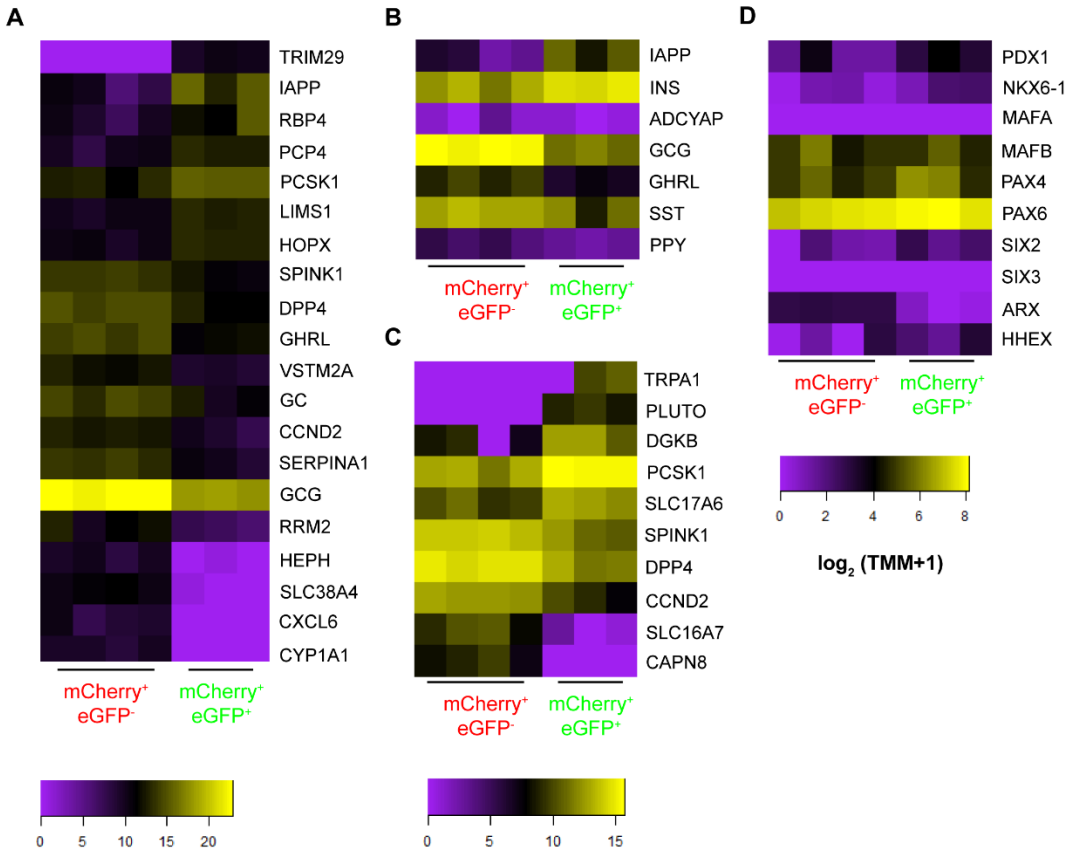

Figure 4-5. RNA seq analysis of ANGIs subpopulations. **A)** Differentially expressed transcripts between IAPP positive and negative subpopulations (P < 0.001, Fold change > 2). **B)** Endocrine hormone expression in sorted cells. **C)** Differentially expressed transcripts pertaining to islet function (P < 0.05). **D)** Expression of lineage-defining transcription factors.

4.7 IAPP-expressing SC-β Cells Retain Stable Insulin Expression

Expression of IAPP is correlated with higher expression of key β cell genes regulating insulin processing and correlated with maturation. It is also associated with decreased expression of other endocrine cell lineages. Our laboratory and others have demonstrated that poly-hormonal cells do not thrive as β cells after transplantation [81, 83, 84]. In addition, polyhormonal cells may resolve into α cells either after transplantation as we observed, or after prolonged culture *in vitro*, as has been observed in α cell differentiation protocols [91]. To determine whether IAPP-expressing cells may be more stable over long-term culture *in vitro* compared to IAPP-negative insulin-expressing cells, we sorted mCherry-positive, eGFP-positive/negative ANGIs subpopulations and reaggregated clusters for up to 50 days *in vitro*. While 72 hours after reaggregation nearly all cells were insulin-positive by epifluorescence imaging **(Fig. 4-6A)**, 6 days post-reaggregation clusters had much lower mCherry signal in the eGFP-negative population **(Fig. 4-6B)**. This trend continued at each time point observed **(Fig. 4-6C)**. To better-quantify this phenomenon we dissociated cells after 12 days of post-reaggregation and analyzed transgene expression. Strikingly, less than one quarter of cells that did not express eGFP at the time of sorting retained mCherry signal after 12 days. In contrast, nearly 70 percent of eGFP positive cells retained their expression of *INS* **(Fig. 4-6D)**. It is unclear if mCherry negative cells in these reaggregates resolved into other lineages or comprised dead cells from the reaggregates. Of the cells that did retain mCherry expression after sorting for lack of eGFP expression, only some of the cell population was able to activate eGFP expression over 12 days, likely reflecting the activation of the transgene observed over normal stage 6 culture. In contrast, most of the cells sorted for eGFP remained eGFP positive after culture, though some of this expression was lost after reaggregation, suggesting that the more mature SC-β state may be in flux with prolonged culture or after stressful processes such as sorting and reaggregation **(Fig. 4-6E)**.

Figure 4-6. Long-term culture of reaggregated ANGIs subpopulations. ANGIs differentiations were sorted and reaggregated into mCherry^{+} and eGFP$^{+/-}$ populations for **A)** 3 days (4x magnification), **B)** 6 days (10x magnification), and **C)** 9 days (10x magnification). **D)** Live cell flow cytometry 12 days after reaggregation for mCherry expression. **E)** Flow cytometry on the mCherry-positive subpopulation from reaggregates.

Figure 4-6 continued.

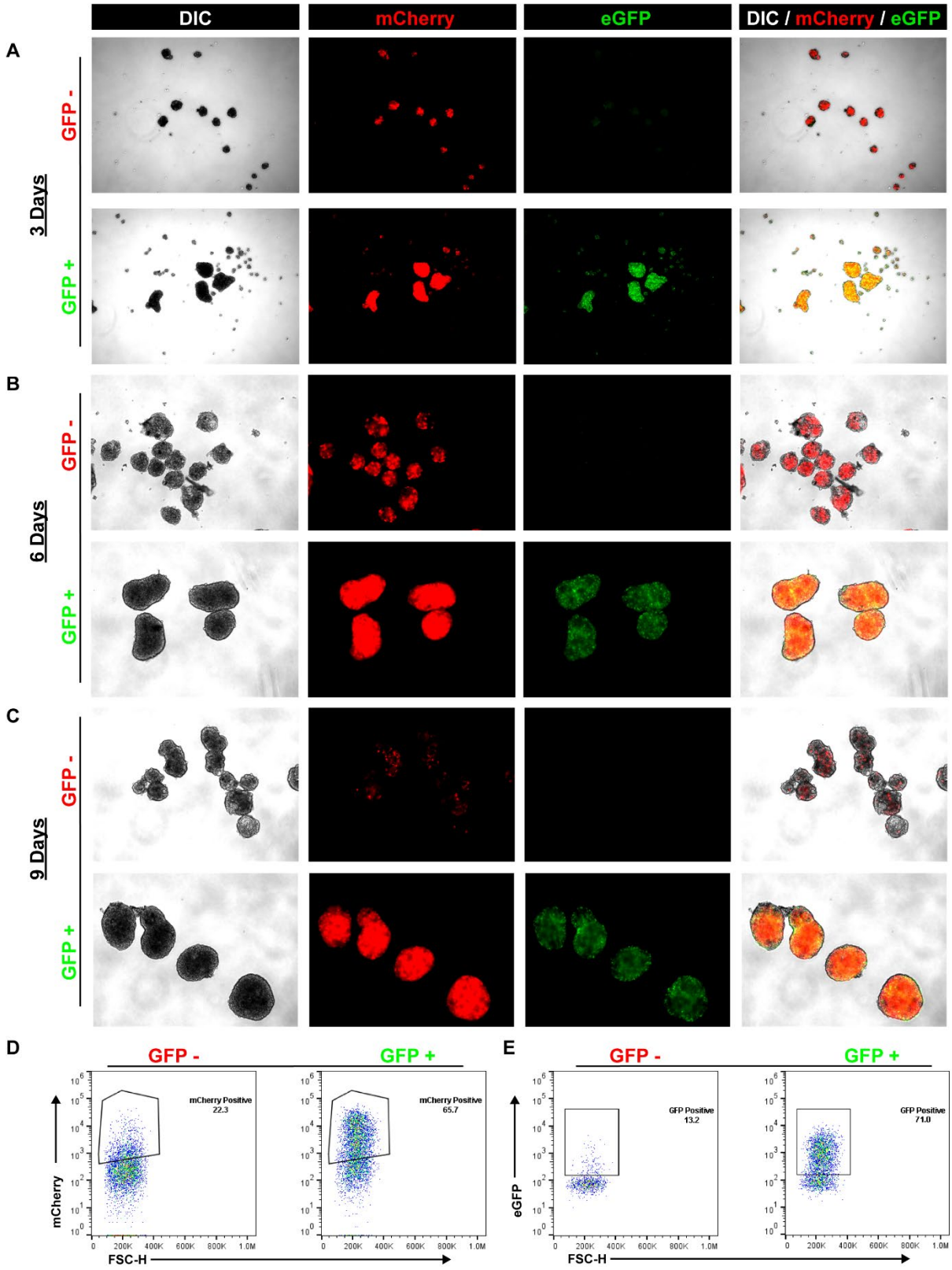

4.8 Discussion:

Maturation of SC-β cells has been a focus of numerous publications after initial reports of protocols to differentiate insulin-producing cells *in vitro* [283]. These approaches have attempted to further mature the function of SC-β cells and GSIS *in vitro*. This was also our initial focus in choosing IAPP, a gene associated with co-expression networks that are dynamically regulated during *in vivo* maturation as SC-β cells improve glucose responsiveness while up-regulating transcripts associated perinatal islet development. While IAPP expression correlates with increased cellular insulin content and expression as well as improved regulation of insulin release, its expression alone does not rescue mature glucose sensing *in vitro*. This may be unsurprising given the metabolic nature of GSIS inhibition in SC-β cells. Nevertheless, it appears that SC-β cells expressing IAPP are a more developmentally mature subpopulation in differentiation, and it our current definition of SC-β cells as Nkx6.1/C-peptide expressing cells could be updated to include IAPP. It remains to be seen whether these cells are the only cells to maintain insulin expression after transplantation, or whether *in vivo* maturation induces IAPP expression from other cells which do not autonomously achieve IAPP expression *in vitro*. These studies are ongoing. Given that IAPP was also identified in the GABA co-expression network in the previous chapter, we also tried culturing ANGIs SC-β clusters for 7 days in the same GABA concentrations used for GSIS experiments. We did not observe a significant change in population ratios after 7 days in culture **(Supplemental Fig. III-5)**.

To date, differentiation of SC-β cells is considered complete after 10-20 days of differentiation into stage 6 of our protocol [81], defined by simple maintenance of SC-β cells in culture medium without additional growth factors. Here, we report that IAPP expression peaks several weeks into stage 6 of differentiation **(Fig. 4-2A)**. An additional 30 days for maximal induction of IAPP is a large burden on the timescale of differentiation and planning for experimental use of cells. Waiting for maximal induction of IAPP would result in a differentiation

that takes 1/6 of a year to complete. It seems that this is a ripe opportunity for small molecule screens to expedite the maturation of SC-β cells *in vitro*, possibly resulting in a seventh stage of culture after IAPP induction. Here we have provided the first steps toward that goal, with a dual knock-in reporter line capable of real time monitoring of both *INS* and *IAPP* expression. This report has also identified a number of potential transcriptional regulators of IAPP including TRIM29, HOPX, and PLAGL1 which are now being tested for the ability to induce IAPP expression and facilitate a more rapid maturation to insulin/IAPP co-positive SC-β cells without the need to wait nearly two months in stage 6 for maturation to occur at its own pace. Such a screen may also increase the overall population size of mature SC-β cells, defined by Nkx6.1/C-peptide/IAPP even after 50 days of culture.

This observation also invokes a question of timing when inducing differentiation of pluripotent stem cells in an attempt to recapitulate normal fetal development. Whether some events that take months to occur naturally can truly, fully occur at the rapid speeds achieved through *in vitro* differentiation remains to be seen. It is likely this step can be facilitated more rapidly, as insulin expression is induced long before IAPP in this protocol, and IAPP expression may even precede insulin induction in the developing pancreas. On the other hand, precocious induction of insulin resulted in poly-hormonal endocrine cell types not observed during normal development in earlier iterations of SC-β protocols, and only by delaying onset of NGN3 induction and allowing a true pancreatic progenitor population co-positive for Nkx61 and PDX1 to undergo endocrine specification was it possible to induce NKX6.1-copositive SC-β cells capable of glucose response and survival post-transplantation [81, 88, 89].

In addition to IAPP expression, it is also apparent that ADCYAP1 is not fully induced as IAPP expression increases over time. It was our hope that cells expressing *IAPP* would also harbor increased levels of *ADCYAP1* transcript. After developing a protocol to induce timely expression of IAPP, it may be worth inducing ADCYAP1 expression; the two secreted hormones

act in opposing roles with IAPP reducing basal secretion of Insulin and ADCYAP1 stimulating cAMP production and amplifying calcium transients in stimulated β cells after glucose exposure. To combine both effects would produce SC-β cells with improved control over stimulus-secretion coupling resulting in a differentiated cell type that will more responsively maintain glucose homeostasis toward a cell-based therapy for diabetes. This work has added IAPP into the discussion for markers and characteristics of SC-β cells *in vitro* and provided a tool to produce more hormonally-mature SC-β cells in the form of the ANGIs dual knock-in reporter line.

Chapter 5: Discussion

5.1 Metabolism and Glucose Sensing in SC-β Cells

Appropriate secretion of insulin is necessary to maintain life and balance energy homeostasis; the ability of SC-β cells to maintain this balance is crucial for their potential therapeutic value. This work is the first to analyze insulin secretion capacity at this depth in SC-β cells and will be among the first report to suggest a molecular target to improve GSIS to the magnitude observed in healthy cadaveric islets.

Insulin secretion assays in SC-β cells have been reported using both static incubation and dynamic perifusion methods [81, 88, 89, 104, 105]. Static GSIS reports have demonstrated much less glucose responsiveness than has been observed in healthy mouse rat and human models, with fold-changes reported less than 5 in all publications to date. These methods have used sequential challenges of large numbers of SC-β cells in a small number of replicates. Here, we demonstrate a more robust and sensitive method to measure Insulin release using reaggregated SC-β cells, with stimulation indices reaching 20-30 for KCl. Using metabolic intermediates, we were able to achieve these levels of Insulin secretion, similar to healthy human islets that also demonstrate a similar magnitude of insulin release in response to glucose and KCl stimulation [98]. This method of insulin secretion analysis also allows for hundreds of measurements to be made at the same time, increasing experimental capacity and allowing for dose-response analysis in multiple conditions. We have also used total insulin content as a normalization method between experiments. This allows for a more direct comparison between differentiations which may have variability in differentiation efficiency as well as differences in insulin content as insulin stores accumulate with time at the end of differentiation. Other methods reported have normalized to total cell numbers and total DNA extracted from samples. Both of these normalization methods are incomplete, as they overestimate the cell mass being measured, as all cells present, regardless of insulin expression are measured in both methods. This method is also easier, as it is incorporated into the insulin measurements necessary for the GSIS protocol.

Our work with SC-β cells demonstrated that in many ways our cells are indistinguishable from the human islet. Encouragingly, many aspects of their physiology which have not yet been investigated were strikingly similar to the human islet, including glucose uptake measurements, mitochondrial mass, early glycolysis, and response to some cell-permeable metabolites. While we knew that SC-β cells expressed similar levels of characteristic β cell transcripts [81], the ability to undergo biphasic Insulin release at the magnitude and timing observed in the human islet is truly remarkable. Previous reports of glucose response have exhibited abnormal patterns of release without a first phase of secretion [89], or a completely absent second phase [104, 105]. In most of these experiments, Insulin release compared to cellular insulin content was not examined. With a more complete understanding of the dynamics of nutrient-dependent Insulin release in SC-β cells, we can be even more confident that these cells accurately recapitulate the mechanisms of insulin secretion observed in healthy cadaveric islets. While this work was not able to fix SC-β metabolism *in vitro*, the similarities between human islet and SC-β cell insulin secretion suggest that fixing this deficiency in GAPDH activity will result in a differentiated cell type poised to replace cadaveric human islets for curative transplantation in diabetic patients and provide a new platform for study of islet biology and *in vitro* diabetes models. These encouraging results leave us excited for studies of insulin secretory vesicle pool dynamics [96], F-actin remodeling in response to glucose challenge [102], calcium flux and homeostasis [94], and regulation of membrane voltage and re-polarization [93]. Regulation of calcium flux may be particularly interesting, as calcium transients were quite brief during methyl-3PG exposure and may reflect differences in SC-β cell calcium homeostasis from human islets. These studies will be tremendously informative and will likely allow us to ask new questions regarding human islet biology with the advantages that come with gene editing approaches and cell numbers that are currently unattainable from cadaveric tissue.

Our identification of GAPDH as the bottleneck in GSIS is striking, as GAPDH has not been described as a regulator of glycolytic flux in the β cell. Inhibition of GAPDH activity has mostly been described in the context of cell stress and apoptosis [188-191, 193, 195-197, 284-287], mediated by post-translational modifications that inhibit its ability to act as an enzyme and simultaneously allow its nuclear translocation by the GAPDH binding protein, SIAH-1 [188]. We have analyzed GAPDH for PTMs described previously and do not observe a significant amount of these modifications that can induce this inhibition and/or translocation. This is not entirely unexpected, as the loss of enzyme activity occurs before nuclear translocation in differentiation. It may not be a coincidence that the active GAPDH tetramer is lost during pancreatic specification in our differentiation protocol. In the healthy adult and rodent pancreas, we observe a mix of cytoplasmic and nuclear GAPDH in both the islet and acinar tissue. We also observe some nuclear GAPDH signal during endocrine specification during embryonic development, though at much lower rates. Whether this difference in enzyme activity is an artifact of *in vitro* culture and differentiation or due to an incomplete step in pancreatic specification will be important to determine. This will be a challenge for future iterations of protocols and will require innovative approaches to overcome. While induction of gene expression can be monitored with fluorescent protein coding transgenes, it will be necessary to devise a high throughput way to analyze GAPDH activity or to identify a novel interaction with GAPDH at the time of its inactivation to pursue a high throughput approach to improve culture conditions with the aim of restoring GAPDH activity.

Alternatively, closer attention to GAPDH during pancreas specification in the developing mouse may also be a model to study correct GAPDH modification and activity during differentiation, though limiting tissue and difficulty of isolating this early fetal structure will be challenging. While we were unable to detect any PTMs that could explain the lack of GAPDH enzymatic activity, there are hundreds of described PTMs that can regulate enzymatic function [288]. A more thorough analysis of the GAPDH PTM repertoire during the specification of

pancreatic endoderm in SC-β cells may be the best approach to identify what processes are inappropriately active or missing during *in vitro* differentiation resulting in inhibition of GAPDH activity and GSIS in the further differentiated SC-β cell. Proteomic analysis is a field that is rapidly advancing and improved sensitivity and ability to detect novel PTMs will be key toward understanding this bottleneck in differentiated islets [289].

Mixed nuclear and cytoplasmic distribution of GAPDH in functional islets poses several questions about the role of GAPDH in pancreas biology. Perhaps most importantly, does nuclear GAPDH play a role in transcription or cell identity in the islet, and how does the localization of GAPDH in a single cell change over time? Modification of GAPDH to manipulate its subcellular localization and fusing GAPDH to a fluorescent protein would be logical approaches to answer these questions [287]. While moonlighting enzymes are thought to be playing roles in different compartments separate from their metabolic activity [202, 204], it is tempting to think that subcellular localization of NADH production from GAPDH could regulate some processes, especially in the nucleus given the role of NADH as a reducing capable of regulating transcription [290, 291].

Use of lineage markers and gene expression profiling alone may not be sufficient to demonstrate that differentiated tissues are equivalent to the *bona fide* human tissues desired, and without a complete understanding of the limitations or shortcomings of stem cell-derived models we may miss or overlook potential caveats in experimental design. It is possible that a biochemical approach similar to our work using MIMOSA could prove valuable in other tissues, especially differentiation of tissues whose metabolism and energy balance plays a critical role in normal function such as liver, kidney, and endothelial cells. Gene expression is in many ways easier to analyze and benefits from the ability to amplify measurable signal from very little starting material as well as its origin from a finite set of molecular instructions from which to produce align-able, readable signals. With advances in mass spectrometry and the development of tools to catalog

and quantify metabolites, metabolomic analysis may have its time in the spotlight in characterizing stem cell-derived tissues.

Our findings that metabolic intermediates such as methyl succinate and glyceric acid can stimulate insulin release suggest that we may be able to supplement current SC-β cell products with these intermediates to simulate diabetic stress or to screen for compounds that generate β cell replication for therapy of T2D. Until it is possible to bypass inefficient GAPDH activity *in vitro*, these compounds may allow us to begin using SC-β cells for *in vitro* disease modeling before we fully recapitulate islet biology in differentiated cells. This may also present other challenges through bypassing normal glucose uptake and early glycolysis, for example if these early metabolites play a permissive role in β cell replication or stress, these aspects of the biology will be missing from disease modeling in our cells until glucose sensing is re-established. These issues have been raised with some of the intermediates used in this study, as super stimulation of mitochondrial metabolism at the expense of glycolysis can in some contexts shift metabolic balances away from physiological conditions [181, 182, 292]. Nonetheless, cell-permeable intermediates may be useful tool compounds to prove human islet biology with current protocols available.

The experiments performed in our analysis of SC-β cells were in many cases validating or repeating classical experiments performed in the islet [98, 176]. This approach may prove valuable in other tissues derived from stem cells. The novel applications and disease models that have become available with differentiated human tissues from pluripotent stem cells are vast and will provide insight into mechanisms of development and disease in the human that would not be possible otherwise. One of the challenges present in rodent models of human disease are the unknown or unavoidable differences in mouse and human biology. It is possible that with the advent of stem cell-derived tissues that similar challenges will become evident. Only by interrogating these models and confirming the biology we take for granted in primary tissues can

we fully trust the models of disease and development that are rapidly becoming available to researchers and avoid potential pitfalls or overly broad interpretation of results.

5.2 in vivo Maturation of SC-β Cells

in vitro GSIS profiles of human islets are not well-correlated with transplantation outcome. Rather, islet health and inflammation are thought to limit transplantation efficacy [45, 293]. This also appears to be true of SC-β cells, as GSIS profiles *in vitro* do not predict functionality of grafts after transplantation. For this reason, rescuing functional glucose sensing in SC-β cells may not be necessary to solve before these cells are clinically useful. However, even if transplantation rescues function of SC-β cells, the processes regulating this phenomenon are not known, and significant variability in transplantation outcome from the same differentiation among host mice suggests that mechanisms underlying this maturation are not a guarantee after each transplantation. In addition, for these cells to be used as a platform for drug discovery and human developmental biology, glucose responsiveness must be further improved. In order to better-understand what aspects of β cell physiology are improved after transplantation we analyzed gene expression changes after maturation *in vivo* for 6 weeks.

Gene expression changes during *in vivo* maturation do not directly implicate metabolic shifts after transplantation. This is not too surprising, as gene expression analysis in other studies have not been able to identify metabolic defects in SC-β cells, GAPDH as a glycolytic bottleneck in GSIS appears to be at a post-translational block. Instead, we observed other aspects of β cell biology maturing that will contribute to a more complete β cell phenotype as metabolism is corrected. It will be of interest to determine how modifications of GAPDH correlate with improved GSIS over time, though without a measurable modification or known process to monitor, it is not yet possible to directly monitor GAPDH activity as transplants mature. When this does become a possibility, we have demonstrated that the 6-week time point may be the appropriate *in vivo* maturation window to examine how GAPDH activity is modified after transplant.

RNA Seq analysis indicates calcium homeostasis, exocytotic machinery, and induced expression of other β cell hormones are components of *in vivo* maturation. While these processes may not directly resolve functionality via bypassing the observed bottleneck in GAPDH activity, we have identified a number of potential transcriptional hubs that could modify insulin secretion and may be markers of more mature SC-β cells. In particular, IAPP and ADCYAP1 would appear to be excellent markers of more mature SC-β cells, as these are both β cell-specific hormones and IAPP is known to play a role in islet dysfunction through the deposition of amyloid plaques that are toxic to cells [250]. More investigation into IAPP as a potential marker of mature SC-β cells is warranted and initial experiments suggest this is a promising avenue to pursue further *in vitro* maturation.

One common characteristic of transplanted SC-β cells is the increase in secreted Insulin over time as transplants mature. Recent reports have demonstrated detectable Insulin secretion in response to glucose challenge as early as three days after transplantation [105], though how these changes are observed before vascularization has been achieved is unclear [235, 236]. A concerted effort to profile and quantify insulin release over time as transplants mature will be necessary in order to measure and predict the number of cells needed to achieve a therapeutic but safe threshold of insulin secretion after transplantation as well as determine how long improvement continues after transplant. If insulin content continues to increase after transplantation, it may be necessary to deliver a sub-therapeutic dose to the patient to prevent hypoglycemic excursions. Alternatively, with the data presented here it may be possible to mature SC-β cells *in vitro* in order to avoid this progressive Increase in secreted Insulin in response to glucose challenge *in vivo*.

Transplantation of stem cell-derived β cells for curative diabetes therapy is a realistic goal in the coming decade. Analysis of transplantation has so far been limited to demonstration of little to no tumor formation after transplant and the ability to maintain survival in transplanted animals

after diabetes induction. The current standard of care for diabetic patients is injection of exogenous Insulin to regulate blood sugar. This therapy is not ideal, as brief but recurring hyperglycemic excursions over time cause microvascular complications, resulting in nephropathies, neuropathies, and retinopathies among other complications [205]. In order for SC-β cells to join human islets in replacing exogenous Insulin therapies, the capacity of these cells to maintain normoglycemia more efficiently than insulin injection and a direct comparison of their efficacy to cadaveric islet tissues must be demonstrated. SC-β cells have been shown to decrease overall glycemic levels in diabetic animals and exhibit improved GSIS with prolonged transplantation time. Studies must now be done using continuous glucose monitoring, HbA1c measurements [294], and analysis of other diabetes comorbidities to insulin pump therapies to demonstrate if SC-β cells are in fact a more efficacious treatment for T1D than insulin therapy [9]. While human islet transplantation using the Edmonton protocol has successfully produced insulin independence in patients [42], long-term transplantation outcome is still less-than-desirable, with fewer than 10% of patients maintaining normoglycemia 10 years after transplantation [43, 45]. In addition, human islets transplanted into the liver may not function as well as islets from whole-pancreas transplants [295]. Reasons for this loss of function are not well-understood but should be considered in the context of *in vivo* function and maturation of these cells. It is possible we need to strive beyond an *in vivo* matured-like cell to fully cure diabetes after transplantation of SC-β cells.

Analysis of SC-β cells after 2 months of maturation *in vivo* reveals that there are still many differences between SC-β cell gene expression and human islets. It is unclear how long SC-β cells must remain under the kidney to achieve as mature a state as possible *in vivo*. Time course analysis and longer *in vivo* experiments may be necessary to address this question, though longer transplant times and large cohorts for analysis will be technically challenging and expensive. Perhaps rather than further gene expression analyses, more detailed study of graft function would

be informative. Experiments using hyperglycemic clamps [296], the *in vivo* counterpart to dynamic perifusion experiments, as well as transplant into sites with more thorough imaging capabilities such as the anterior chamber of the eye may allow us more detailed access to monitor the transplants [297, 298]. Combination of genetic reporters for β cell markers along with biosensors such as the GCaMP Calcium sensor or membrane Voltage sensors would be useful to analyze Insulin release and glucose sensing in real time in the same animal [299, 300]. These experiments may also pose more or less stress to the animal, and the environmental effects on Insulin release in live animals is hard to understate: adrenaline and other stress-related hormone signaling is undoubtedly in flux as animals are handled and bled during *in vivo* GSIS assays. Analysis of transplanted SC-β cells in other models may also be informative, as previous work has demonstrated that rats are a more suitable transplantation host than mice for pancreatic progenitors [301]. It may be necessary to observe SC-β cells in diabetic non-human primate models to observe functional maturation in a more human-like model.

5.3 IAPP Dual Reporter

Our identification of IAPP as a maturation marker for stem cell-derived β cells is both useful and surprising. IAPP is a β cell-specific peptide hormone co-secreted with Insulin at a ratio of 100:1 (INS:IAPP) and modulates the activity of Insulin by regulating satiety and glucose utilization after Insulin-dependent glucose uptake and suppressing its secretion in an autocrine manner [220, 250, 253, 254, 260]. We chose IAPP as a potential marker of mature SC-β cells because it was known to be β cell specific, was strongly up-regulated after transplantation and functional maturation, and clustered with other functionally important β cell genes after MEGENA co-expression network analysis.

SC-β cells expressing IAPP are more stable than IAPP-negative cells which may revert into other endocrine cell lineages with prolonged culture. These cells have nearly 10 times more insulin content per cell, better-regulate basal Insulin secretion, and express *in vivo* maturation

associated genes at a higher level than IAPP-negative SC-β cells, even though NKX6.1 expression is present in both sub-populations at similar levels. The ANGIs iPS line now gives us a chance to study aspects of SC-β cell induction including epigenetic states of polyhormonal and mono-hormonal SC-β cells and is a tool to enrich more mature SC-β cells than Insulin reporter lines alone are capable of. This line will also be facilitate small molecule screens to identify inducers of SC-β cell maturation more quickly *in vitro* as well as compounds that can increase induction efficiency of SC-β cells over time.

It is curious that the insulin::P2A-mCherry transgene does not fully cleave and results in a fusion protein localized to the secretory vesicles, as the same construct design was used to create the IAPP::P2A-eGFP sequence. Both peptides are flanked by a triple nuclear localization sequence signal on the N and C-termini of the cleaved peptide, but in the same cell one peptide sequence is successfully cleaved and properly localized while the other peptide sequence survives translation, resulting in an Insulin fusion protein. It is possible that the translational machinery responsible for Insulin translation may be different than that for IAPP. This could be at the level of Ribosomal ribonucleoprotein structure, or Insulin-specific chaperones located at the ER membrane as translation occurs. While this was not the original intent of the reporter line, it is an unexpected finding and hints at unique regulation of insulin synthesis. Perhaps this is not surprising for a transcript that accounts for such a large percentage of translation occurring within the cell [302].

In addition to maturation, it is also in the interest of the SC-β field to induce IAPP expression in SC-β cells, as it would be invaluable to have a human islet model to study toxic oligomer formation in SC-β cells [250, 252, 254, 272, 276, 303-307]. IAPP is the first amyloidogenic protein discovered, which was identified by biochemical analysis of plaques present in diabetic pancreata [275]. The IAPP peptide sequence in rodents is not amyloidogenic, and thus the potential role of amyloid fibrils in driving or exacerbating diabetic stress in the islet

has not been well-studied [247, 259, 278]. A model in which to visualize expression of a potential dysregulated and toxic protein as well as understand the independent regulation of IAPP from insulin in the islet β cell could prove invaluable, offering a chance to both identify therapeutic targets to avoid amyloid fibril toxicity as well as produce SC-β cells with a higher capacity to secrete Insulin and exist stably after transplantation. Going forward it will be interesting to determine if the stability of IAPP-expressing SC-β cells *in vitro* is also true after transplantation and could be analyzed by sorting for eGFP-positive and negative cells expressing mCherry and transplanting each population under a different kidney in the same mouse, asking how much mCherry expression persists after several weeks *in vivo*.

5.4 The Next 10 Years of Stem Cell-derived B Cells:

The first reports of SC-β cells able to respond to glucose and thrive after transplantation was published 4.5 years ago [81, 89]. Since that time protocols have been developed to produce more functionally mature cells as defined by gene expression and by GSIS profiles *in vitro* [104, 105, 116]. With this report and others, it is possible that newer protocols will transition from broader characterization-based approaches to more targeted screens to improve cell identity and function. It may also be beneficial for groups to stop examining a generic GSIS phenotype of Insulin secretion and focus on individual processes, such as maintaining de- and re-polarization, calcium flux dynamics, or even GAPDH activity. These approaches may be more applicable between protocols and will provide a more hypothesis-driven method to improve SC-β cell differentiation protocols.

It is our hope that GSIS assays will also become more standardized in the years to come. At the moment, each SC-β cell publication appears to have performed GSIS differently and choosing a standardized protocol with the best sensitivity and reproducibility will be valuable. In the same vein, it would be prudent to require groups claiming improved function or a modification of current SC-β protocols to demonstrate efficacy in more than one genetic background in order

to ensure lessons learned are applicable to most differentiations and protocols do not drift apart from line-to-line as they evolve. Differentiating SC-β cells and changing differentiation protocols will also require authors to address an important question: are the cells being produced fundamentally more or less functional or has a media or culture-based modification changed Insulin secretion profiles without addressing a more basic deficiency in the cells. For example, GSIS phenotype in SC-β cells is easily manipulated by adding or subtracting serum in the final stage of differentiation [104]. However, switching culture conditions again reverts phenotypes and does not have a stable effect on the cells. Whether this is an actual improvement in differentiation protocol or whether this is a work-around for a larger issue needs to be addressed and agreed upon. This is analogous to culturing human islets in low or high glucose for 24 hours before GSIS [99]. Higher basal glucose culture can disrupt the insulin secretion phenotype, but changes in basal media are not permanently changing the cell types within the islet. This is in part a semantic argument, but certainly not in the context of therapeutic potential of SC-β cells or the proper characterization of cells for transplantation into humans.

Other cell types present within the SC-β differentiations have so far been referred to as “poly-hormonal” cells [81, 84, 86, 89], and their presence has been dismissed as a hurdle to be addressed. However, the human islet does not only contain β cells. Controlling ratios of other endocrine lineages either through a single protocol or reaggregation of multiple cell types differentiated in separate protocols may be an interesting approach to model intra-islet interactions as well as produce islets capable of maintaining normoglycemia but ensuring the transplant recipient is equally protected from hypoglycemic episodes. Complexity of differentiation protocols will increase dramatically with multiple cell types generated at once, but this may be the only way to generate a fully islet-like cluster of cells from a pluripotent source. Indeed, it is known that α cell function is lost in diabetes and without replacing the β cell population of the endogenous islet it may be necessary to supply new α cells to regain control of glucagon secretion [308].

Disease modeling in SC-β cells will likely far-outlast the current challenges we face in producing a fully functional islet. T2D modeling in SC-β cells will allow for screens and models incorporating IAPP oligomeric studies as mentioned earlier as well as insulinotropic and replication-based screens ensuring results are applicable to human biology. The combination of non-replicative β cells as starting material as well as the ability to conduct extensive gene editing in these cells makes SC-β cells a promising model for the study of T2D stress and replication *in vitro*. Recapitulating T1D will be more complicated but is a completely unexplored space for *ex vivo* disease modeling. Only with the ability to make genetically matched SC-β cells to donor blood samples can we observe autoimmune β cell destruction *ex vivo* [57, 58, 309]. These studies allow us to bypass species barriers that exist in replicating T1D autoimmunity as well as begin to observe the initial events that precede and proceed interaction of the healthy, unstressed islet with autoreactive T cells. This will likely be the most promising SC-β application other than direct cell therapies in patients and may be the most revealing set of experiments to learn new human islet biology. In order to fully realize this goal for *ex vivo* disease modeling, the most islet-like tissue will be a necessary starting point. The work described here has identified several approaches and tools toward that goal.

Appendix I

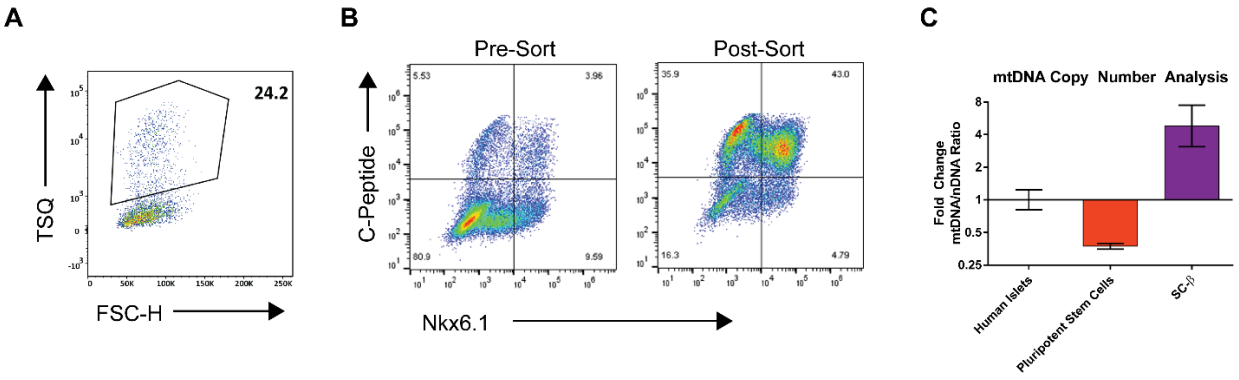

Supplemental Figure I-2. Enrichment of SC-β Cells A) Sorting based on zinc content using the TSQ dye reveals a zinc-containing sub-population. **B)** Flow cytometry analysis of cells before and after TSQ-based sorting for C-Peptide and Nkx6.1. **C)** Real Time RT-PCR analysis of cDNA for mitochondrial DNA normalized to genomic DNA.

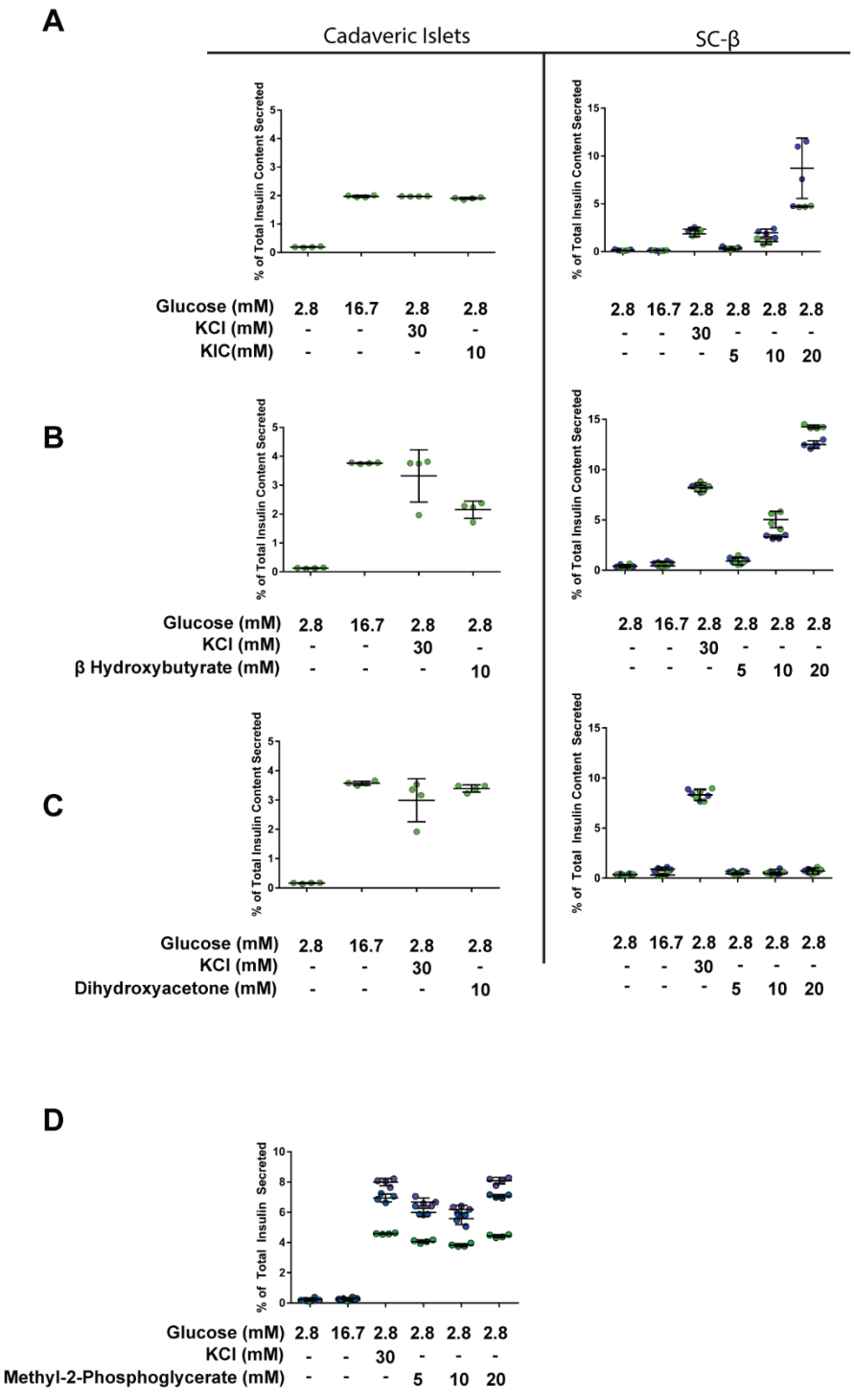

Supplemental Figure I-4. Secretagogues Continued. A) Cadaveric islet and SC-β cell response to ketoisocaproate (KIC) in static GSIS. **B)** Human islet and SC-β cell response to β hydroxybutyrate. **C)** Human islet and SC-β response to Dihydroxyacetone. **D)** SC-β cell response to methyl-2-Phosphoglycerate.

Supplemental Figure I-6. GAPDH Localization During Differentiation. A) GAPDH immunofluorescence staining throughout differentiation of SC-β cells. **B)** GSIS profiles of SC-β cells cultured in previously described basal media and current protocol “V8” medium with KCl stimulation for comparison. **C)** Western blot of lysates from DSS-crosslinked samples from SC-β differentiations in serum-supplemented (v1) or BCA-supplemented media (v8).

Supplemental Figure I-6 continued.

A

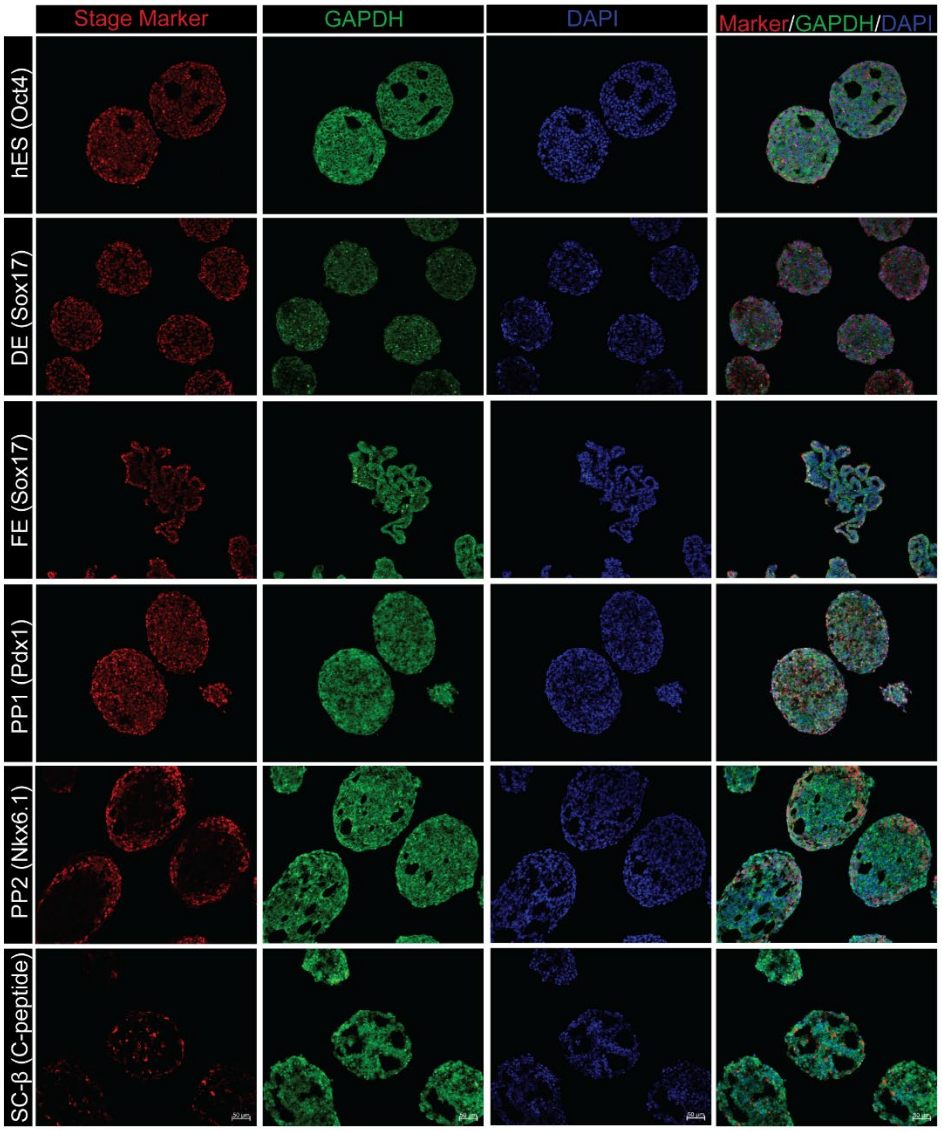

B

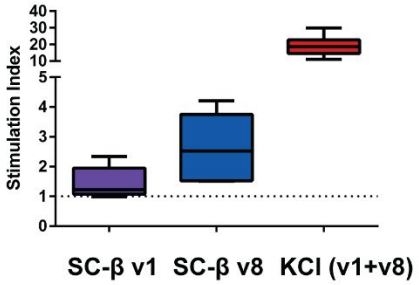

C

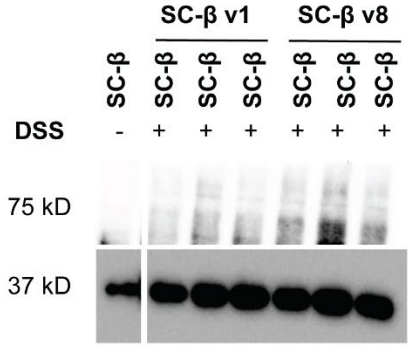

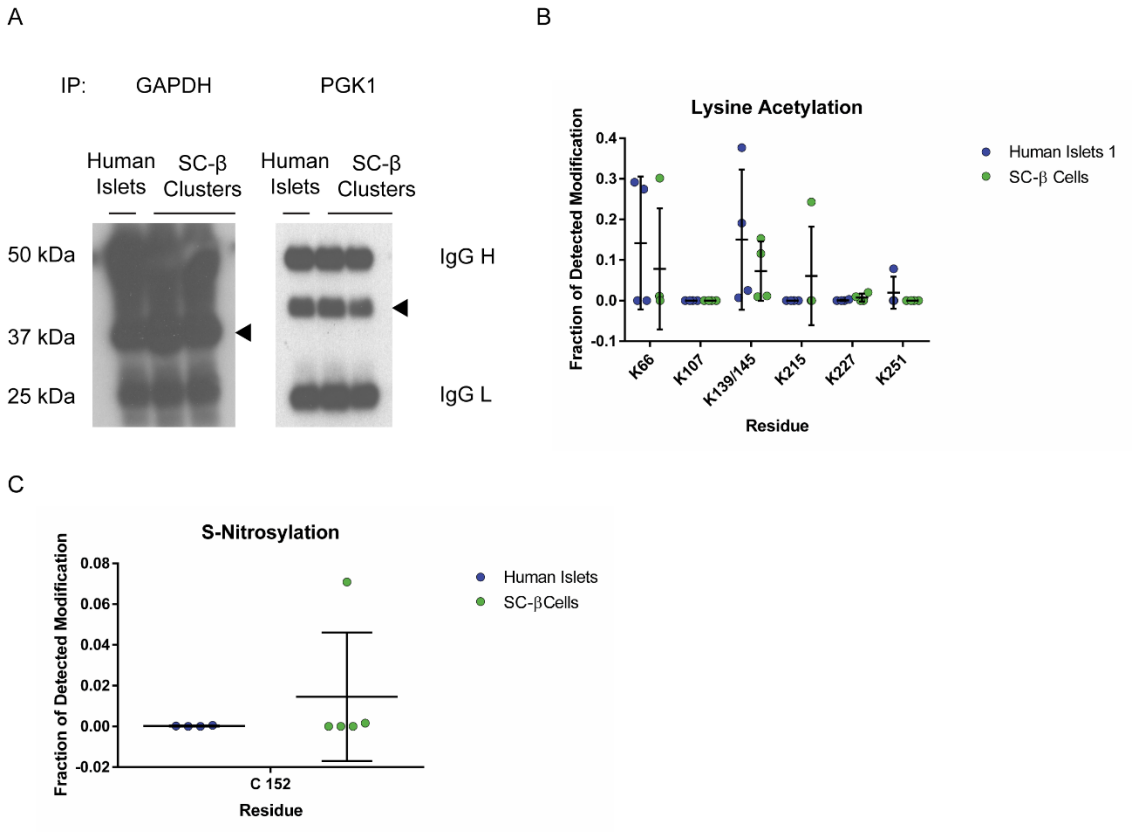

Supplemental Figure I-7. PTM Profiles of GAPDH A) Western blot of immunoprecipitation of GADH and PGK1. **B)** Acetylation of GAPDH Lysine Residues detected by mass spectrometry in human islets and SC-β cells. **C)** S-Nitrosylation of Cysteine 152 of GAPDH from human islets and SC-β cells.

Appendix II

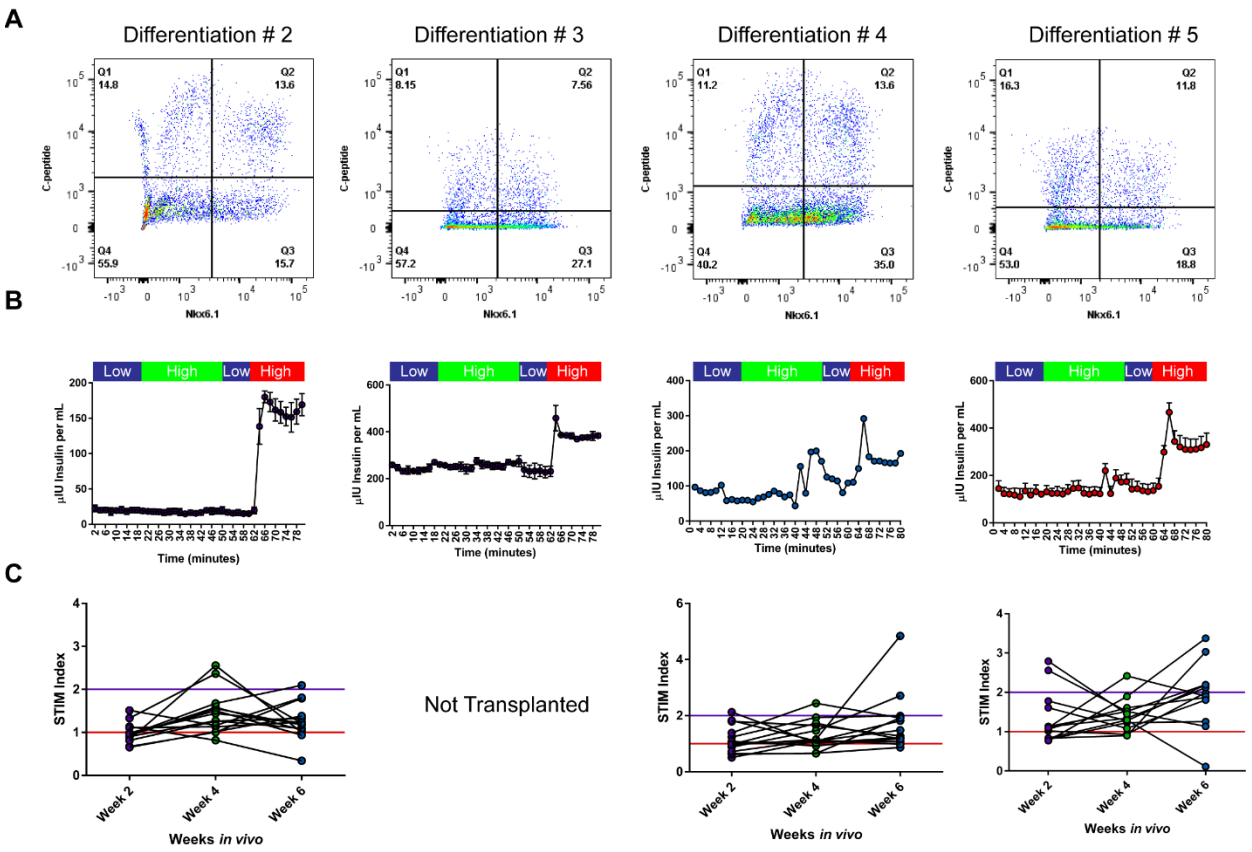

Supplemental Figure II-1. SC-β Profiles. A) Flow cytometric analysis of SC-β cell differentiations used in this study. **B)** *in vitro* GSIS profiles of SC-β cell differentiations. **C)** *in vivo* GSIS profiles of transplanted cells after 6 weeks of *in vivo* maturation.

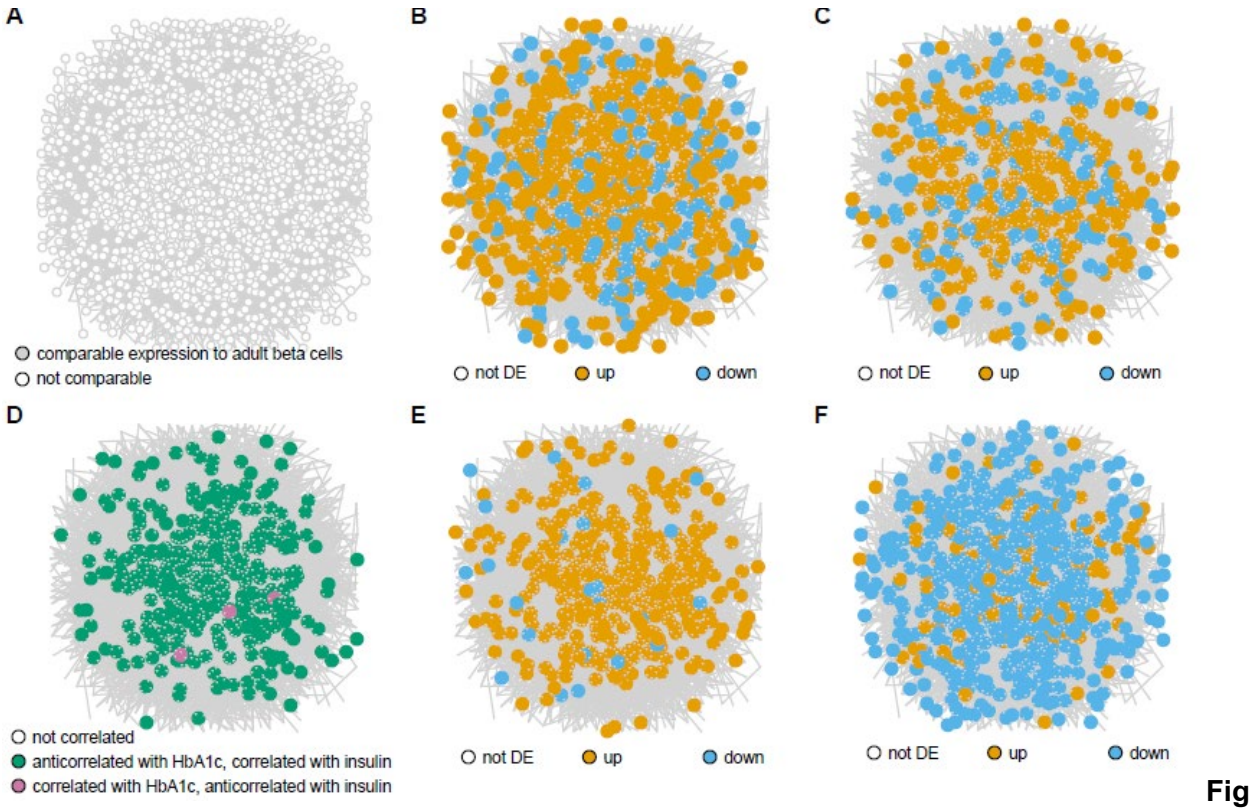

Fig

Supplemental Figure II-3. Candidate module c1_8. c1_8 contained 2,606 genes and was partially mature at stage 6 as 44.8% genes were not DE vs adult β cells (**A**). c1_8 was maturing, i.e., enriched in up-regulated DEGs in the *in vivo* maturation experiment (**B**) and maturation of fetal β cells in human (GSE56130) [86] (**C**). c1_8 was functionally important as indicated by enrichment in GSIS-associated genes [228] (**D**) and markers of successful islet graft function (GSE75062) [227] (**E**)

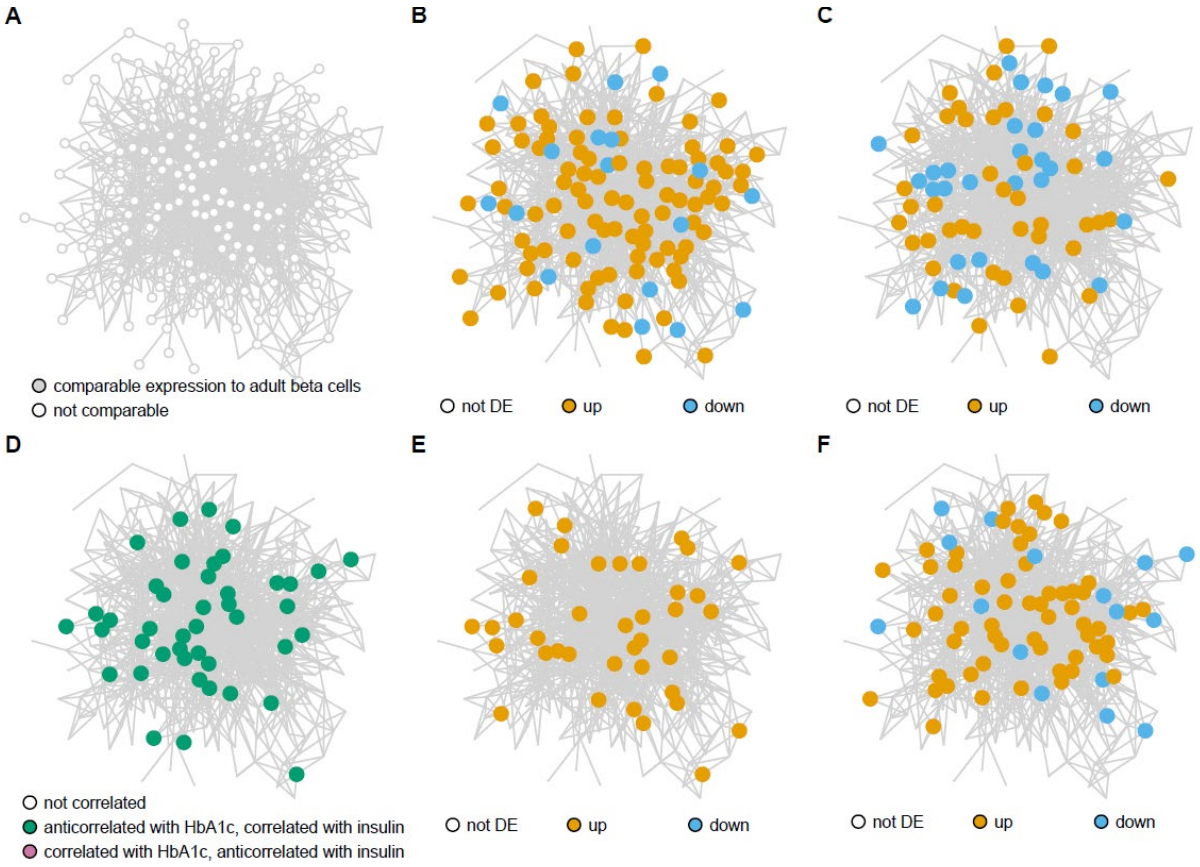

Supplemental Fig II-4. Candidate module c1_21. A) c1_21 contained 357 genes and had 52.7% mature genes with comparable expression to adult β cells at stage 6. **B)** c1_21 was maturing, i.e., enriched in up-regulated DEGs the *in vivo* maturation experiment **C)** and to a lesser extend in maturation of fetal β cells in human pancreata [86]. **D)** c1_21 was functionally important as indicated by enrichment in GSIS-associated genes in healthy and diabetic islets [228] **E)** and markers of successful islet graft function after transplantation into mice [227]. **F)** Genes in c1_21 trended to increase in expression during hyperglycemic stress after islet transplantation into diabetic mice [110].

Supplemental Table II-1. Major biological themes in modules c1_8 and c1_21.

Module c1_8

Biological theme (N GO terms)	Example enriched GO terms at FDR 5%
Hormone secretion (10)	regulation of GSIS (GO:0061178)
	insulin secretion (GO:0030073)
	regulation of insulin secretion (GO:0050796)
Differentiation and development (64)	neuron development (GO:0048666)
	axonogenesis (GO:0007409)
	synapse assembly (GO:0007416)
Vesicle transport, exocytosis and secretion (59)	vesicle-mediated transport (GO:0016192)
	exocytosis (GO:0006887)
	secretion (GO:0046903)
Electrophysiology (27)	membrane depolarization (GO:0051899)
	action potential (GO:0001508)
	ion transmembrane transport (GO:0034220)
Cell-cell communication (14)	trans-synaptic signaling (GO:0099537)
	cell-cell adhesion (GO:0098609)
	cell-cell signaling (GO:0007267)

Supplemental Table II-1 continued.

Lipid metabolism (5)	glycolipid metabolic process (GO:0006664)
Other (56)	receptor clustering (GO:0043113)
Module c1_21	
Differentiation and development (3)	neuron differentiation (GO:0030182)

Supplemental Table II-2. Validation candidate modules for relevance to β cell function.

Gene set	Module c1_8	Module c1_21
Mendelian disease genes: diabetes or related	*ABCC8, GCK, GCKR, HADH, NEUROD1, PAX6, PRPS1, RFX6, WFS1*	*HNF1A, MAFA, PDX1*
Type 1 diabetes autoantigens	*GAD2, G6PC2, PTPRN, SLC30A8, IGF2*	*PTPRN2, INS-IGF2, SOX13*
Anti-diabetes drug targets	*GLP1R, DPP4*	
β cell – relevant transcription regulators	*DACH1, DACH2, ELAVL4, FOXO1, ISL1, INSM1, JAZF1, MAFB, NKX6-3, TSHZ1*	*MAPK8IP1, MEIS3, NKX6-1, TFEB*
Formation or acidification or trafficking of insulin granules	*vacuolar-type H+-ATPases ATP6V0A1, ATP6V1A, ATP6V1B2, ATP6V1C1, ATP6AP2, SNAP25, synaptotagmins SYT1, SYT4, SYT7, SYT11, SYT13,*	*ATP6V0D1, ATP6V0E2, ATP6AP1, CHGA (1), WDR5 (2)*

Supplemental Table II-2 continued.

	SYT14, SYT16, SYT17	
Glucose transport	*SLC2A11, SLC2A12*	*SLC45A1*
Elements of GSIS		
Glucose sensors:	*SLC2A2, SLC5A4*	
K_{ATP} channels:	*ABCC8, ABCC9, KCNJ8*	
Voltage-gated Ca2+ channels:	*CACNA1A, CACNA1B, CACNA1C, CACNA1D, CACNA2D1, CACNA2D2, CACNA2D3*	
Insulin processing	*CPE, ERO1B, PCSK1, PCSK2*	

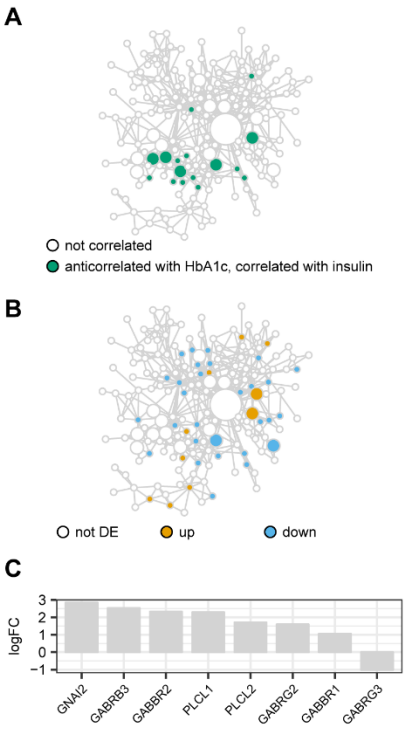

Supplemental Figure II-5. A) Submodule c1_66 was associated with GSIS [228], and **B)** tended to be down-regulated in hyperglycemic stress [110]. **C)** Other elements of GABA signaling were also up-regulated during *in vivo* maturation.

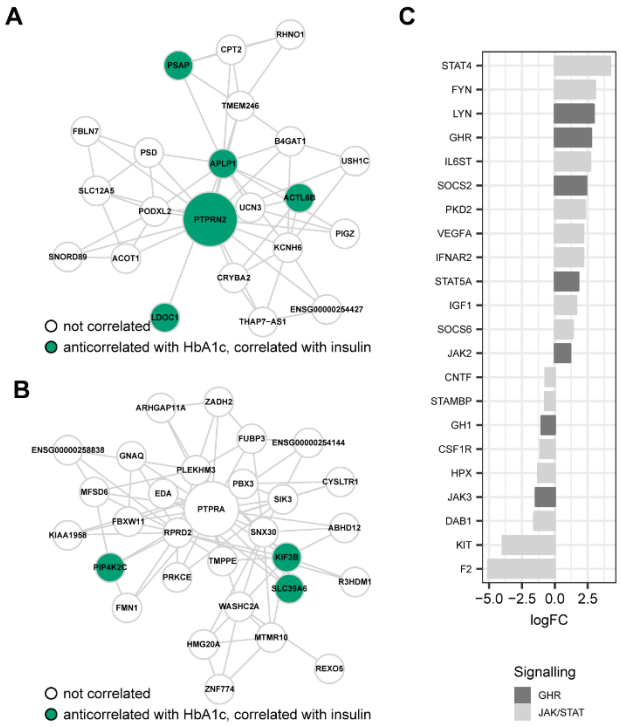

Supplemental Figure II-6. JAK/STAT signaling as candidate inducer of maturation. A) Submodule c1_409 and **B)** submodule c1_291 were previously associated with GSIS in cadaveric islets [310]. **C)** Genes in JAK/STAT cascade and specifically growth hormone receptor *GHR* pathway tended to be up-regulated in the *in vivo* maturation experiment.

Supplemental Table II-3. Other candidate inducers of β cell maturation. Genes are identified based on network topology analysis of modules c1_21 and c1_8. All genes had high betweenness centrality, were "immature" at stage 6 and differentially expressed in the in vivo maturation experiment. *MAPK8IP2* (c1_2, c1_21, c1_155), *PRUNE1* (c1_73, c1_286), *NMNAT2* (c1_56) were also hubs for the submodules indicated in brackets. "-" denotes negative correlation while "+" denotes positive correlation.

Gene	**Module hierarchy**	***in vivo* maturation Log_2FC (FDR)**	**Correlation with GSIS [228]**
ABHD14A	c1_2,c1_21,c1_153,c1_411	1.9 (0.0069)	no
ADORA2A	c1_8,c1_55	-0.7 (0.0199)	no
CDS2	c1_8,c1_67,c1_278	1.1 (0.0136)	no
CNTN1	c1_8,c1_62	1.8 (0.0204)	no
DACH1	c1_8,c1_59,c1_265	0.8 (0.0275)	- HbA_{1c}, + insulin
GLT1D1	c1_8,c1_53	2.0 (0.0046)	no
GPRASP1	c1_8,c1_62	1 (0.0335)	- HbA_{1c}, + insulin
GPRASP2	c1_8,c1_62	0.9 (0.0024)	no
HMGCLL1	c1_8,c1_57,c1_262	2.7 (0.0069)	no
HTR1F	c1_8,c1_68,c1_280	1.6 (0.0267)	no
KIAA1324	c1_8,c1_62	2.3 (9e-04)	- HbA_{1c}, + insulin
KIF13A	c1_8,c1_79	2.8 (0.0131)	- HbA_{1c}, + insulin
MAGEE1	c1_8,c1_62	-3 (0.02)	no
MAPK10	c1_8,c1_80,c1_293	1.2 (0.0164)	no
MAPK8IP2	c1_2,c1_21,c1_155	2.7 (0.0405)	no
NCALD	c1_8,c1_84,c1_297	1.2 (0.0459)	no

Supplemental Table II-3 continued.

NMNAT2	c1_8,c1_56	1.7 (0.0181)	- HbA_{1c}, + insulin
NOL4	c1_8,c1_80,c1_293	0.6 (0.0283)	- HbA_{1c}, + insulin
NUDT3	c1_8,c1_59,c1_266	2.4 (0.0305)	- HbA_{1c}, + insulin
OGFOD3	c1_2,c1_21,c1_156	3.4 (0.0261)	no
PCDHB10	c1_8,c1_66	3.0 (0.0305)	no
PRUNE1	c1_8,c1_73,c1_286	1.0 (0.0062)	no
RAVER2	c1_8,c1_74	2.5 (0.0144)	no
RCAN2	c1_8,c1_66	3.5 (0.011)	no
RTN1	c1_8,c1_63,c1_271	2.1 (0.013)	- HbA_{1c}, + insulin
SLC4A10	c1_8,c1_61,c1_270	2.2 (0.0035)	- HbA_{1c}, + insulin
TMCC2	c1_2,c1_21,c1_155	2.4 (0.0129)	no
ZHX3	c1_8,c1_60	2.6 (0.0329)	- HbA_{1c}, + insulin

Appendix III

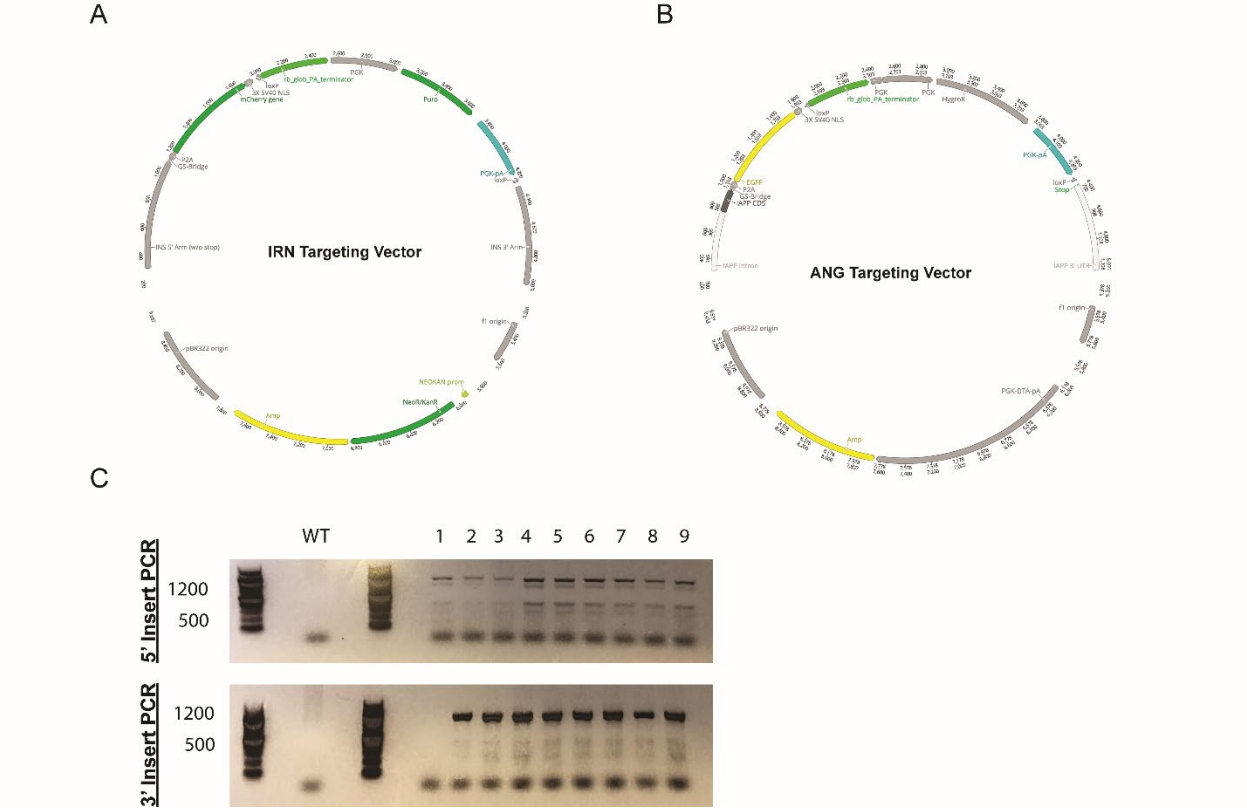

Supplemental Figure III-1. ***Gene Targeting in 1016 iPS*****. A)** Complete vector used for Insulin targeting toward IRN clones. **B)** Complete vector used for IAPP gene targeting for ANG clone. **C)** PCR validation of correct ANG insertion to make ANGIs clones (Clone 1 in 3' insert was due to evaporation of mix during PCR. Second clone PCR is shown in Fig. 4-1).

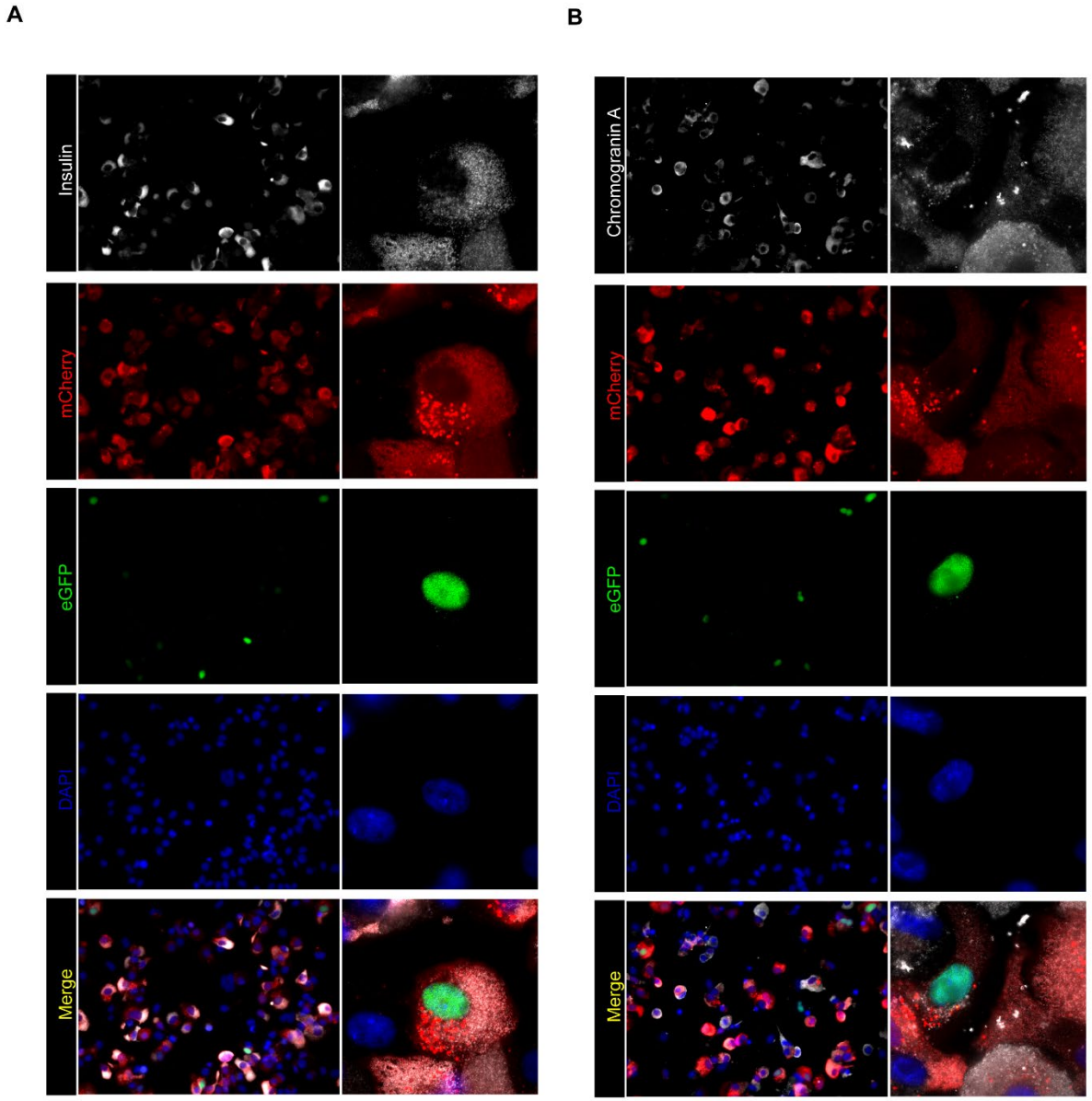

Supplemental Figure III-2. Immunofluorescent staining of ANGIs Differentiations. A) Immunofluorescence stain of Insulin, mCherry, eGFP, and DAPI at 20x (left) and 100x (right) and **B)** Chromogranin A, mCherry, eGFP, and DAPI at 20x (left) and 100x (right).

Supplemental Figure III-4. *Complete in vivo* Cohort Data from ANGIs Clones 1 and 2. A) *in vivo* GSIS data from ANGIs Clone 1 transplantation cohort. **B)** Circulating human Insulin before and after injection one-week post-transplantation. **C)** Circulating human Insulin before and after injection 5 weeks post-transplantation. **D)** Circulating human Insulin before and after injection 9 weeks post-transplantation. **E)** *in vivo* GSIS data from ANGIs Clone 2 transplantation cohort. **F)** Circulating human Insulin before and after injection one-week post-transplantation. **G)** Circulating human Insulin before and after injection 5 weeks post-transplantation. **H)** Circulating human Insulin before and after injection 9 weeks post-transplantation

Supplemental Figure III-4 continued.

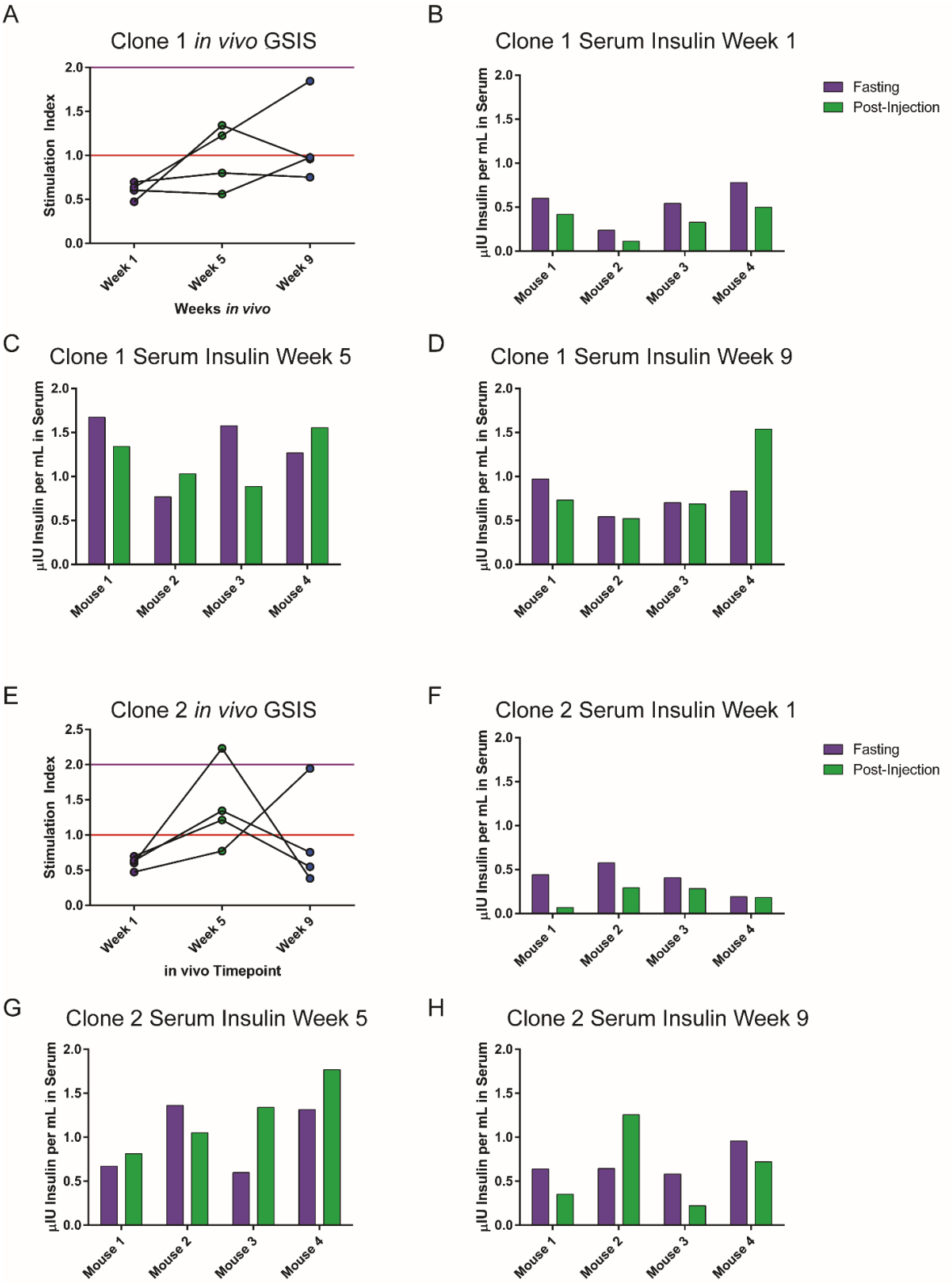

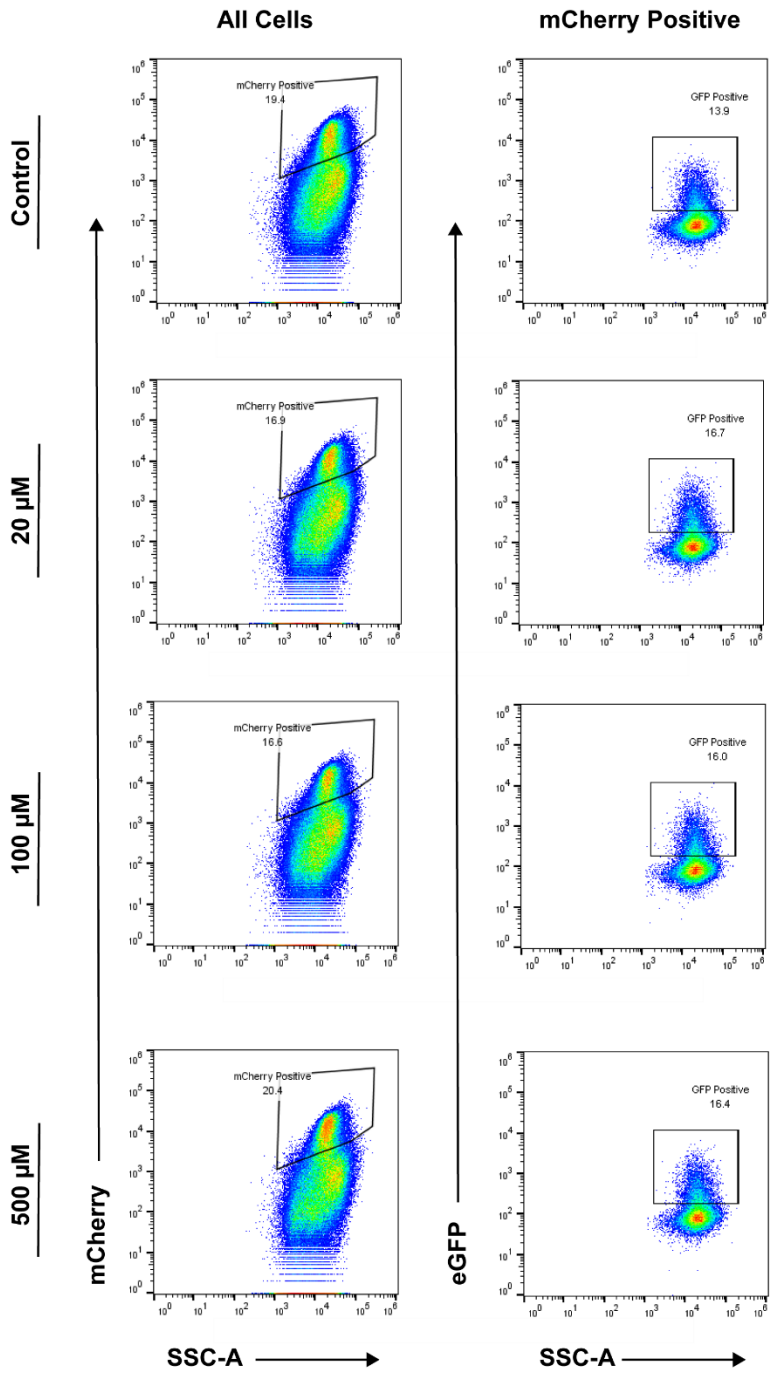

Supplemental Figure III-5. Incubation of ANGIs Clone 1 with GABA for 7 days.

Materials and Methods

Culture and passage of Pluripotent Stem Cells

Pluripotent stem cell lines were cultured in mTeSR 1 media. Both planar and suspension cultures were fed with fresh medium every 24 hours. After dissociation with TrypLE trypsin or Accutase for planar or suspension cultures, respectively, cells were re-plated using a 1:1000 dilution of Rho Kinase inhibitor for the first 24 hours-post split to maintain cell survival. Planar cultures were maintained on tissue culture plates pre-coated using maintenance Matrigel from Stem Cell Technologies. After dissociation cells were counted using a Vicell automated cell counter and plated at a density of 65,000 cells per cm^2. Suspension maintenance lines were dissociated and re-seeded every 72 hours and planar cells were dissociated and re-plated every 72-96 hours depending on survival and confluency at the time of passage.

Differentiation of SC-β Cells

Differentiation of SC-β cells were accomplished using the protocol previously published with the following adjustments [81]. Suspension cultures were differentiated 48- or 72-hours post-seeding once clusters achieved an average diameter or approximately 200 μm. Stage 2 induction of foregut endoderm was carried out for 48 hours rather than 72 hours. Stage 3 induction was performed in the absence of the BMP inhibitor LDN, and stage 4 differentiations were performed including 1:1000 dilutions of Rho kinase inhibitor to improve cell survival and cluster integrity as well as a 1:2000 dilution of Activin A. Finally, stage 6 clusters were either maintained in CMRLS + 10% FBS as previously described, or in a simpler MCDB131-based medium used in stages 3 and 4 of the differentiation protocol. CMRLS was used when comparing metabolism of SC-β cells and human islets. For other GSIS-based experiments S3 base medium was used.

Flow Cytometry

Flow cytometry was performed after dissociating cells in Accutase, washing in PBS and either using live cells in FACS buffer (PBS with 5% FBS, 0.1M EDTA, 1:1000 Rho kinase inhibitor, and 0.5% BSA) or fixed in 4% PFA for 20 minutes followed by washing and analysis in PBS. Stains were performed overnight at 4 degrees with manufacturer-recommended dilutions. Analyses were performed on the BD LSR II, BD Fortessa, and the Attune NxT. .fcs files were analyzed using FlowJo software. Stained cells were analyzed using alexafluor dyes 488, 594, and 647. TSQ samples were analyzed using the violet channel and analyzed for fluorescence at 405 nm.

Immunofluorescence

Immunofluorescence was performed on 10 μm sections of tissues fixed in 4% PFA and stored either in paraffin wax or cryo-preserved in OCT freeze medium. Sections were cut using a cryostat for frozen sections or microtome for paraffin-embedded samples. Slides were stained after rehydration and antigen retrieval in boiling citrate buffer. Samples were blocked in 10% Donkey serum in PBST for 30 minutes after antigen retrieval. Primary antibody concentrations were used as directed by manufacturers and allowed to incubate in blocking buffer on slides overnight at 4 degrees. Secondary antibodies were used at a 1:500 dilution of Alexafluor-conjugated donkey secondary antibody and DAPI. After washing slides were mounted using Fluoromount-G and sealed with nail polish before being allowed to dry in a light-protected chamber. Images were collected using the Zeiss Imager Z2 microscope and figures were generated using the Zen Blue software to generate individual channel images. Some images were generated using Photoshop to combine channels. These images were not altered after generation in the ZEN software.

Use of Fluorescent Zinc Dyes

SC-β cells were sorted using TSQ live cell dye. TSQ was resuspended at a concentration of 25 mg / mL in DMSO and diluted at 1:2000 in PBS or FACS buffer before analysis by flow cytometry. Analysis when sorting or on the LSR II was performed using an ultraviolet light source. Use of TSQ with the Fortessa or Attune NxT was performed using the violet channel.

FACS Isolation of SC-β Cells

SC-β cells were dissociated and resuspended in FACS buffer as previously described. After resuspension and addition of TSQ and Propidium Iodide (1:100) where applicable, cells were kept on ice and sorted using either the FACSARIA III, MoFlow XDP, or MoFlo Astrios in the Harvard Bauer Flow Cytometry Core. After enrichment of SC-β cells samples were spun down at 350 rcf and used for their downstream applications as described elsewhere.

Cell-permeable Live Cell Dyes

The following live cell dyes were used at these concentrations. Fluo-4 calcium sensitive dye was used at a dilution of 1:50 in Kreb's Ringer Buffer during imaging. DisCap voltage potential dye was used at manufacturer recommended concentration and allowed to remain on cells for the duration of experiments. TSQ was used at a concentration of 12.5 µg/ mL and also allowed to remain on cells for the duration of each experiment. Propidium Iodide (Thermo Fisher) was used at a concentration of 10 µg/mL.

Static GSIS Assays

Stage 6 cells were dissociated using Accutase and quenched. After resuspension in basal medium with a 1:1000 dilution of Rho Kinase inhibitor cells were counted and resuspended at a concentration of 50,000 cells per mL. Using a multichannel pipette and trough, 96-well V-bottom low attachment plates were filled with 100 µL per well of cell suspension and spun at 230 rcf for

5 minutes in plates. Clusters were allowed to re-aggregate for at least 48 hours and fed at 48-hour intervals after reaggregation. Medium was aspirated using a 12-well aspirating manifold after spinning re-aggregates to the bottom of each well. Fresh Kreb's Ringer Buffer was prepared for each experiment from salts to improve reproducibility of results. Plates were spun down and cells were washed twice in 2.8 mM Glucose KRB. Plates were allowed to fast for 120 minutes at 37 degrees followed by another wash step and replacement of KRB with low, high, KCl, or other treatments in KRB. Plates were spun, incubated for 1 hour at 37 degrees, re-spun and the top 70 µL of supernatant collected and some representative wells lysed in RIPA to calculate total insulin content per cell. Supernatant was re-spun in 96 well PCR plates and the top 50 µL of supernatant was collected and frozen at -20 degrees until analysis.

Dynamic GSIS Perifusion Assays

KRB was prepared the same as described above. Clusters were allowed to fast in low glucose for 2 hours followed by loading into dynamic perifusion chambers as described previously in the BioRep perifusion system [103]. After loading low glucose KRB was flowed over chambers for 30 minutes at a rate of 100 µL per minute to allow clusters to adjust to the change in flow pressure. Supernatant was then collected and frozen at -20 degrees before analysis.

Insulin ELISAs

Insulin samples were stored as previously described before thawing at room temperature on the day of analysis. Samples were loaded into either the Alpco human Insulin elisa for *in vitro* GSIS analysis or ultrasensitive human Insulin ELISAs for *in vivo* maturation GSIS samples as described in the manufacturer's protocol. After developing ELISA plates and stopping the reaction, absorbance was read at 450 nm and 605 nm for sample and background absorbance, respectively. Lysed insulin content samples were also run at a 1:100 dilution simultaneously. Each plate run contained its own standard set for internal control.

Quantification of Mitochondrial Content

Mitochondrial mtDNA content was analyzed using Real Time RT-PCR and primers as previously described [174]. Primers were custom-ordered through Thermo Fisher using the same sequences. Mitochondrial mass was also measured using MitoTracker Green as a measure of total mass. After incubation in MitoTracker Green as described by the manufacturer in suspension, cells were washed and analyzed by flow cytometry.

MIMOSA ^{13}C Tracing

SC-β clusters were enriched using TSQ-based sorting and reaggregation. After reaggregation cells were washed and incubated in simple DMEM medium created from powder on the day of analysis using 4 mM Glutamine and 9 mM Glucose as previously described [176]. After allowing clusters to reach steady state metabolism for 3 hours, clusters were treated with either ^{13}C labeled glucose or glutamine for 0-180 minutes followed by lysis in quench buffer described by Alves *et al*. After quenching, samples were frozen on dry ice and shipped overnight to Yale University for Mass Spectrometric analysis. Values were generated as a function of signal enrichment and described at Atomic Percent Enrichment (APE). Final values were calculated at Yale University by Tiago Alves using Wave software.

Western Blot

Protein samples were collected in RIPA buffer containing Protease and Phosphatase inhibitors. After lysis samples were quantified using Pierce BCA Rapid Gold Protein Assay. After calculation, samples were diluted to a mass of 5 ug protein and combined with Pierce loading buffer and reducing reagent. After boiling for 10 minutes samples were run using BioRad AnyKD gels and transferred onto nitrocellulose membranes. Membranes were blocked for 30 minutes in 3% BCA in TBST and primary antibodies were incubated overnight in 0.1% BCA in TBST according to manufacturer suggested primary antibody dilutions. HRP-conjugated secondary

antibodies were incubated at a 1:10,000 dilution and developed either on film or in the BioRad ChemiDoc instrument.

Intermediate Metabolite Treatment

Intermediate metabolite GSIS assays were performed as described above, using low glucose basal KRB solution and supplemented with 5, 10, and 20 mM metabolite mixture. Metabolites were measured as powder and added to KRB.

Small Molecule GSIS Assays

To test efficacy of small molecules and biomolecules for improved GSIS, SC-β clusters were incubated in concentrations described previously for 72 hours before GSIS was performed. Compounds were not included in KRB at the time of assay for ease of experiments. Medium was changed after 24 and 48 hours after treatment to maintain drug efficacy. Concentrations were used at the reported IC_{50} or EC_{50} and 0.2x and 5x those reported values for each experiment.

Calcium Flux Imaging

TSQ-sorted clusters were plated in maintenance Matrigel as described previously. Fluorescence was quantified using the Axiozoom V16 instrument in the Harvard Center for Biological Imaging. Image analysis was performed in ImageJ after collection and generation of image files in ZEN software. Clusters were allowed to fast for 2 hours before dye incorporation. Clusters were then washed 3 times and maintained in low glucose KRB until replacement with KRB with indicated additions.

Immunoprecipitation

Clusters were lysed in Pierce IP Lysis buffer containing HALT protease/phosphatase inhibitor cocktail dilution at 1:100. After quantifying protein concentration 500 µg of lysate was incubated

in primary antibody overnight at 4 degrees according to manufacturer recommended antibody dilutions. After overnight incubation Protein G Dynabeads were washed in IP Lysis buffer and incubated with shaking for 1 hour at 4 degrees. After incubation beads were washed in IP Lysis buffer and protein was eluted from beads using boiling in SDS-Urea buffer. Samples were evenly diluted and run in western blot without quantification but normalized using H+L bands.

Mass Spectrometry Analysis of Post-translational modifications

After immunoprecipitation and confirmation via western blot, SDS-PAGE gels were run and expected bands for GAPDH and PGK1 were cut out from the gel without stain. After bands were cut from the gels, the samples were washed in 50% acetonitrile for 2 hours at room temperature to dehydrate samples. Gel blocks were then stored at 4 degrees until analysis by the Bauer Proteomics Core.

Transplantation

In vivo maturation experiments were carried out using immunocompromised SCID-Beige male mice from Jackson Laboratories (CB17.Cg-*Prkdc*^{scid}*Lyst*$^{bg\text{-}J}$/Crl). Surgeries were performed under the Melton protocol 10-18 for Harvard University. Animals were anesthetized using avertin and 5 million total cells of SC-β differentiations were transplanted underneath the left kidney capsule using a 27-gauge butterfly needle in ice cold low glucose DMEM. Animals were allowed to recover on a heated pad under supervision until active before individual housing after surgery.

Recovery of Transplanted Cells

Animals were sacrificed using CO_2 asphyxiation and secondary cervical dislocation as per our animal protocol regulations. Individual kidneys were removed from the body cavity after sacrifice. Under a fluorescent dissecting microscope (Leica X) the kidney capsule was peeled from the body of the kidney, taking with it the GFP-positive graft. After isolation in PBS, 1/3 of each graft was fixed in 4% PFA as described. The rest of the graft was incubated in Accutase for 10 minutes

at 37 degrees followed by passing through progressively higher gauge needles from 10/15/27 gauge. After dissociation cell suspensions were filtered through a 40 μM filter and resuspended in stage 6 medium and immediately sorted.

Generation of 1016 iPS GFP Line

The 1016 iPS cell line was purchased from Columbia University. Constitutive GFP-expressing 1016 iPS cells were generated using the constructs previously described [311]. Cells were selected using Puromycin and expanded and adapted to 3D suspension culture. All experiments using human embryonic or other pluripotent stem cells were reviewed and approved by the Harvard University Embryonic Stem Cell Research Oversight (ESCRO) Committee.

Donor islets

Islets for study were purchased from Prodo Laboratories, NDRI, and the University of Miami. All islets were isolated from healthy donors at the time of death and used within 7 days of shipment. All islet studies were performed in accordance with IRB approved procedures at Harvard University under protocol IRB16-0013.

In vivo GSIS

After transplantation SCID-Beige mice were allowed to recover for 2 weeks followed by *in vivo* GSIS analysis at 2, 4, and 6 weeks post-transplant. Animals were fasted overnight prior to beginning the GSIS assay. After overnight fast blood was collected by a facial puncture, immediately followed by intraperitoneal injection of 1 mg/kg glucose. After 30 minutes blood was again collected by facial puncture. Blood was spun down and serum isolated and frozen at -20 degrees Celsius until analysis by Insulin ELISA.

RNA Seq Expression profiling of SC-β Cells

After RNA collection via TriZol extraction, RNA samples were analyzed using the Agilent Bioanalyzer RNA Pico kit to determine concentration and RNA Integrity Number score. After analysis libraries were prepared by the biopolymer facility at Harvard Medical School and sequenced using the Illumina NextSeq platform. Resulting sequencing files were analyzed using the Trinity pipeline utilizing RSEM and aligned to the human HG19 reference genome.

Live Cell Protein Cross-linking

Live cells were crosslinked using the cell-permeable DSS compound from Thermo Fisher. Cells were incubated in PBS with 5mM DSS compound for 30 minutes. The reaction was quenched by addition of 1M Tris-HCl. Clusters were spun down and quenched using RIPA. Protein concentration was determined as described for western blots above and bands for monomer and multimers were cut apart in the membrane and developed separately for improved clarity.

GAPDH Activity Assays

GAPDH activity was determined using the Abcam GAPDH activity assay kit. Lysates were collected as instructed and quantified while lysates remained on ice. After quantification the same amount of protein was loaded into 4 replicates with a single background replicate for control. Absorbance was measured at 450 and 605 nm on kinetic mode for 30 minutes every 120 seconds. After data collection, timepoints with linear curves were selected to quantify and compare GAPDH activity across all samples as described.

MEGENA Co-expression Network Analysis

All coexpression network analysis and bioinformatic analysis was performed by Maria Ryoboshapkina using computing resources at AstraZeneca.

Gene Targeting in pluripotent Stem Cells

Gene targeting was performed in pluripotent stem cells after dissociation in TrypLE trypsin and washing in PBS. Electroporations were carried out according to manufacturer instructions for the Invitrogen Neon instrument. 11 Million live cells were resuspended in 440 µL of R buffer containing 24 µg of plasmid DNA containing a 1:4 molar ratio of vector to guide RNA.

Homologous Recombination Construct Design

Homologous recombination constructs were generously provided by JRF and modified to contain 5' and 3' homology regions determined by the UCSC genome browser. After design homology arms were generated by IDT and cloned into the vector using restriction cloning. After modification plasmids were sequenced. Guide RNA design and CRISPR vectors were used as described previously using the px330 cloning system.

Validation of Targeted Clones

Genomic DNA from clones was isolated using the Qiagen DNA-Easy kit and tested using PCR targeted to the transgene with a forward primer lying upstream of the 5' homology region or inside of the 3' homology arm with reverse primers lying inside of the 5' homology region or outside of the 3' homology region, respectively. Clones containing expected band sizes were then differentiated and sorted for their expected fluorescence profiles. After sorting RNA was collected and Real Time RT-PCR was used to confirm enrichment of transcripts corresponding to knock-in reporter lines.

Real Time RT-PCR Analysis

Real Time RT-PCR was performed using the Reverse Transcriptase cDNA supermix system. cDNA was then diluted and used with Taqman designed primers. Real Time reactions were performed using the ABI7500 thermal cycler. Determination of fold-change in transcript values was performed using the ddCt method using *UBC* as a housekeeping gene.

Co-culture of SC-β Cells with HUVECs

Co-culture of SC-β cells with HUVECs was done maintaining a 5,000 SC-β cell count in each well and adding HUVECs from a dilution range of 1:4 to 1:1. Cells were allowed to reaggregate in normal S3 medium supplemented with Rho Kinase inhibitor for the first 24 hours. GSIS on these clusters was performed as described above. Endothelial cells were cultured by Edwin Rosado-Olivieri

References

1. Meier, U. and A.M. Gressner, *Endocrine regulation of energy metabolism: review of pathobiochemical and clinical chemical aspects of leptin, ghrelin, adiponectin, and resistin.* Clin Chem, 2004. **50**(9): p. 1511-25.

2. Kaur, J., *A comprehensive review on metabolic syndrome.* Cardiol Res Pract, 2014. **2014**: p. 943162.

3. Pan, F.C. and C. Wright, *Pancreas organogenesis: from bud to plexus to gland.* Dev Dyn, 2011. **240**(3): p. 530-65.

4. Slack, J.M., *Developmental biology of the pancreas.* Development, 1995. **121**(6): p. 1569-80.

5. Petersen, M.C. and G.I. Shulman, *Mechanisms of Insulin Action and Insulin Resistance.* Physiol Rev, 2018. **98**(4): p. 2133-2223.

6. Brissova, M., et al., *Assessment of human pancreatic islet architecture and composition by laser scanning confocal microscopy.* J Histochem Cytochem, 2005. **53**(9): p. 1087-97.

7. Olerud, J., A. Johansson, and P.O. Carlsson, *Vascular niche of pancreatic islets.* Expert Rev Endocrinol Metab, 2009. **4**(5): p. 481-491.

8. Thorens, B., *Neural regulation of pancreatic islet cell mass and function.* Diabetes Obes Metab, 2014. **16 Suppl 1**: p. 87-95.

9. Russell, S.J., et al., *Outpatient glycemic control with a bionic pancreas in type 1 diabetes.* N Engl J Med, 2014. **371**(4): p. 313-325.

10. Kittah, N.E. and A. Vella, *MANAGEMENT OF ENDOCRINE DISEASE: Pathogenesis and management of hypoglycemia.* Eur J Endocrinol, 2017. **177**(1): p. R37-R47.

11. Morales, J. and D. Schneider, *Hypoglycemia.* Am J Med, 2014. **127**(10 Suppl): p. S17-24.

12. Fazeli Farsani, S., et al., *Incidence and prevalence of diabetic ketoacidosis (DKA) among adults with type 1 diabetes mellitus (T1D): a systematic literature review.* BMJ Open, 2017. **7**(7): p. e016587.

13. Buysschaert, M., et al., *Definitions (and Current Controversies) of Diabetes and Prediabetes.* Curr Diabetes Rev, 2016. **12**(1): p. 8-13.

14. Fu, Z., E.R. Gilbert, and D. Liu, *Regulation of insulin synthesis and secretion and pancreatic Beta-cell dysfunction in diabetes.* Curr Diabetes Rev, 2013. **9**(1): p. 25-53.

15. Banting, F.G., et al., *Pancreatic Extracts in the Treatment of Diabetes Mellitus.* Can Med Assoc J, 1922. **12**(3): p. 141-6.

16. Bertuzzi, F., et al., *Brittle type 1 diabetes mellitus.* Curr Med Chem, 2007. **14**(16): p. 1739-44.

17. Tattersall, R., et al., *Course of brittle diabetes: 12 year follow up.* BMJ, 1991. **302**(6787): p. 1240-3.

18. Tekin, Z., et al., *Outcomes of Pancreatic Islet Allotransplantation Using the Edmonton Protocol at the University of Chicago.* Transplant Direct, 2016. **2**(10): p. e105.

19. Roglic, G. and World Health Organization, *Global report on diabetes*. 2016, Geneva, Switzerland: World Health Organization. 86 pages.

20. Kahn, B.B. and J.S. Flier, *Obesity and insulin resistance.* J Clin Invest, 2000. **106**(4): p. 473-81.

21. Kahn, C.R., *Insulin resistance, insulin insensitivity, and insulin unresponsiveness: a necessary distinction.* Metabolism, 1978. **27**(12 Suppl 2): p. 1893-902.

22. Kahn, S.E., R.L. Hull, and K.M. Utzschneider, *Mechanisms linking obesity to insulin resistance and type 2 diabetes.* Nature, 2006. **444**(7121): p. 840-6.

23. Olefsky, J.M., O.G. Kolterman, and J.A. Scarlett, *Insulin action and resistance in obesity and noninsulin-dependent type II diabetes mellitus.* Am J Physiol, 1982. **243**(1): p. E15-30.

24. Ren, J.M., et al., *Evidence from transgenic mice that glucose transport is rate-limiting for glycogen deposition and glycolysis in skeletal muscle.* J Biol Chem, 1993. **268**(22): p. 16113-5.

25. Butler, A.E., et al., *Beta-cell deficit and increased beta-cell apoptosis in humans with type 2 diabetes.* Diabetes, 2003. **52**(1): p. 102-10.

26. Meyre, D., *Give GWAS a Chance.* Diabetes, 2017. **66**(11): p. 2741-2742.

27. Weir, G.C. and S. Bonner-Weir, *Islet beta cell mass in diabetes and how it relates to function, birth, and death.* Ann N Y Acad Sci, 2013. **1281**: p. 92-105.

28. Kahn, S.E., *The relative contributions of insulin resistance and beta-cell dysfunction to the pathophysiology of Type 2 diabetes.* Diabetologia, 2003. **46**(1): p. 3-19.

29. Kasuga, M., *Insulin resistance and pancreatic beta cell failure.* J Clin Invest, 2006. **116**(7): p. 1756-60.

30. Schwartz, S.S., et al., *A Unified Pathophysiological Construct of Diabetes and its Complications.* Trends Endocrinol Metab, 2017. **28**(9): p. 645-655.

31. Katsarou, A., et al., *Type 1 diabetes mellitus.* Nat Rev Dis Primers, 2017. **3**: p. 17016.

32. Gepts, W., *Pathologic anatomy of the pancreas in juvenile diabetes mellitus.* Diabetes, 1965. **14**(10): p. 619-33.

33. Kondrashova, A., et al., *The 'Hygiene hypothesis' and the sharp gradient in the incidence of autoimmune and allergic diseases between Russian Karelia and Finland.* APMIS, 2013. **121**(6): p. 478-93.

34. Nerup, J., et al., *HL-A antigens and diabetes mellitus.* Lancet, 1974. **2**(7885): p. 864-6.

35. Cudworth, A.G. and J.C. Woodrow, *Letter: HL-A antigens and diabetes mellitus.* Lancet, 1974. **2**(7889): p. 1153.

36. Singal, D.P. and M.A. Blajchman, *Histocompatibility (HL-A) antigens, lymphocytotoxic antibodies and tissue antibodies in patients with diabetes mellitus.* Diabetes, 1973. **22**(6): p. 429-32.

37. Rosenfeld, L., *Insulin: discovery and controversy.* Clin Chem, 2002. **48**(12): p. 2270-88.

38. Papatheodorou, K., et al., *Complications of Diabetes.* J Diabetes Res, 2015. **2015**: p. 189525.

39. Kloppel, G., et al., *Islet pathology and the pathogenesis of type 1 and type 2 diabetes mellitus revisited.* Surv Synth Pathol Res, 1985. **4**(2): p. 110-25.

40. Rahier, J., et al., *Pancreatic beta-cell mass in European subjects with type 2 diabetes.* Diabetes Obes Metab, 2008. **10 Suppl 4**: p. 32-42.

41. Shapiro, A.M. and J.R. Lakey, *Future trends in islet cell transplantation.* Diabetes Technol Ther, 2000. **2**(3): p. 449-52.

42. Shapiro, A.M., et al., *Islet transplantation in seven patients with type 1 diabetes mellitus using a glucocorticoid-free immunosuppressive regimen.* N Engl J Med, 2000. **343**(4): p. 230-8.

43. Gamble, A., et al., *The journey of islet cell transplantation and future development.* Islets, 2018. **10**(2): p. 80-94.

44. Ryan, E.A., et al., *Five-year follow-up after clinical islet transplantation.* Diabetes, 2005. **54**(7): p. 2060-9.

45. Barton, F.B., et al., *Improvement in outcomes of clinical islet transplantation: 1999-2010.* Diabetes Care, 2012. **35**(7): p. 1436-45.

46. Cohen, D.E. and D. Melton, *Turning straw into gold: directing cell fate for regenerative medicine.* Nat Rev Genet, 2011. **12**(4): p. 243-52.

47. Thomson, J.A., et al., *Embryonic stem cell lines derived from human blastocysts.* Science, 1998. **282**(5391): p. 1145-7.

48. Takahashi, K., et al., *Induction of pluripotent stem cells from adult human fibroblasts by defined factors.* Cell, 2007. **131**(5): p. 861-72.

49. Vegas, A.J., et al., *Long-term glycemic control using polymer-encapsulated human stem cell-derived beta cells in immune-competent mice.* Nat Med, 2016. **22**(3): p. 306-11.

50. Hart, N.J. and A.C. Powers, *Use of human islets to understand islet biology and diabetes: progress, challenges and suggestions.* Diabetologia, 2019. **62**(2): p. 212-222.

51. Atkinson, M.A., G.S. Eisenbarth, and A.W. Michels, *Type 1 diabetes.* Lancet, 2014. **383**(9911): p. 69-82.

52. Atkinson, M.A., *Evaluating preclinical efficacy.* Sci Transl Med, 2011. **3**(96): p. 96cm22.

53. Skelin Klemen, M., et al., *The triggering pathway to insulin secretion: Functional similarities and differences between the human and the mouse beta cells and their translational relevance.* Islets, 2017. **9**(6): p. 109-139.

54. Rorsman, P. and M. Braun, *Regulation of insulin secretion in human pancreatic islets.* Annu Rev Physiol, 2013. **75**: p. 155-79.

55. Evans, M.J. and M.H. Kaufman, *Establishment in culture of pluripotential cells from mouse embryos.* Nature, 1981. **292**(5819): p. 154-6.

56. Martin, G.R., *Isolation of a pluripotent cell line from early mouse embryos cultured in medium conditioned by teratocarcinoma stem cells.* Proc Natl Acad Sci U S A, 1981. **78**(12): p. 7634-8.

57. Millman, J.R., et al., *Generation of stem cell-derived beta-cells from patients with type 1 diabetes.* Nat Commun, 2016. **7**: p. 11463.

58. Maehr, R., et al., *Generation of pluripotent stem cells from patients with type 1 diabetes.* Proc Natl Acad Sci U S A, 2009. **106**(37): p. 15768-73.

59. Wells, J.M. and D.A. Melton, *Early mouse endoderm is patterned by soluble factors from adjacent germ layers.* Development, 2000. **127**(8): p. 1563-72.

60. Lammert, E., O. Cleaver, and D. Melton, *Induction of pancreatic differentiation by signals from blood vessels.* Science, 2001. **294**(5542): p. 564-7.

61. Hebrok, M., S.K. Kim, and D.A. Melton, *Notochord repression of endodermal Sonic hedgehog permits pancreas development.* Genes Dev, 1998. **12**(11): p. 1705-13.

62. Ohlsson, H., K. Karlsson, and T. Edlund, *IPF1, a homeodomain-containing transactivator of the insulin gene.* EMBO J, 1993. **12**(11): p. 4251-9.

63. Sherwood, R.I., T.Y. Chen, and D.A. Melton, *Transcriptional dynamics of endodermal organ formation.* Dev Dyn, 2009. **238**(1): p. 29-42.

64. Burlison, J.S., et al., *Pdx-1 and Ptf1a concurrently determine fate specification of pancreatic multipotent progenitor cells.* Dev Biol, 2008. **316**(1): p. 74-86.

65. Solar, M., et al., *Pancreatic exocrine duct cells give rise to insulin-producing beta cells during embryogenesis but not after birth.* Dev Cell, 2009. **17**(6): p. 849-60.

66. Xuan, S., et al., *Pancreas-specific deletion of mouse Gata4 and Gata6 causes pancreatic agenesis.* J Clin Invest, 2012. **122**(10): p. 3516-28.

67. Decker, K., et al., *Gata6 is an important regulator of mouse pancreas development.* Dev Biol, 2006. **298**(2): p. 415-29.

68. Zhou, Q., et al., *A multipotent progenitor domain guides pancreatic organogenesis.* Dev Cell, 2007. **13**(1): p. 103-14.

69. Schaffer, A.E., et al., *Nkx6 transcription factors and Ptf1a function as antagonistic lineage determinants in multipotent pancreatic progenitors.* Dev Cell, 2010. **18**(6): p. 1022-9.

70. Murtaugh, L.C., et al., *Notch signaling controls multiple steps of pancreatic differentiation.* Proc Natl Acad Sci U S A, 2003. **100**(25): p. 14920-5.

71. Gradwohl, G., et al., *neurogenin3 is required for the development of the four endocrine cell lineages of the pancreas.* Proc Natl Acad Sci U S A, 2000. **97**(4): p. 1607-11.

72. Sharon, N., et al., *A Peninsular Structure Coordinates Asynchronous Differentiation with Morphogenesis to Generate Pancreatic Islets.* Cell, 2019. **176**(4): p. 790-804 e13.

73. Gu, G., J. Dubauskaite, and D.A. Melton, *Direct evidence for the pancreatic lineage: NGN3+ cells are islet progenitors and are distinct from duct progenitors.* Development, 2002. **129**(10): p. 2447-57.

74. Nelson, S.B., A.E. Schaffer, and M. Sander, *The transcription factors Nkx6.1 and Nkx6.2 possess equivalent activities in promoting beta-cell fate specification in Pdx1+ pancreatic progenitor cells.* Development, 2007. **134**(13): p. 2491-500.

75. Naya, F.J., et al., *Diabetes, defective pancreatic morphogenesis, and abnormal enteroendocrine differentiation in BETA2/neuroD-deficient mice.* Genes Dev, 1997. **11**(18): p. 2323-34.

76. Schaffer, A.E., et al., *Nkx6.1 controls a gene regulatory network required for establishing and maintaining pancreatic Beta cell identity.* PLoS Genet, 2013. **9**(1): p. e1003274.

77. Collombat, P., et al., *Opposing actions of Arx and Pax4 in endocrine pancreas development.* Genes Dev, 2003. **17**(20): p. 2591-603.

78. Zhang, J., et al., *The diabetes gene Hhex maintains delta-cell differentiation and islet function.* Genes Dev, 2014. **28**(8): p. 829-34.

79. Johansson, K.A., et al., *Temporal control of neurogenin3 activity in pancreas progenitors reveals competence windows for the generation of different endocrine cell types.* Dev Cell, 2007. **12**(3): p. 457-65.

80. Stanger, B.Z., A.J. Tanaka, and D.A. Melton, *Organ size is limited by the number of embryonic progenitor cells in the pancreas but not the liver.* Nature, 2007. **445**(7130): p. 886-91.

81. Pagliuca, F.W., et al., *Generation of functional human pancreatic beta cells in vitro.* Cell, 2014. **159**(2): p. 428-39.

82. Nostro, M.C., et al., *Pancreatic differentiation*, in *StemBook*. 2008: Cambridge (MA).

83. Kroon, E., et al., *Pancreatic endoderm derived from human embryonic stem cells generates glucose-responsive insulin-secreting cells in vivo.* Nat Biotechnol, 2008. **26**(4): p. 443-52.

84. D'Amour, K.A., et al., *Production of pancreatic hormone-expressing endocrine cells from human embryonic stem cells.* Nat Biotechnol, 2006. **24**(11): p. 1392-401.

85. D'Amour, K.A., et al., *Efficient differentiation of human embryonic stem cells to definitive endoderm.* Nat Biotechnol, 2005. **23**(12): p. 1534-41.

86. Hrvatin, S., et al., *Differentiated human stem cells resemble fetal, not adult, beta cells.* Proc Natl Acad Sci U S A, 2014. **111**(8): p. 3038-43.

87. Bayha, E., et al., *Retinoic acid signaling organizes endodermal organ specification along the entire antero-posterior axis.* PLoS One, 2009. **4**(6): p. e5845.

88. Russ, H.A., et al., *Controlled induction of human pancreatic progenitors produces functional beta-like cells in vitro.* EMBO J, 2015. **34**(13): p. 1759-72.

89. Rezania, A., et al., *Reversal of diabetes with insulin-producing cells derived in vitro from human pluripotent stem cells.* Nat Biotechnol, 2014. **32**(11): p. 1121-33.

90. Rezania, A., et al., *Maturation of human embryonic stem cell-derived pancreatic progenitors into functional islets capable of treating pre-existing diabetes in mice.* Diabetes, 2012. **61**(8): p. 2016-29.

91. Rezania, A., et al., *Production of functional glucagon-secreting alpha-cells from human embryonic stem cells.* Diabetes, 2011. **60**(1): p. 239-47.

92. Rezania, A., et al., *Enrichment of human embryonic stem cell-derived NKX6.1-expressing pancreatic progenitor cells accelerates the maturation of insulin-secreting cells in vivo.* Stem Cells, 2013. **31**(11): p. 2432-42.

93. Braun, M., et al., *Voltage-gated ion channels in human pancreatic beta-cells: electrophysiological characterization and role in insulin secretion.* Diabetes, 2008. **57**(6): p. 1618-28.

94. Ashcroft, F.M. and P. Rorsman, *Electrophysiology of the pancreatic beta-cell.* Prog Biophys Mol Biol, 1989. **54**(2): p. 87-143.

95. Gerber, S.H. and T.C. Sudhof, *Molecular determinants of regulated exocytosis.* Diabetes, 2002. **51 Suppl 1**: p. S3-11.

96. Rorsman, P. and E. Renstrom, *Insulin granule dynamics in pancreatic beta cells.* Diabetologia, 2003. **46**(8): p. 1029-45.

97. Henquin, J.C., et al., *Pharmacological approach to understanding the control of insulin secretion in human islets.* Diabetes Obes Metab, 2017. **19**(8): p. 1061-1070.

98. Henquin, J.C., et al., *Dynamics of glucose-induced insulin secretion in normal human islets.* Am J Physiol Endocrinol Metab, 2015. **309**(7): p. E640-50.

99. Henquin, J.C., D. Dufrane, and M. Nenquin, *Nutrient control of insulin secretion in isolated normal human islets.* Diabetes, 2006. **55**(12): p. 3470-7.

100. Henquin, J.C., et al., *Insulin secretion: movement at all levels.* Diabetes, 2002. **51 Suppl 1**: p. S1-2.

101. Henquin, J.C., N.I. Mourad, and M. Nenquin, *Disruption and stabilization of beta-cell actin microfilaments differently influence insulin secretion triggered by intracellular Ca2+ mobilization or store-operated Ca2+ entry.* FEBS Lett, 2012. **586**(1): p. 89-95.

102. Kalwat, M.A. and D.C. Thurmond, *Signaling mechanisms of glucose-induced F-actin remodeling in pancreatic islet beta cells.* Exp Mol Med, 2013. **45**: p. e37.

103. Bentsi-Barnes, K., et al., *Detailed protocol for evaluation of dynamic perifusion of human islets to assess beta-cell function.* Islets, 2011. **3**(5): p. 284-90.

104. Velazco-Cruz, L., et al., *Acquisition of Dynamic Function in Human Stem Cell-Derived beta Cells.* Stem Cell Reports, 2019. **12**(2): p. 351-365.

105. Nair, G.G., et al., *Recapitulating endocrine cell clustering in culture promotes maturation of human stem-cell-derived beta cells.* Nat Cell Biol, 2019. **21**(2): p. 263-274.

106. Lamontagne, J., et al., *Identification of the signals for glucose-induced insulin secretion in INS1 (832/13) beta-cells using metformin-induced metabolic deceleration as a model.* J Biol Chem, 2017. **292**(47): p. 19458-19468.

107. Blum, B., et al., *Functional beta-cell maturation is marked by an increased glucose threshold and by expression of urocortin 3.* Nat Biotechnol, 2012. **30**(3): p. 261-4.

108. Bonner-Weir, S., et al., *Compensatory growth of pancreatic beta-cells in adult rats after short-term glucose infusion.* Diabetes, 1989. **38**(1): p. 49-53.

109. Talchai, C., et al., *Pancreatic beta cell dedifferentiation as a mechanism of diabetic beta cell failure.* Cell, 2012. **150**(6): p. 1223-34.

110. Kennedy, J., et al., *Protective unfolded protein response in human pancreatic beta cells transplanted into mice.* PLoS One, 2010. **5**(6): p. e11211.

111. Accili, D., et al., *What ails the beta-cell?* Diabetes Obes Metab, 2010. **12 Suppl 2**: p. 1-3.

112. Sims, E.K., et al., *Biomarkers of islet beta cell stress and death in type 1 diabetes.* Diabetologia, 2018. **61**(11): p. 2259-2265.

113. Hunter, C.S. and R.W. Stein, *Evidence for Loss in Identity, De-Differentiation, and Trans-Differentiation of Islet beta-Cells in Type 2 Diabetes.* Front Genet, 2017. **8**: p. 35.

114. Blum, B., et al., *Reversal of beta cell de-differentiation by a small molecule inhibitor of the TGFbeta pathway.* Elife, 2014. **3**: p. e02809.

115. Nostro, M.C., et al., *Efficient generation of NKX6-1+ pancreatic progenitors from multiple human pluripotent stem cell lines.* Stem Cell Reports, 2015. **4**(4): p. 591-604.

116. Yoshihara, E., et al., *ERRgamma Is Required for the Metabolic Maturation of Therapeutically Functional Glucose-Responsive beta Cells.* Cell Metab, 2016. **23**(4): p. 622-34.

117. Talavera-Adame, D., et al., *Effective endothelial cell and human pluripotent stem cell interactions generate functional insulin-producing beta cells.* Diabetologia, 2016. **59**(11): p. 2378-2386.

118. Ghazizadeh, Z., et al., *ROCKII inhibition promotes the maturation of human pancreatic beta-like cells.* Nat Commun, 2017. **8**(1): p. 298.

119. Accili, D., et al., *Early neonatal death in mice homozygous for a null allele of the insulin receptor gene.* Nat Genet, 1996. **12**(1): p. 106-9.

120. Bunner, A.E., P.C. Chandrasekera, and N.D. Barnard, *Knockout mouse models of insulin signaling: Relevance past and future.* World J Diabetes, 2014. **5**(2): p. 146-59.

121. Lemaire, K., L. Thorrez, and F. Schuit, *Disallowed and Allowed Gene Expression: Two Faces of Mature Islet Beta Cells.* Annu Rev Nutr, 2016. **36**: p. 45-71.

122. Pullen, T.J., et al., *Identification of genes selectively disallowed in the pancreatic islet.* Islets, 2010. **2**(2): p. 89-95.

123. De Vos, A., et al., *Human and rat beta cells differ in glucose transporter but not in glucokinase gene expression.* J Clin Invest, 1995. **96**(5): p. 2489-95.

124. Dai, C., et al., *Islet-enriched gene expression and glucose-induced insulin secretion in human and mouse islets.* Diabetologia, 2012. **55**(3): p. 707-18.

125. Becker, T.C., et al., *Differential effects of overexpressed glucokinase and hexokinase I in isolated islets. Evidence for functional segregation of the high and low Km enzymes.* J Biol Chem, 1996. **271**(1): p. 390-4.

126. Giroix, M.H., et al., *Hexose metabolism in pancreatic islets. Inhibition of hexokinase.* Biochem J, 1984. **223**(2): p. 447-53.

127. Prentki, M., F.M. Matschinsky, and S.R. Madiraju, *Metabolic signaling in fuel-induced insulin secretion.* Cell Metab, 2013. **18**(2): p. 162-85.

128. Meglasson, M.D. and F.M. Matschinsky, *New perspectives on pancreatic islet glucokinase.* Am J Physiol, 1984. **246**(1 Pt 1): p. E1-13.

129. Henquin, J.C., et al., *Congenital hyperinsulinism caused by hexokinase I expression or glucokinase-activating mutation in a subset of beta-cells.* Diabetes, 2013. **62**(5): p. 1689-96.

130. Otonkoski, T., et al., *Physical exercise-induced hypoglycemia caused by failed silencing of monocarboxylate transporter 1 in pancreatic beta cells.* Am J Hum Genet, 2007. **81**(3): p. 467-74.

131. Pullen, T.J., et al., *Overexpression of monocarboxylate transporter-1 (SLC16A1) in mouse pancreatic beta-cells leads to relative hyperinsulinism during exercise.* Diabetes, 2012. **61**(7): p. 1719-25.

132. Maechler, P., *Mitochondrial function and insulin secretion.* Mol Cell Endocrinol, 2013. **379**(1-2): p. 12-8.

133. Yoshihara, E., et al., *ERRγ Is Required for the Metabolic Maturation of Therapeutically Functional Glucose-Responsive β Cells.* Cell Metabolism, 2016. **23**(4): p. 622-634.

134. Owen, O.E., S.C. Kalhan, and R.W. Hanson, *The key role of anaplerosis and cataplerosis for citric acid cycle function.* J Biol Chem, 2002. **277**(34): p. 30409-12.

135. Jensen, M.V., et al., *Metabolic cycling in control of glucose-stimulated insulin secretion.* Am J Physiol Endocrinol Metab, 2008. **295**(6): p. E1287-97.

136. Jitrapakdee, S., et al., *Regulation of insulin secretion: role of mitochondrial signalling.* Diabetologia, 2010. **53**(6): p. 1019-32.

137. Li, X., et al., *The MDM2-p53-pyruvate carboxylase signalling axis couples mitochondrial metabolism to glucose-stimulated insulin secretion in pancreatic beta-cells.* Nat Commun, 2016. **7**: p. 11740.

138. Jensen, M.V., et al., *Compensatory responses to pyruvate carboxylase suppression in islet beta-cells. Preservation of glucose-stimulated insulin secretion.* J Biol Chem, 2006. **281**(31): p. 22342-51.

139. Stark, R. and R.G. Kibbey, *The mitochondrial isoform of phosphoenolpyruvate carboxykinase (PEPCK-M) and glucose homeostasis: has it been overlooked?* Biochim Biophys Acta, 2014. **1840**(4): p. 1313-30.

140. Stark, R., et al., *Phosphoenolpyruvate cycling via mitochondrial phosphoenolpyruvate carboxykinase links anaplerosis and mitochondrial GTP with insulin secretion.* J Biol Chem, 2009. **284**(39): p. 26578-90.

141. Kibbey, R.G., et al., *Mitochondrial GTP regulates glucose-stimulated insulin secretion.* Cell Metab, 2007. **5**(4): p. 253-64.

142. Pongratz, R.L., et al., *Cytosolic and mitochondrial malic enzyme isoforms differentially control insulin secretion.* J Biol Chem, 2007. **282**(1): p. 200-7.

143. Tengholm, A. and E. Gylfe, *cAMP signalling in insulin and glucagon secretion.* Diabetes Obes Metab, 2017. **19 Suppl 1**: p. 42-53.

144. Drucker, D.J., *The biology of incretin hormones.* Cell Metab, 2006. **3**(3): p. 153-65.

145. Bae, J., et al., *Differential Effects of Thiazolidinediones and Dipeptidyl Peptidase-4 Inhibitors on Insulin Resistance and beta-Cell Function in Type 2 Diabetes Mellitus: A Propensity Score-Matched Analysis.* Diabetes Ther, 2019. **10**(1): p. 149-158.

146. Meloni, A.R., et al., *GLP-1 receptor activated insulin secretion from pancreatic beta-cells: mechanism and glucose dependence.* Diabetes Obes Metab, 2013. **15**(1): p. 15-27.

147. Brun, T., et al., *Evidence for an anaplerotic/malonyl-CoA pathway in pancreatic beta-cell nutrient signaling.* Diabetes, 1996. **45**(2): p. 190-8.

148. Prentki, M., *New insights into pancreatic beta-cell metabolic signaling in insulin secretion.* Eur J Endocrinol, 1996. **134**(3): p. 272-86.

149. Wollheim, C.B. and P. Maechler, *Beta-cell mitochondria and insulin secretion: messenger role of nucleotides and metabolites.* Diabetes, 2002. **51 Suppl 1**: p. S37-42.

150. O'Sullivan-Murphy, B. and F. Urano, *ER stress as a trigger for beta-cell dysfunction and autoimmunity in type 1 diabetes.* Diabetes, 2012. **61**(4): p. 780-1.

151. Brunzell, J.D., et al., *Relationships between fasting plasma glucose levels and insulin secretion during intravenous glucose tolerance tests.* J Clin Endocrinol Metab, 1976. **42**(2): p. 222-9.

152. Anello, M., et al., *Fast reversibility of glucose-induced desensitization in rat pancreatic islets. Evidence for an involvement of ionic fluxes.* Diabetes, 1996. **45**(4): p. 502-6.

153. Bonner-Weir, S., et al., *Limited B cell regeneration in a B cell deficient rat model: studies with dexamethasone.* Metabolism, 1981. **30**(9): p. 914-8.

154. Jonas, J.C., et al., *Chronic hyperglycemia triggers loss of pancreatic beta cell differentiation in an animal model of diabetes.* J Biol Chem, 1999. **274**(20): p. 14112-21.

155. Lowell, B.B. and G.I. Shulman, *Mitochondrial dysfunction and type 2 diabetes.* Science, 2005. **307**(5708): p. 384-7.

156. Lu, H., et al., *Molecular and metabolic evidence for mitochondrial defects associated with beta-cell dysfunction in a mouse model of type 2 diabetes.* Diabetes, 2010. **59**(2): p. 448-59.

157. Chan, C.B., et al., *Uncoupling protein 2 and islet function.* Diabetes, 2004. **53 Suppl 1**: p. S136-42.

158. Chan, C.B., et al., *Overexpression of uncoupling protein 2 inhibits glucose-stimulated insulin secretion from rat islets.* Diabetes, 1999. **48**(7): p. 1482-6.

159. Wikstrom, J.D., et al., *A novel high-throughput assay for islet respiration reveals uncoupling of rodent and human islets.* PLoS One, 2012. **7**(5): p. e33023.

160. Aguayo-Mazzucato, C., et al., *Mafa expression enhances glucose-responsive insulin secretion in neonatal rat beta cells.* Diabetologia, 2011. **54**(3): p. 583-93.

161. Nishimura, W., et al., *A switch from MafB to MafA expression accompanies differentiation to pancreatic β-cells.* Developmental Biology, 2006. **293**(2): p. 526-539.

162. Dhawan, S., et al., *DNA methylation directs functional maturation of pancreatic beta cells.* J Clin Invest, 2015. **125**(7): p. 2851-60.

163. Stolovich-Rain, M., et al., *Weaning triggers a maturation step of pancreatic beta cells.* Dev Cell, 2015. **32**(5): p. 535-45.

164. Aguayo-Mazzucato, C., et al., *Thyroid hormone promotes postnatal rat pancreatic beta-cell development and glucose-responsive insulin secretion through MAFA.* Diabetes, 2013. **62**(5): p. 1569-80.

165. Kitamura, Y.I., et al., *FoxO1 protects against pancreatic beta cell failure through NeuroD and MafA induction.* Cell Metab, 2005. **2**(3): p. 153-63.

166. Aguayo-Mazzucato, C., et al., *MAFA and T3 Drive Maturation of Both Fetal Human Islets and Insulin-Producing Cells Differentiated From hESC.* J Clin Endocrinol Metab, 2015. **100**(10): p. 3651-9.

167. van der Meulen, T., et al., *Urocortin3 mediates somatostatin-dependent negative feedback control of insulin secretion.* Nat Med, 2015. **21**(7): p. 769-76.

168. van der Meulen, T. and M.O. Huising, *Maturation of stem cell-derived beta-cells guided by the expression of urocortin 3.* Rev Diabet Stud, 2014. **11**(1): p. 115-32.

169. Arda, H.E., et al., *Age-Dependent Pancreatic Gene Regulation Reveals Mechanisms Governing Human beta Cell Function.* Cell Metab, 2016. **23**(5): p. 909-20.

170. Ravassard, P., et al., *A genetically engineered human pancreatic beta cell line exhibiting glucose-inducible insulin secretion.* J Clin Invest, 2011. **121**(9): p. 3589-97.

171. Haeusler, R.A., T.E. McGraw, and D. Accili, *Biochemical and cellular properties of insulin receptor signalling.* Nat Rev Mol Cell Biol, 2018. **19**(1): p. 31-44.

172. Lakey, J.R., et al., *Variables in organ donors that affect the recovery of human islets of Langerhans.* Transplantation, 1996. **61**(7): p. 1047-53.

173. Meeusen, J.W., et al., *TSQ (6-methoxy-8-p-toluenesulfonamido-quinoline), a common fluorescent sensor for cellular zinc, images zinc proteins.* Inorg Chem, 2011. **50**(16): p. 7563-73.

174. Phillips, N.R., M.L. Sprouse, and R.K. Roby, *Simultaneous quantification of mitochondrial DNA copy number and deletion ratio: a multiplex real-time PCR assay.* Sci Rep, 2014. **4**: p. 3887.

175. Komatsu, M., et al., *Glucose-stimulated insulin secretion: A newer perspective.* J Diabetes Investig, 2013. **4**(6): p. 511-6.

176. Alves, Tiago C., et al., *Integrated, Step-Wise, Mass-Isotopomeric Flux Analysis of the TCA Cycle.* Cell Metabolism, 2015. **22**(5): p. 936-947.

177. Mugabo, Y., et al., *Metabolic fate of glucose and candidate signaling and excess-fuel detoxification pathways in pancreatic beta-cells.* J Biol Chem, 2017. **292**(18): p. 7407-7422.

178. Li, C., et al., *A signaling role of glutamine in insulin secretion.* J Biol Chem, 2004. **279**(14): p. 13393-401.

179. Jain, K., J. Logothetopoulos, and P. Zucker, *The effects of D- and L-glyceraldehyde on glucose oxidation, insulin secretion and insulin biosynthesis by pancreatic islets of the rat.* Biochim Biophys Acta, 1975. **399**(2): p. 384-94.

180. Kabra, U.D., et al., *Direct Substrate Delivery Into Mitochondrial Fission-Deficient Pancreatic Islets Rescues Insulin Secretion.* Diabetes, 2017. **66**(5): p. 1247-1257.

181. MacDonald, M.J., *Metabolism of the insulin secretagogue methyl succinate by pancreatic islets.* Arch Biochem Biophys, 1993. **300**(1): p. 201-5.

182. Heissig, H., et al., *Mechanism of the insulin-releasing action of alpha-ketoisocaproate and related alpha-keto acid anions.* Mol Pharmacol, 2005. **68**(4): p. 1097-105.

183. Juntti-Berggren, L., et al., *Dihydroxyacetone-induced oscillations in cytoplasmic free Ca2+ and the ATP/ADP ratio in pancreatic beta-cells at substimulatory glucose.* J Biol Chem, 2003. **278**(42): p. 40710-6.

184. Marsh, J.J. and H.G. Lebherz, *Fructose-bisphosphate aldolases: an evolutionary history.* Trends Biochem Sci, 1992. **17**(3): p. 110-3.

185. Hitosugi, T., et al., *Phosphoglycerate mutase 1 coordinates glycolysis and biosynthesis to promote tumor growth.* Cancer Cell, 2012. **22**(5): p. 585-600.

186. Hoagland, V.D., Jr. and D.C. Teller, *Influence of substrates on the dissociation of rabbit muscle D-glyceraldehyde 3-phosphate dehydrogenase.* Biochemistry, 1969. **8**(2): p. 594-602.

187. Tomokuni, Y., et al., *Loose interaction between glyceraldehyde-3-phosphate dehydrogenase and phosphoglycerate kinase revealed by fluorescence resonance energy transfer-fluorescence lifetime imaging microscopy in living cells.* FEBS J, 2010. **277**(5): p. 1310-8.

188. Suarez, S., et al., *High Glucose-induced Retinal Pericyte Apoptosis Depends on Association of GAPDH and Siah1.* J Biol Chem, 2015. **290**(47): p. 28311-20.

189. Jayaguru, P. and S. Mohr, *Nuclear GAPDH: changing the fate of Muller cells in diabetes.* J Ocul Biol Dis Infor, 2011. **4**(1-2): p. 34-41.

190. Yego, E.C. and S. Mohr, *siah-1 Protein is necessary for high glucose-induced glyceraldehyde-3-phosphate dehydrogenase nuclear accumulation and cell death in Muller cells.* J Biol Chem, 2010. **285**(5): p. 3181-90.

191. Kornberg, M.D., et al., *GAPDH mediates nitrosylation of nuclear proteins.* Nat Cell Biol, 2010. **12**(11): p. 1094-100.

192. Yego, E.C., et al., *Differential regulation of high glucose-induced glyceraldehyde-3-phosphate dehydrogenase nuclear accumulation in Muller cells by IL-1beta and IL-6.* Invest Ophthalmol Vis Sci, 2009. **50**(4): p. 1920-8.

193. Kanwar, M. and R.A. Kowluru, *Role of glyceraldehyde 3-phosphate dehydrogenase in the development and progression of diabetic retinopathy.* Diabetes, 2009. **58**(1): p. 227-34.

194. Sen, N., et al., *Nitric oxide-induced nuclear GAPDH activates p300/CBP and mediates apoptosis.* Nat Cell Biol, 2008. **10**(7): p. 866-73.

195. Kim, C.I., et al., *Nuclear translocation and overexpression of GAPDH by the hyper-pressure in retinal ganglion cell.* Biochem Biophys Res Commun, 2006. **341**(4): p. 1237-43.

196. Hara, M.R., et al., *S-nitrosylated GAPDH initiates apoptotic cell death by nuclear translocation following Siah1 binding.* Nat Cell Biol, 2005. **7**(7): p. 665-74.

197. Joo, H.Y., et al., *SIRT1 interacts with and protects glyceraldehyde-3-phosphate dehydrogenase (GAPDH) from nuclear translocation: implications for cell survival after irradiation.* Biochem Biophys Res Commun, 2012. **424**(4): p. 681-6.

198. Kim, J.J. and M.Y. Lee, *p53 is not necessary for nuclear translocation of GAPDH during NO-induced apoptosis.* BMB Rep, 2011. **44**(12): p. 782-6.

199. Lenzen, S., *A fresh view of glycolysis and glucokinase regulation: history and current status.* J Biol Chem, 2014. **289**(18): p. 12189-94.

200. Sener, A., et al., *Hexose metabolism in pancreatic islets: compartmentation of hexokinase in islet cells.* Arch Biochem Biophys, 1986. **251**(1): p. 61-7.

201. Hutton, J.C. and R.M. O'Brien, *Glucose-6-phosphatase catalytic subunit gene family.* J Biol Chem, 2009. **284**(43): p. 29241-5.

202. Jeffery, C.J., *Protein moonlighting: what is it, and why is it important?* Philos Trans R Soc Lond B Biol Sci, 2018. **373**(1738).

203. Jeffery, C.J., *Protein species and moonlighting proteins: Very small changes in a protein's covalent structure can change its biochemical function.* J Proteomics, 2016. **134**: p. 19-24.

204. Jeffery, C.J., *An introduction to protein moonlighting.* Biochem Soc Trans, 2014. **42**(6): p. 1679-83.

205. Pantalone, K.M., et al., *Clinical characteristics, complications, comorbidities and treatment patterns among patients with type 2 diabetes mellitus in a large integrated health system.* BMJ Open Diabetes Res Care, 2015. **3**(1): p. e000093.

206. Fraga, D.W., et al., *A comparison of media supplement methods for the extended culture of human islet tissue.* Transplantation, 1998. **65**(8): p. 1060-6.

207. Diedisheim, M., et al., *Modeling human pancreatic beta cell dedifferentiation.* Mol Metab, 2018. **10**: p. 74-86.

208. Jabs, N., et al., *Reduced insulin secretion and content in VEGF-a deficient mouse pancreatic islets.* Exp Clin Endocrinol Diabetes, 2008. **116 Suppl 1**: p. S46-9.

209. Lammert, E., et al., *Role of VEGF-A in vascularization of pancreatic islets.* Curr Biol, 2003. **13**(12): p. 1070-4.

210. Azizoglu, D.B., et al., *Vascular development in the vertebrate pancreas.* Dev Biol, 2016. **420**(1): p. 67-78.

211. Thorens, B., *Brain glucose sensing and neural regulation of insulin and glucagon secretion.* Diabetes Obes Metab, 2011. **13 Suppl 1**: p. 82-8.

212. Ahren, B., *Autonomic regulation of islet hormone secretion--implications for health and disease.* Diabetologia, 2000. **43**(4): p. 393-410.

213. Sneddon, J.B., M. Borowiak, and D.A. Melton, *Self-renewal of embryonic-stem-cell-derived progenitors by organ-matched mesenchyme.* Nature, 2012. **491**(7426): p. 765-8.

214. Borg, D.J., et al., *Mesenchymal stromal cells improve transplanted islet survival and islet function in a syngeneic mouse model.* Diabetologia, 2014. **57**(3): p. 522-31.

215. de Souza, B.M., et al., *Effect of co-culture of mesenchymal stem/stromal cells with pancreatic islets on viability and function outcomes: a systematic review and meta-analysis.* Islets, 2017. **9**(2): p. 30-42.

216. Hibsher, D., et al., *Pancreatic Mesenchyme Regulates Islet Cellular Composition in a Patched/Hedgehog-Dependent Manner.* Sci Rep, 2016. **6**: p. 38008.

217. Lukowiak, B., et al., *Identification and purification of functional human beta-cells by a new specific zinc-fluorescent probe.* J Histochem Cytochem, 2001. **49**(4): p. 519-28.

218. Figlewicz, D.P., et al., *65Zinc and endogenous zinc content and distribution in islets in relationship to insulin content.* Endocrinology, 1984. **115**(3): p. 877-81.

219. van der Meulen, T., et al., *Urocortin 3 marks mature human primary and embryonic stem cell-derived pancreatic alpha and beta cells.* PLoS One, 2012. **7**(12): p. e52181.

220. Kahn, S.E., et al., *Evidence of cosecretion of islet amyloid polypeptide and insulin by beta-cells.* Diabetes, 1990. **39**(5): p. 634-8.

221. Portela-Gomes, G.M., et al., *PACAP is expressed in secretory granules of insulin and glucagon cells in human and rodent pancreas. Evidence for generation of cAMP compartments uncoupled from hormone release in diabetic islets.* Regul Pept, 2003. **113**(1-3): p. 31-9.

222. Ishihara, H., et al., *Overexpression of monocarboxylate transporter and lactate dehydrogenase alters insulin secretory responses to pyruvate and lactate in beta cells.* J Clin Invest, 1999. **104**(11): p. 1621-9.

223. Yang, Y., et al., *Different effects of LDH-A inhibition by oxamate in non-small cell lung cancer cells.* Oncotarget, 2014. **5**(23): p. 11886-96.

224. Sekine, N., et al., *Low lactate dehydrogenase and high mitochondrial glycerol phosphate dehydrogenase in pancreatic beta-cells. Potential role in nutrient sensing.* J Biol Chem, 1994. **269**(7): p. 4895-902.

225. Fadista, J., et al., *Global genomic and transcriptomic analysis of human pancreatic islets reveals novel genes influencing glucose metabolism.* Proc Natl Acad Sci U S A, 2014. **111**(38): p. 13924-9.

226. Song, W.M. and B. Zhang, *Multiscale Embedded Gene Co-expression Network Analysis.* PLoS Comput Biol, 2015. **11**(11): p. e1004574.

227. Kurian, S.M., et al., *Gene expression signature predicts human islet integrity and transplant functionality in diabetic mice.* PLoS One, 2017. **12**(10): p. e0185331.

228. Taneera, J., et al., *Identification of novel genes for glucose metabolism based upon expression pattern in human islets and effect on insulin secretion and glycemia.* Hum Mol Genet, 2015. **24**(7): p. 1945-55.

229. Baron, M., et al., *A Single-Cell Transcriptomic Map of the Human and Mouse Pancreas Reveals Inter- and Intra-cell Population Structure.* Cell Syst, 2016. **3**(4): p. 346-360 e4.

230. Segerstolpe, A., et al., *Single-Cell Transcriptome Profiling of Human Pancreatic Islets in Health and Type 2 Diabetes.* Cell Metab, 2016. **24**(4): p. 593-607.

231. Thomas, P.D., et al., *PANTHER: a browsable database of gene products organized by biological function, using curated protein family and subfamily classification.* Nucleic Acids Res, 2003. **31**(1): p. 334-41.

232. Braun, M., et al., *Regulated exocytosis of GABA-containing synaptic-like microvesicles in pancreatic beta-cells.* J Gen Physiol, 2004. **123**(3): p. 191-204.

233. Taneera, J., et al., *gamma-Aminobutyric acid (GABA) signalling in human pancreatic islets is altered in type 2 diabetes.* Diabetologia, 2012. **55**(7): p. 1985-94.

234. Kapp, K., et al., *The protein tyrosine phosphatase alpha modifies insulin secretion in INS-1E cells.* Biochem Biophys Res Commun, 2003. **311**(2): p. 361-4.

235. Brissova, M., et al., *Pancreatic islet production of vascular endothelial growth factor--a is essential for islet vascularization, revascularization, and function.* Diabetes, 2006. **55**(11): p. 2974-85.

236. Brissova, M. and A.C. Powers, *Revascularization of transplanted islets: can it be improved?* Diabetes, 2008. **57**(9): p. 2269-71.

237. Dai, C., et al., *Pancreatic islet vasculature adapts to insulin resistance through dilation and not angiogenesis.* Diabetes, 2013. **62**(12): p. 4144-53.

238. Peiris, H., et al., *The beta-cell/EC axis: how do islet cells talk to each other?* Diabetes, 2014. **63**(1): p. 3-11.

239. Kalousova, A., et al., *Dachshund homologues play a conserved role in islet cell development.* Dev Biol, 2010. **348**(2): p. 143-52.

240. Ma, R.C., et al., *Familial young-onset diabetes, pre-diabetes and cardiovascular disease are associated with genetic variants of DACH1 in Chinese.* PLoS One, 2014. **9**(1): p. e84770.

241. Williams, M.J., et al., *The Obesity-Linked Gene Nudt3 Drosophila Homolog Aps Is Associated With Insulin Signaling.* Mol Endocrinol, 2015. **29**(9): p. 1303-19.

242. Ezanno, H., et al., *JNK3 is required for the cytoprotective effect of exendin 4.* J Diabetes Res, 2014. **2014**: p. 814854.

243. Cao, X., et al., *Novel human ZAKI-4 isoforms: hormonal and tissue-specific regulation and function as calcineurin inhibitors.* Biochem J, 2002. **367**(Pt 2): p. 459-66.

244. Bizzoca, A., et al., *F3/Contactin acts as a modulator of neurogenesis during cerebral cortex development.* Dev Biol, 2012. **365**(1): p. 133-51.

245. Gilley, J. and M.P. Coleman, *Endogenous Nmnat2 is an essential survival factor for maintenance of healthy axons.* PLoS Biol, 2010. **8**(1): p. e1000300.

246. Zollo, M., et al., *PRUNE is crucial for normal brain development and mutated in microcephaly with neurodevelopmental impairment.* Brain, 2017. **140**(4): p. 940-952.

247. Betsholtz, C., et al., *Sequence divergence in a specific region of islet amyloid polypeptide (IAPP) explains differences in islet amyloid formation between species.* FEBS Lett, 1989. **251**(1-2): p. 261-4.

248. Shintani, N., et al., *Functional roles of the neuropeptide PACAP in brain and pancreas.* Life Sci, 2003. **74**(2-3): p. 337-43.

249. Carboneau, B.A., et al., *Unexpected effects of the MIP-CreER transgene and tamoxifen on beta-cell growth in C57Bl6/J male mice.* Physiol Rep, 2016. **4**(18).

250. Akter, R., et al., *Islet Amyloid Polypeptide: Structure, Function, and Pathophysiology.* J Diabetes Res, 2016. **2016**: p. 2798269.

251. Lutz, T.A., *The interaction of amylin with other hormones in the control of eating.* Diabetes Obes Metab, 2013. **15**(2): p. 99-111.

252. Montane, J., et al., *Metabolic stress, IAPP and islet amyloid.* Diabetes Obes Metab, 2012. **14 Suppl 3**: p. 68-77.

253. Henson, M.S., et al., *Evaluation of plasma islet amyloid polypeptide and serum glucose and insulin concentrations in nondiabetic cats classified by body condition score and in cats with naturally occurring diabetes mellitus.* Am J Vet Res, 2011. **72**(8): p. 1052-8.

254. Westermark, P., A. Andersson, and G.T. Westermark, *Islet amyloid polypeptide, islet amyloid, and diabetes mellitus.* Physiol Rev, 2011. **91**(3): p. 795-826.

255. Lutz, T.A., *The role of amylin in the control of energy homeostasis.* Am J Physiol Regul Integr Comp Physiol, 2010. **298**(6): p. R1475-84.

256. Ohsawa, H., et al., *Islet amyloid polypeptide inhibits glucose-stimulated insulin secretion from isolated rat pancreatic islets.* Biochem Biophys Res Commun, 1989. **160**(2): p. 961-7.

257. Yamamoto, K., et al., *Overexpression of PACAP in transgenic mouse pancreatic beta-cells enhances insulin secretion and ameliorates streptozotocin-induced diabetes.* Diabetes, 2003. **52**(5): p. 1155-62.

258. Yada, T., et al., *Pituitary adenylate cyclase-activating polypeptide (PACAP) is an islet substance serving as an intra-islet amplifier of glucose-induced insulin secretion in rats.* J Physiol, 1997. **505 (Pt 2)**: p. 319-28.

259. Leffert, J.D., et al., *Rat amylin: cloning and tissue-specific expression in pancreatic islets.* Proc Natl Acad Sci U S A, 1989. **86**(9): p. 3127-30.

260. Sanke, T., et al., *An islet amyloid peptide is derived from an 89-amino acid precursor by proteolytic processing.* J Biol Chem, 1988. **263**(33): p. 17243-6.

261. Leighton, B. and G.J. Cooper, *Pancreatic amylin and calcitonin gene-related peptide cause resistance to insulin in skeletal muscle in vitro.* Nature, 1988. **335**(6191): p. 632-5.

262. Potes, C.S. and T.A. Lutz, *Brainstem mechanisms of amylin-induced anorexia.* Physiol Behav, 2010. **100**(5): p. 511-8.

263. Trevaskis, J.L., D.G. Parkes, and J.D. Roth, *Insights into amylin-leptin synergy.* Trends Endocrinol Metab, 2010. **21**(8): p. 473-9.

264. Turek, V.F., et al., *Mechanisms of amylin/leptin synergy in rodent models.* Endocrinology, 2010. **151**(1): p. 143-52.

265. Butler, P.C., et al., *Effects of meal ingestion on plasma amylin concentration in NIDDM and nondiabetic humans.* Diabetes, 1990. **39**(6): p. 752-6.

266. Bailey, R.J., et al., *Pharmacological characterization of rat amylin receptors: implications for the identification of amylin receptor subtypes.* Br J Pharmacol, 2012. **166**(1): p. 151-67.

267. Muff, R., et al., *An amylin receptor is revealed following co-transfection of a calcitonin receptor with receptor activity modifying proteins-1 or -3.* Endocrinology, 1999. **140**(6): p. 2924-7.

268. Christopoulos, G., et al., *Multiple amylin receptors arise from receptor activity-modifying protein interaction with the calcitonin receptor gene product.* Mol Pharmacol, 1999. **56**(1): p. 235-42.

269. Lutz, T.A., et al., *Amylin Selectively Signals Onto POMC Neurons in the Arcuate Nucleus of the Hypothalamus.* Diabetes, 2018. **67**(5): p. 805-817.

270. Trevaskis, J.L., et al., *Interaction of leptin and amylin in the long-term maintenance of weight loss in diet-induced obese rats.* Obesity (Silver Spring), 2010. **18**(1): p. 21-6.

271. Wilson, M.E., J.A. Kalamaras, and M.S. German, *Expression pattern of IAPP and prohormone convertase 1/3 reveals a distinctive set of endocrine cells in the embryonic pancreas.* Mech Dev, 2002. **115**(1-2): p. 171-6.

272. Haataja, L., et al., *Islet amyloid in type 2 diabetes, and the toxic oligomer hypothesis.* Endocr Rev, 2008. **29**(3): p. 303-16.

273. Westermark, P., et al., *Islet amyloid in type 2 human diabetes mellitus and adult diabetic cats contains a novel putative polypeptide hormone.* Am J Pathol, 1987. **127**(3): p. 414-7.

274. Cooper, G.J., et al., *Purification and characterization of a peptide from amyloid-rich pancreases of type 2 diabetic patients.* Proc Natl Acad Sci U S A, 1987. **84**(23): p. 8628-32.

275. Ehrlich, J.C. and I.M. Ratner, *Amyloidosis of the islets of Langerhans. A restudy of islet hyalin in diabetic and non-diabetic individuals.* Am J Pathol, 1961. **38**: p. 49-59.

276. Halban, P.A., et al., *beta-cell failure in type 2 diabetes: postulated mechanisms and prospects for prevention and treatment.* J Clin Endocrinol Metab, 2014. **99**(6): p. 1983-92.

277. Margittai, M. and R. Langen, *Spin labeling analysis of amyloids and other protein aggregates.* Methods Enzymol, 2006. **413**: p. 122-39.

278. Westermark, P., et al., *Islet amyloid polypeptide: pinpointing amino acid residues linked to amyloid fibril formation.* Proc Natl Acad Sci U S A, 1990. **87**(13): p. 5036-40.

279. Liu, Z., et al., *Systematic comparison of 2A peptides for cloning multi-genes in a polycistronic vector.* Sci Rep, 2017. **7**(1): p. 2193.

280. Dicker, D., *DPP-4 inhibitors: impact on glycemic control and cardiovascular risk factors.* Diabetes Care, 2011. **34 Suppl 2**: p. S276-8.

281. Akerman, I., et al., *Human Pancreatic beta Cell lncRNAs Control Cell-Specific Regulatory Networks.* Cell Metab, 2017. **25**(2): p. 400-411.

282. Murao, N., et al., *Essential roles of aspartate aminotransferase 1 and vesicular glutamate transporters in beta-cell glutamate signaling for incretin-induced insulin secretion.* PLoS One, 2017. **12**(11): p. e0187213.

283. !!! INVALID CITATION !!! [10, 36, 100].

284. Butera, G., et al., *Mutant p53 prevents GAPDH nuclear translocation in pancreatic cancer cells favoring glycolysis and 2-deoxyglucose sensitivity.* Biochim Biophys Acta Mol Cell Res, 2018. **1865**(12): p. 1914-1923.

285. Zhai, D., et al., *Disruption of the nuclear p53-GAPDH complex protects against ischemia-induced neuronal damage.* Mol Brain, 2014. **7**: p. 20.

286. Mazzola, J.L. and M.A. Sirover, *Subcellular localization of human glyceraldehyde-3-phosphate dehydrogenase is independent of its glycolytic function.* Biochim Biophys Acta, 2003. **1622**(1): p. 50-6.

287. Shashidharan, P., et al., *Nuclear translocation of GAPDH-GFP fusion protein during apoptosis.* Neuroreport, 1999. **10**(5): p. 1149-53.

288. Duan, G. and D. Walther, *The roles of post-translational modifications in the context of protein interaction networks.* PLoS Comput Biol, 2015. **11**(2): p. e1004049.

289. Hu, A., W.S. Noble, and A. Wolf-Yadlin, *Technical advances in proteomics: new developments in data-independent acquisition.* F1000Res, 2016. **5**.

290. Imai, S.I. and L. Guarente, *It takes two to tango: NAD(+) and sirtuins in aging/longevity control.* NPJ Aging Mech Dis, 2016. **2**: p. 16017.

291. Fjeld, C.C., W.T. Birdsong, and R.H. Goodman, *Differential binding of NAD+ and NADH allows the transcriptional corepressor carboxyl-terminal binding protein to serve as a metabolic sensor.* Proc Natl Acad Sci U S A, 2003. **100**(16): p. 9202-7.

292. Lembert, N., et al., *Methyl pyruvate initiates membrane depolarization and insulin release by metabolic factors other than ATP.* Biochem J, 2001. **354**(Pt 2): p. 345-50.

293. Johansson, H., et al., *Tissue factor produced by the endocrine cells of the islets of Langerhans is associated with a negative outcome of clinical islet transplantation.* Diabetes, 2005. **54**(6): p. 1755-62.

294. Weykamp, C., *HbA1c: a review of analytical and clinical aspects.* Ann Lab Med, 2013. **33**(6): p. 393-400.

295. Dy, E.C., D.M. Harlan, and K.I. Rother, *Assessment of islet function following islet and pancreas transplantation.* Curr Diab Rep, 2006. **6**(4): p. 316-22.

296. DeFronzo, R.A., J.D. Tobin, and R. Andres, *Glucose clamp technique: a method for quantifying insulin secretion and resistance.* Am J Physiol, 1979. **237**(3): p. E214-23.

297. Abdulreda, M.H., A. Caicedo, and P.O. Berggren, *Transplantation into the anterior chamber of the eye for longitudinal, non-invasive in vivo imaging with single-cell resolution in real-time.* J Vis Exp, 2013(73): p. e50466.

298. Speier, S., et al., *Noninvasive high-resolution in vivo imaging of cell biology in the anterior chamber of the mouse eye.* Nat Protoc, 2008. **3**(8): p. 1278-86.

299. Nakai, J., M. Ohkura, and K. Imoto, *A high signal-to-noise Ca(2+) probe composed of a single green fluorescent protein.* Nat Biotechnol, 2001. **19**(2): p. 137-41.

300. Akemann, W., et al., *Imaging neural circuit dynamics with a voltage-sensitive fluorescent protein.* J Neurophysiol, 2012. **108**(8): p. 2323-37.

301. Bruin, J.E., et al., *Accelerated Maturation of Human Stem Cell-Derived Pancreatic Progenitor Cells into Insulin-Secreting Cells in Immunodeficient Rats Relative to Mice.* Stem Cell Reports, 2015. **5**(6): p. 1081-1096.

302. Evans-Molina, C., et al., *Glucose regulation of insulin gene transcription and pre-mRNA processing in human islets.* Diabetes, 2007. **56**(3): p. 827-35.

303. Kayatekin, C., et al., *Translocon Declogger Ste24 Protects against IAPP Oligomer-Induced Proteotoxicity.* Cell, 2018. **173**(1): p. 62-73 e9.

304. Antoni, G., et al., *In vivo visualization of amyloid deposits in the heart with 11C-PIB and PET.* J Nucl Med, 2013. **54**(2): p. 213-20.

305. Bohman, S. and G.T. Westermark, *Extensive amyloid formation in transplanted microencapsulated mouse and human islets.* Amyloid, 2012. **19**(2): p. 87-93.

306. Sjolander, J., et al., *Islet amyloid polypeptide triggers limited complement activation and binds complement inhibitor C4b-binding protein, which enhances fibril formation.* J Biol Chem, 2012. **287**(14): p. 10824-33.

307. Udayasankar, J., et al., *Amyloid formation results in recurrence of hyperglycaemia following transplantation of human IAPP transgenic mouse islets.* Diabetologia, 2009. **52**(1): p. 145-53.

308. Yosten, G.L.C., *Alpha cell dysfunction in type 1 diabetes.* Peptides, 2018. **100**: p. 54-60.

309. Tan, S., et al., *Type 1 diabetes induction in humanized mice.* Proc Natl Acad Sci U S A, 2017. **114**(41): p. 10954-10959.

310. Taneera, J., et al., *A systems genetics approach identifies genes and pathways for type 2 diabetes in human islets.* Cell Metab, 2012. **16**(1): p. 122-34.

311. Hockemeyer, D., et al., *Genetic engineering of human pluripotent cells using TALE nucleases.* Nat Biotechnol, 2011. **29**(8): p. 731-4.